



**HAL**  
open science

# Deeper understanding of the homography decomposition for vision-based control

Ezio Malis, Manuel Vargas

► **To cite this version:**

Ezio Malis, Manuel Vargas. Deeper understanding of the homography decomposition for vision-based control. [Research Report] RR-6303, INRIA. 2007, pp.90. inria-00174036v3

**HAL Id: inria-00174036**

**<https://inria.hal.science/inria-00174036v3>**

Submitted on 25 Sep 2007

**HAL** is a multi-disciplinary open access archive for the deposit and dissemination of scientific research documents, whether they are published or not. The documents may come from teaching and research institutions in France or abroad, or from public or private research centers.

L'archive ouverte pluridisciplinaire **HAL**, est destinée au dépôt et à la diffusion de documents scientifiques de niveau recherche, publiés ou non, émanant des établissements d'enseignement et de recherche français ou étrangers, des laboratoires publics ou privés.



INSTITUT NATIONAL DE RECHERCHE EN INFORMATIQUE ET EN AUTOMATIQUE

*Deeper understanding of the homography  
decomposition for vision-based control*

Ezio Malis and Manuel Vargas

**N° 6303**

Septembre 2007

Thème NUM

*R*apport  
de recherche





## Deeper understanding of the homography decomposition for vision-based control

Ezio Malis <sup>\*</sup> and Manuel Vargas <sup>†</sup>

Thème NUM — Systèmes numériques  
Projet AROBAS

Rapport de recherche n° 6303 — Septembre 2007 — 90 pages

**Abstract:** The displacement of a calibrated camera between two images of a planar object can be estimated by decomposing a homography matrix. The aim of this document is to propose a new method for solving the homography decomposition problem. This new method provides analytical expressions for the solutions of the problem, instead of the traditional numerical procedures. As a result, expressions of the translation vector, rotation matrix and object-plane normal are explicitly expressed as a function of the entries of the homography matrix. The main advantage of this method is that it will provide a deeper understanding on the homography decomposition problem. For instance, it allows to obtain the relations among the possible solutions of the problem. Thus, new vision-based robot control laws can be designed. For example the control schemes proposed in this report combine the two final solutions of the problem (only one of them being the true one) assuming that there is no a priori knowledge for discerning among them.

**Key-words:** Visual servoing, planar objects, homography, decomposition, camera calibration errors, structure from motion, Euclidean reconstruction.

<sup>\*</sup> Ezio Malis is with INRIA Sophia Antipolis

<sup>†</sup> Manuel Vargas is with the *Dpto. de Ingeniería de Sistemas y Automática* in the University of Seville, Spain.

## Mieux comprendre la décomposition de la matrice d'homographie pour l'asservissement visuel

**Résumé :** Le déplacement d'une caméra calibrée peut être estimé à partir de deux images d'un objet planaire en décomposant une matrice d'homographie. L'objectif de ce rapport de recherche est de proposer une nouvelle méthode pour résoudre le problème de la décomposition de l'homographie. Cette nouvelle méthode donne une expression analytique des solutions du problème au lieu des solutions numériques classiques. Finalement, nous obtenons explicitement le vecteur de translation, la matrice de rotation et la normale au plan exprimés en fonction des éléments de la matrice d'homographie. Le principal avantage de cette méthode est qu'elle aide à mieux comprendre le problème de la décomposition. En particulier, elle permet d'obtenir analytiquement les relations entre les solutions possibles. Donc, des nouveaux schémas de commande de référence vision peuvent être conçus. Par exemple, les méthodes d'asservissement visuel proposées dans ce rapport combinent les deux solutions de la décomposition (une seule des deux est la vraie solution) en supposant qu'il n'est pas possible de distinguer a priori quelle est la bonne solution.

**Mots-clés :** Asservissement visuel, objets plans, homographie, décomposition, erreurs de calibration de la caméra, reconstruction Euclidienne

## Contents

<b>1</b>	<b>Introduction</b>	<b>5</b>
<b>2</b>	<b>Theoretical background</b>	<b>5</b>
2.1	Perspective projection . . . . .	5
2.2	The homography matrix . . . . .	7
<b>3</b>	<b>The numerical method for homography decomposition</b>	<b>8</b>
3.1	Faugeras SVD-based decomposition . . . . .	8
3.2	Zhang SVD-based decomposition . . . . .	9
3.3	Elimination of impossible solutions . . . . .	10
3.3.1	Reference-plane non-crossing constraint . . . . .	10
3.3.2	Reference-point visibility . . . . .	12
<b>4</b>	<b>A new analytical method for homography decomposition</b>	<b>13</b>
4.1	Summary of the analytical decomposition . . . . .	14
4.2	Detailed development of the analytical decomposition . . . . .	19
4.2.1	First method . . . . .	19
4.2.2	Second method . . . . .	33
<b>5</b>	<b>Relations among the possible solutions</b>	<b>37</b>
5.1	Summary of the relations among the possible solutions . . . . .	37
5.2	Preliminary relations . . . . .	39
5.3	Relations for the rotation matrices . . . . .	41
5.3.1	Relations for the rotation axes and angles . . . . .	42
5.4	Relations for translation and normal vectors . . . . .	46
<b>6</b>	<b>Position-based visual servoing based on analytical decomposition</b>	<b>48</b>
6.1	Introduction . . . . .	48
6.2	Vision-based control . . . . .	48
6.2.1	Homography-based state observer with full information . . . . .	50
6.3	A modified control objective . . . . .	50
6.3.1	Mean-based control law . . . . .	51
6.3.2	Parametrization of the mean of two rotations . . . . .	52
6.4	Stability analysis . . . . .	59
6.4.1	Stability of the translation error $\mathbf{e}_t$ . . . . .	59
6.4.2	Stability in the orientation error $\mathbf{e}_r$ . . . . .	62
6.4.3	Conclusions on the stability of the mean-based control . . . . .	63
6.4.4	Practical considerations bounding global stability . . . . .	64
6.5	Switching control law . . . . .	66
6.5.1	Alternatives for the detection of the false solution . . . . .	67
6.6	Simulation results . . . . .	68

6.6.1	Control using the true solution . . . . .	68
6.6.2	Mean-based control . . . . .	70
6.6.3	Switching control . . . . .	70
<b>7</b>	<b>Hybrid visual servoing based on analytical decomposition</b>	<b>72</b>
<b>8</b>	<b>Conclusions</b>	<b>74</b>
	<b>Acknowledgments</b>	<b>74</b>
<b>A</b>	<b>Useful relations for the homography decomposition</b>	<b>75</b>
<b>B</b>	<b>On the normalization of the homography matrix</b>	<b>76</b>
<b>C</b>	<b>Proofs of several properties</b>	<b>77</b>
C.1	Proof of properties on minors of matrix $\mathbf{S}$ . . . . .	77
C.2	Geometrical aspects related to minors of matrix $\mathbf{S}$ . . . . .	78
C.3	Components of vectors $\mathbf{x}$ and $\mathbf{y}$ are always real . . . . .	79
C.4	Proof of the equivalence of different expressions for $\nu$ . . . . .	81
C.5	Proof of condition $\rho > 1$ . . . . .	81
<b>D</b>	<b>Stability proofs</b>	<b>82</b>
D.1	Positivity of matrix $\mathbf{S}_{11}$ . . . . .	82
D.1.1	When is $\mathbf{S}_{11}$ singular ? . . . . .	86
D.2	Positivity of matrix $\mathbf{S}_{11-}$ . . . . .	87
D.2.1	When is $\mathbf{S}_{11-}$ singular ? . . . . .	89
	<b>References</b>	<b>89</b>

## 1 Introduction

Several methods for vision-based robot control need an estimation of the camera displacement (i.e. rotation and translation) between two views of an object [3, 4, 6, 5]. When the object is a plane, the camera displacement can be extracted (assuming that the intrinsic camera parameters are known) from the homography matrix that can be measured from two views. This process is called homography decomposition. The standard algorithms for homography decomposition obtain numerical solutions using the singular value decomposition of the matrix [1, 11]. It is shown that in the general case there are two possible solutions to the homography decomposition. This numerical decomposition has been sufficient for many computer and robot vision applications. However, when dealing with robot control applications, an analytical procedure to solve the decomposition problem would be preferable (i.e. analytical expressions for the computation of the camera displacement directly in terms of the components of the homography matrix). Indeed, the analytical decomposition allows us the analytical study of the variations of the estimated camera pose in the presence of camera calibration errors. Thus, we can obtain insights on the robustness of vision-based control laws.

The aim of this document is to propose a new method for solving the homography decomposition problem. This new method provides analytical expressions for the solutions of the problem, instead of the traditional numerical procedures. The main advantage of this method is that it will provide a deeper understanding on the homography decomposition problem. For instance, it allows to obtain the relations among the possible solutions of the problem. Thus, new vision-based robot control laws can be designed. For example the control schemes proposed in this report combine the two final solutions of the problem (only one of them being the true one) assuming that there is no a priori knowledge for discerning among them.

The document is organized as follows. Section 2 provides the theoretical background and introduce the notation that will be used in the report. In Section 3, we briefly remind the standard numerical method for homography decomposition. In Section 4, we describe the proposed analytical decomposition method. In Section 5, we find the relation between the two solutions of the decomposition. In Section 6 we propose a new position-based visual servoing scheme. Next, in Section 7 we propose a new hybrid visual servoing scheme. Finally, Section 8 gives the main conclusions of the report.

## 2 Theoretical background

### 2.1 Perspective projection

We consider two different camera frames: the current and desired camera frames,  $\mathcal{F}$  and  $\mathcal{F}^*$  in the figure, respectively. We assume that the absolute frame coincides with the reference camera frame  $\mathcal{F}^*$ . We suppose that the camera observes a planar object, consisting of a set



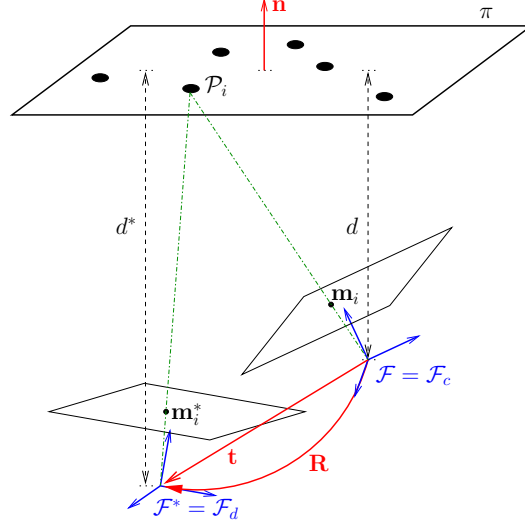


Figure 1: Desired and current camera frames and involved notation.

of  $n$  3D feature points,  $\mathcal{P}$ , with Cartesian coordinates:

$$\mathcal{P} = (X, Y, Z)$$

These points can be referred either to the desired camera frame or to the current one, being denoted as  ${}^d\mathcal{P}$  and  ${}^c\mathcal{P}$ , respectively. The homogeneous transformation matrix, converting 3D point coordinates from the desired frame to the current frame is:

$${}^c\mathbf{T}_d = \begin{bmatrix} {}^c\mathbf{R}_d & {}^c\mathbf{t}_d \\ \mathbf{0} & 1 \end{bmatrix}$$

where  ${}^c\mathbf{R}_d$  and  ${}^c\mathbf{t}_d$  are the rotation matrix and translation vector, respectively.

In the figure, the distances from the object plane to the corresponding camera frame are denoted as  $d^*$  and  $d$ . The normal  $\mathbf{n}$  to the plane can be also referred to the reference or current frames ( ${}^d\mathbf{n}$  or  ${}^c\mathbf{n}$ , respectively). The camera grabs an image of the mentioned object from both, the desired and the current configurations. This image acquisition implies the projection of the 3D points on a plane so they have the same depth from the corresponding camera origin. The normalized projective coordinates of each point will be referred as:

$$\mathbf{m}^* = (x^*, y^*, 1) = {}^d\mathbf{m}; \quad \mathbf{m} = (x, y, 1) = {}^c\mathbf{m}$$

for the desired and current camera frames. Finally, we obtain the homogeneous image coordinates  $\mathbf{p} = (u, v, 1)$ , in pixels, of each point using the following transformation:

$$\mathbf{p} = \mathbf{K} \mathbf{m}$$

where  $\mathbf{K}$  is the upper triangular matrix containing the camera intrinsic parameters.

All along the document, we will make use of an abbreviated notation:

$$\begin{cases} \mathbf{R} &= & {}^c\mathbf{R}_d \\ \mathbf{t} &= & {}^c\mathbf{t}_d/d^* \\ \mathbf{n} &= & {}^d\mathbf{n} \end{cases}$$

Where we see that the translation vector  $\mathbf{t}$  is normalized respect to the plane depth  $d^*$ . Also we can notice that  $\mathbf{t}$  and  $\mathbf{n}$  are not referred to the same frame.

## 2.2 The homography matrix

Let  $\mathbf{p}^* = (u^*, v^*, 1)$  be the  $(3 \times 1)$  vector containing the homogeneous coordinates of a point in the reference image and let  $\mathbf{p} = (u, v, 1)$  be the vector containing the homogeneous coordinates of a point in the current image. The projective homography matrix  $\mathbf{G}$  transforms one vector into the other, up to a scale factor:

$$\alpha_g \mathbf{p} = \mathbf{G} \mathbf{p}^*$$

The projective homography matrix can be measured from the image information by matching several coplanar points. At least 4 points are needed (at least three of them must be non-collinear). This matrix is related to the transformation elements  $\mathbf{R}$  and  $\mathbf{t}$  and to the normal of the plane  $\mathbf{n}$  according to:

$$\mathbf{G} = \gamma \mathbf{K} (\mathbf{R} + \mathbf{t} \mathbf{n}^\top) \mathbf{K}^{-1} \quad (1)$$

where the matrix  $\mathbf{K}$  is the camera calibration matrix. The homography in the Euclidean space can be computed from the projective homography matrix, using an estimated camera calibration matrix  $\hat{\mathbf{K}}$ :

$$\hat{\mathbf{H}} = \hat{\mathbf{K}}^{-1} \mathbf{G} \hat{\mathbf{K}} \quad (2)$$

In this report, we suppose that we have no uncertainty in the intrinsic camera parameters. Then, we assume that  $\hat{\mathbf{K}} = \mathbf{K}$ , so that  $\hat{\mathbf{H}} = \gamma (\mathbf{R} + \mathbf{t} \mathbf{n}^\top)$ . In a future work, we will try to study the influence of camera-calibration errors on the Euclidean reconstruction, taking advantage of the analytical decomposition method presented here. The equivalent to the homography matrix  $\mathbf{G}$  in the Euclidean space is the *Euclidean homography matrix*  $\mathbf{H}$ . It transforms one 3D point in projective coordinates from one frame to the other, again up to a scale factor:

$$\alpha_h \mathbf{m} = \mathbf{H} \mathbf{m}^*$$

where  $\mathbf{m}^* = (x^*, y^*, 1)$  is the vector containing the normalized projective coordinates of a point viewed from the reference camera pose, and  $\mathbf{m} = (x, y, 1)$  is the vector containing these normalized projective coordinates when the point is viewed from the current camera pose. This homography matrix is:

$$\mathbf{H} = \frac{\hat{\mathbf{H}}}{\gamma} = \mathbf{R} + \mathbf{t} \mathbf{n}^\top \quad (3)$$

Notice that  $\text{med}(\text{svd}(\mathbf{H})) = 1$ . Thus, after obtaining  $\widehat{\mathbf{H}}$ , the scale factor  $\gamma$  can be computed as follows:

$$\gamma = \text{med}(\text{svd}(\widehat{\mathbf{H}}))$$

by solving a third order equation (see Appendix B).

The problem of Euclidean homography decomposition, also called *Euclidean reconstruction from homography*, is that of retrieving the elements  $\mathbf{R}$ ,  $\mathbf{t}$  and  $\mathbf{n}$  from matrix  $\mathbf{H}$ :

$$\mathbf{H} \implies \{\mathbf{R}, \mathbf{t}, \mathbf{n}\}$$

Notice that the translation is estimated up to a positive scalar factor (as  $\mathbf{t}$  has been normalized with respect to  $d^*$ ).

### 3 The numerical method for homography decomposition

Before presenting the analytical decomposition method itself, it is convenient to concisely remind the traditional methods based on SVD [1, 11].

#### 3.1 Faugeras SVD-based decomposition

If we perform the singular value decomposition of the homography matrix [1]:

$$\mathbf{H} = \mathbf{U} \mathbf{\Lambda} \mathbf{V}^\top$$

we get the orthogonal matrices  $\mathbf{U}$  and  $\mathbf{V}$  and a diagonal matrix  $\mathbf{\Lambda}$ , which contains the singular values of matrix  $\mathbf{H}$ . We can consider this diagonal matrix as an homography matrix as well, and hence apply relation (3) to it:

$$\mathbf{\Lambda} = \mathbf{R}_\Lambda + \mathbf{t}_\Lambda \mathbf{n}_\Lambda^\top \tag{4}$$

Computing the components of the rotation matrix, translation and normal vectors is simple when the matrix being decomposed is a diagonal one. First,  $\mathbf{t}_\Lambda$  can be easily eliminated from the three vector equations coming out from (4) (one for each column of this matrix equation). Then, imposing that  $\mathbf{R}_\Lambda$  is an orthogonal matrix, we can linearly solve for the components of  $\mathbf{n}_\Lambda$ , from a new set of equations relating only these components with the three singular values (see [1] for the detailed development). As a result of the decomposition algorithm, we can get up to 8 different solutions for the triplets:  $\{\mathbf{R}_\Lambda, \mathbf{t}_\Lambda, \mathbf{n}_\Lambda\}$ . Then, assuming that the decomposition of matrix  $\mathbf{\Lambda}$  is done, in order to compute the final decomposition elements, we just need to use the following expressions:

$$\begin{aligned} \mathbf{R} &= \mathbf{U} \mathbf{R}_\Lambda \mathbf{V}^\top \\ \mathbf{t} &= \mathbf{U} \mathbf{t}_\Lambda \\ \mathbf{n} &= \mathbf{V} \mathbf{n}_\Lambda \end{aligned}$$

It is clear that this algorithm does not allow us to obtain an analytical expression of the decomposition elements  $\{\mathbf{R}, \mathbf{t}, \mathbf{n}\}$ , in terms of the components of matrix  $\mathbf{H}$ . This is the aim of this report: to develop a method that gives us such analytical expressions. As already said, there are up to 8 solutions in general for this problem. These are 8 mathematical solutions, but not all of them are physically possible, as we will see. Several constraints can be applied in order to reduce this number of solutions.

### 3.2 Zhang SVD-based decomposition

Notice that a similar method to obtain this decomposition is proposed in [11]. The authors claim that closed-form expressions for the translation vector, normal vector and rotation matrix are obtained. However, the closed-form solutions are obtained numerically, again from SVD decomposition of the homography matrix.

They propose to compute the eigenvalues and eigenvectors of matrix  $\mathbf{H}^\top \mathbf{H}$ :

$$\mathbf{H}^\top \mathbf{H} = \mathbf{V} \mathbf{\Lambda}^2 \mathbf{V}^\top$$

Where the eigenvalues and corresponding eigenvectors are:

$$\mathbf{\Lambda} = \text{diag}(\lambda_1, \lambda_2, \lambda_3); \quad \mathbf{V} = [\mathbf{v}_1 \ \mathbf{v}_2 \ \mathbf{v}_3]$$

with the unitary eigenvalue  $\lambda_2$  and ordered as:

$$\lambda_1 \geq \lambda_2 = 1 \geq \lambda_3$$

Then, defining  $\mathbf{t}^*$  as the normalized translation vector in the desired camera frame,  $\mathbf{t}^* = \mathbf{R}^\top \mathbf{t}$ , they propose to use the following relations:

$$\|\mathbf{t}^*\| = \lambda_1 - \lambda_3; \quad \mathbf{n}^\top \mathbf{t}^* = \lambda_1 \lambda_3 - 1$$

and

$$\begin{aligned} \mathbf{v}_1 &\propto \mathbf{v}'_1 = \zeta_1 \mathbf{t}^* + \mathbf{n} \\ \mathbf{v}_2 &\propto \mathbf{v}'_2 = \mathbf{t}^* \times \mathbf{n} \\ \mathbf{v}_3 &\propto \mathbf{v}'_3 = \zeta_3 \mathbf{t}^* + \mathbf{n} \end{aligned}$$

where  $\mathbf{v}_i$  are unitary vectors, while  $\mathbf{v}'_i$  are not, and  $\zeta_{1,3}$  are scalar functions of the eigenvalues given below.

These relations are derived from the fact that  $(\mathbf{t}^* \times \mathbf{n})$  is an eigenvector associated to the unitary eigenvalue of matrix  $\mathbf{H}^\top \mathbf{H}$  and that all the eigenvectors must be orthogonal.

Then, the authors propose to use the following expressions to compute the first solution for the couple translation vector and normal vector:

$$\mathbf{t}^* = \pm \frac{\mathbf{v}'_1 - \mathbf{v}'_3}{\zeta_1 - \zeta_3} \quad \mathbf{n} = \pm \frac{\zeta_1 \mathbf{v}'_3 - \zeta_3 \mathbf{v}'_1}{\zeta_1 - \zeta_3}$$

and for the second solution:

$$\mathbf{t}^* = \pm \frac{\mathbf{v}'_1 + \mathbf{v}'_3}{\zeta_1 - \zeta_3} \quad \mathbf{n} = \pm \frac{\zeta_1 \mathbf{v}'_3 + \zeta_3 \mathbf{v}'_1}{\zeta_1 - \zeta_3}$$

In order to use these relations, after SVD,  $\zeta_{1,3}$  must be computed as:

$$\zeta_{1,3} = \frac{1}{2 \lambda_1 \lambda_3} \left( -1 \pm \sqrt{1 + 4 \frac{\lambda_1 \lambda_3}{(\lambda_1 - \lambda_3)^2}} \right)$$

Also, the norms of  $\mathbf{v}'_{1,3}$  can be computed from the eigenvalues:

$$\|\mathbf{v}'_i\|^2 = \zeta_i^2 (\lambda_1 - \lambda_3)^2 + 2 \zeta_i (\lambda_1 \lambda_3 - 1) + 1 \quad i = 1, 3$$

Then,  $\mathbf{v}'_{1,3}$  are obtained from the unitary eigenvectors using:

$$\mathbf{v}'_i = \|\mathbf{v}'_i\| \mathbf{v}_i \quad i = 1, 3$$

Finally, the rotation matrix can be obtained:

$$\mathbf{R} = \mathbf{H} (\mathbf{I} + \mathbf{t}^* \mathbf{n}^\top)^{-1}$$

As we see, this is not an analytical decomposition procedure, since we don't obtain  $\{\mathbf{R}, \mathbf{t}, \mathbf{n}\}$  as explicit function of  $\mathbf{H}$ . On the contrary, the computations fully rely on the singular value decomposition as in Faugeras' method.

Moreover, in order to compute the rotation matrix, the right couples should be chosen, but there is a +/- ambiguity. This means that, a priori, there is no way to know if the right couple for the choice of the plus sign in the expression of  $\mathbf{t}^*$  is the vector obtained using the plus or the minus sign in the expression of  $\mathbf{n}$ . With the proposed analytical procedure that ambiguity can be a priori solved.

### 3.3 Elimination of impossible solutions

We describe now how the set of solutions of the homography decomposition problem can be reduced from the 8 mathematical solutions to the only 2 verifying some physical constraints. Of course, this is valid not only for the numerical decomposition method, but in general, whatever the method used.

#### 3.3.1 Reference-plane non-crossing constraint

This is the first physical constraint that allows to reduce the number of solutions from 8 to 4. This constraint imposes that:

*Both frames,  $\mathcal{F}^*$  and  $\mathcal{F}$  must be in the same side of the object plane.*

This means that the camera cannot go in the direction of the plane normal further than the distance to the plane. Otherwise, the camera crosses the plane and the situation can be interpreted as the camera seeing a transparent object from both sides. In Figure 2, the translation vector from one frame to the other,  ${}^d\mathbf{t}_c$ , gives the position of the origin of  $\mathcal{F}$  with respect to  $\mathcal{F}^*$ . This is not the same as vector  $\mathbf{t}$  used in our reduced notation, but they are related by:

$$\mathbf{t} = -{}^c\mathbf{R}_d \frac{{}^d\mathbf{t}_c}{d^*}$$

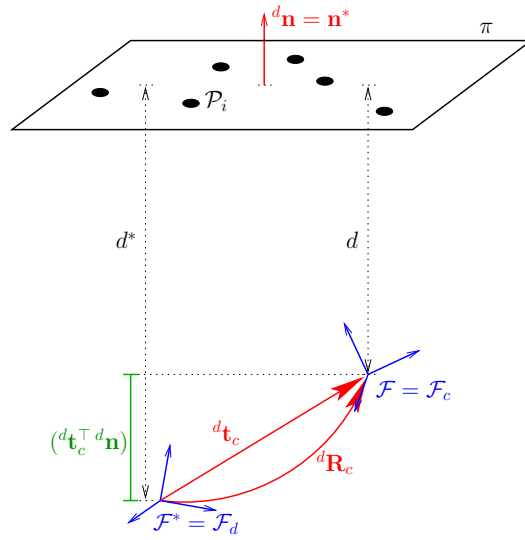


Figure 2: Reference-plane non-crossing constraint.

That way, the translation vector  ${}^d\mathbf{t}_c$ , the normal vector  $\mathbf{n} = {}^d\mathbf{n}$  and the distance to the plane  $d^*$  are referred to the same frame,  $\mathcal{F}^*$ . With this notation, it is clear that the reference-plane non-crossing constraint is satisfied when:

$${}^d\mathbf{t}_c^\top {}^d\mathbf{n} < d^* \quad (5)$$

That is, the projection of the translation vector  ${}^d\mathbf{t}_c$  on the normal direction, must be less than  $d^*$ . Written in terms of our reduced notation:

$$1 + \mathbf{n}^\top \mathbf{R}^\top \mathbf{t} > 0 \quad (6)$$

As we will see in Section 4, only 4 of the 8 solutions derived using the analytic method verify this condition. In fact, the set of four solutions verifying the reference-plane non-crossing

constraint are, in general, two completely different solutions and their "opposites":

$$\begin{aligned} Rtn_a &= \{\mathbf{R}_a, \mathbf{t}_a, \mathbf{n}_a\} \\ Rtn_b &= \{\mathbf{R}_b, \mathbf{t}_b, \mathbf{n}_b\} \\ Rtn_{a-} &= \{\mathbf{R}_a, -\mathbf{t}_a, -\mathbf{n}_a\} \\ Rtn_{b-} &= \{\mathbf{R}_b, -\mathbf{t}_b, -\mathbf{n}_b\} \end{aligned}$$

### 3.3.2 Reference-point visibility

This additional constraint allows to reduce from 4 to 2 the number of feasible solutions. The following additional information is required:

- The set of reference image points:  $\mathbf{p}^*$
- The matrix containing the camera intrinsic parameters:  $\mathbf{K}$

First, the projective coordinates of the reference points are retrieved:

$$\mathbf{m}^* = \mathbf{K}^{-1}\mathbf{p}^*$$

Then, each normal candidate is considered and the projection of each one of the points  $\mathbf{m}^*$  on the direction of that normal is computed. For the solution being valid, this projection must be positive for all the points:

$$\mathbf{m}^{*\top} \mathbf{n}^* > 0$$

The same can be done regarding to the current frame:

$$\mathbf{m}^\top (\mathbf{R} \mathbf{n}) > 0$$

The geometric interpretation of this constraint is that (see Figure 3):

*For all the reference points being visible, they must be in front of the camera.*

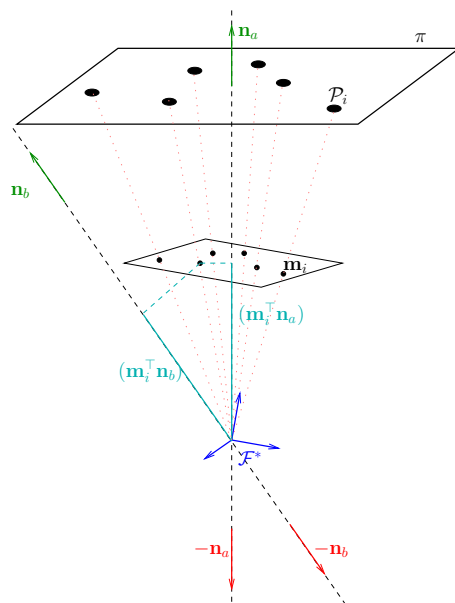


Figure 3: Reference points visibility constraint.

From the four solutions verifying the reference-plane non-crossing constraint, two of them have normals opposite to the other two's, then at least two of them can be discarded with the new constraint. It may occur that even three of them could be discarded, but it is not the usual situation.

## 4 A new analytical method for homography decomposition

In this section, we introduce a new analytical method for solving the homography decomposition problem. Contrarily to [1], where a numerical method based on SVD is used, we provide the expressions of  $\{\mathbf{R}, \mathbf{t}, \mathbf{n}\}$  as a function of matrix  $\mathbf{H}$ .

The four solutions we will achieve following the procedure will be denoted as:

$$Rtn_a = \{\mathbf{R}_a, \mathbf{t}_a, \mathbf{n}_a\} \quad (7)$$

$$Rtn_b = \{\mathbf{R}_b, \mathbf{t}_b, \mathbf{n}_b\} \quad (8)$$

$$Rtn_{a-} = \{\mathbf{R}_a, -\mathbf{t}_a, -\mathbf{n}_a\} \quad (9)$$

$$Rtn_{b-} = \{\mathbf{R}_b, -\mathbf{t}_b, -\mathbf{n}_b\} \quad (10)$$

as said before, these solutions are, in general, two completely different solutions and their opposites.



First, we will summarize the complete set of formulas and after that we will give the details of the development.

## 4.1 Summary of the analytical decomposition

### First method: computing the normal vector first

We can get closed forms of the analytical expressions by introducing a symmetric matrix,  $\mathbf{S}$ , obtained from the homography matrix as:

$$\mathbf{S} = \mathbf{H}^\top \mathbf{H} - \mathbf{I} = \begin{bmatrix} s_{11} & s_{12} & s_{13} \\ s_{12} & s_{22} & s_{23} \\ s_{13} & s_{23} & s_{33} \end{bmatrix}$$

We represent by  $M_{\mathbf{S}_{ij}}$ ,  $i, j = 1..3$ , the expressions of the opposites of minors (minor corresponding to element  $s_{ij}$ ) of matrix  $\mathbf{S}$ . For instance:

$$M_{\mathbf{S}_{11}} = - \begin{vmatrix} s_{22} & s_{23} \\ s_{23} & s_{33} \end{vmatrix} = s_{23}^2 - s_{22}s_{33} \geq 0$$

In general, there are three different alternatives for obtaining the expressions of the normal vectors  $\mathbf{n}_e$  (and from this,  $\mathbf{t}_e$  and  $\mathbf{R}_e$ ) of the homography decomposition from the components of matrix  $\mathbf{S}$ . We will write:

$$\mathbf{n}_e(s_{ii}) = \frac{\mathbf{n}'_e(s_{ii})}{\|\mathbf{n}'_e(s_{ii})\|}; \quad e = \{a, b\}, \quad i = \{1, 2, 3\}$$

Where  $\mathbf{n}_e(s_{ii})$  means for  $\mathbf{n}_e$  developed using  $s_{ii}$ . Then, the three possible cases are:

$$\mathbf{n}'_a(s_{11}) = \begin{bmatrix} s_{11} \\ s_{12} + \sqrt{M_{\mathbf{S}_{33}}} \\ s_{13} + \epsilon_{23} \sqrt{M_{\mathbf{S}_{22}}} \end{bmatrix}; \quad \mathbf{n}'_b(s_{11}) = \begin{bmatrix} s_{11} \\ s_{12} - \sqrt{M_{\mathbf{S}_{33}}} \\ s_{13} - \epsilon_{23} \sqrt{M_{\mathbf{S}_{22}}} \end{bmatrix} \quad (11)$$

$$\mathbf{n}'_a(s_{22}) = \begin{bmatrix} s_{12} + \sqrt{M_{\mathbf{S}_{33}}} \\ s_{22} \\ s_{23} - \epsilon_{13} \sqrt{M_{\mathbf{S}_{11}}} \end{bmatrix}; \quad \mathbf{n}'_b(s_{22}) = \begin{bmatrix} s_{12} - \sqrt{M_{\mathbf{S}_{33}}} \\ s_{22} \\ s_{23} + \epsilon_{13} \sqrt{M_{\mathbf{S}_{11}}} \end{bmatrix} \quad (12)$$

$$\mathbf{n}'_a(s_{33}) = \begin{bmatrix} s_{13} + \epsilon_{12} \sqrt{M_{\mathbf{S}_{22}}} \\ s_{23} + \sqrt{M_{\mathbf{S}_{11}}} \\ s_{33} \end{bmatrix}; \quad \mathbf{n}'_b(s_{33}) = \begin{bmatrix} s_{13} - \epsilon_{12} \sqrt{M_{\mathbf{S}_{22}}} \\ s_{23} - \sqrt{M_{\mathbf{S}_{11}}} \\ s_{33} \end{bmatrix} \quad (13)$$

where  $\epsilon_{ij} = \text{sign}(M_{\mathbf{S}_{ij}})$ . In particular, the  $\text{sign}(\cdot)$  function should be implemented like:

$$\text{sign}(a) = \begin{cases} 1 & \text{if } a \geq 0 \\ -1 & \text{otherwise} \end{cases}$$

in order to avoid problems in the cases when  $M_{\mathbf{S}_{ii}} = 0$ , as it will see later on.

These formulas give all the same result. However, not all of them can be applied in every case, as the computation of  $\mathbf{n}_e(s_{ii})$ , implies a division by  $s_{ii}$ . That means that this formula cannot be applied in the particular case when  $s_{ii} = 0$  (this happens for instance when the  $i$ -th component of  $\mathbf{n}$  is null).

The right procedure is to compute  $\mathbf{n}_a$  and  $\mathbf{n}_b$  using the alternative among the three given corresponding to the  $s_{ii}$  with largest absolute value. That will be the most well conditioned option. The only singular case, then, is the pure rotation case, when  $\mathbf{H}$  is a rotation matrix. In this case, all the components of matrix  $\mathbf{S}$  become null. Nevertheless, this is a trivial case, and there is no need to apply any formulas. It must be taken into account that the four solutions obtained by these formulas (that is  $\{\mathbf{n}_a, -\mathbf{n}_a, \mathbf{n}_b, -\mathbf{n}_b\}$ ) are all the same, but are not always given in the same order. That means that, for instance,  $\mathbf{n}_a(s_{22})$  may correspond to  $-\mathbf{n}_a(s_{11})$ ,  $\mathbf{n}_b(s_{11})$  or  $-\mathbf{n}_b(s_{11})$ , instead of corresponding to  $\mathbf{n}_a(s_{11})$ .

We can also write the expression of  $\mathbf{n}_e$  directly in terms of the columns of matrix  $\mathbf{H}$ :

$$\mathbf{H} = [ \mathbf{h}_1 \quad \mathbf{h}_2 \quad \mathbf{h}_3 ]$$

We give, as an example, the result derived from  $s_{22}$  (equivalent to (12)):

$$\mathbf{n}'_a(s_{22}) = \begin{bmatrix} \mathbf{h}_1^\top \mathbf{h}_2 + \sqrt{(\mathbf{h}_1^\top \mathbf{h}_2)^2 - (\|\mathbf{h}_1\|^2 - 1)(\|\mathbf{h}_2\|^2 - 1)} \\ (\|\mathbf{h}_2\|^2 - 1) \\ \mathbf{h}_2^\top \mathbf{h}_3 - \epsilon_{13} \sqrt{(\mathbf{h}_2^\top \mathbf{h}_3)^2 - (\|\mathbf{h}_2\|^2 - 1)(\|\mathbf{h}_3\|^2 - 1)} \end{bmatrix} \quad (14)$$

$$\mathbf{n}'_b(s_{22}) = \begin{bmatrix} \mathbf{h}_1^\top \mathbf{h}_2 - \sqrt{(\mathbf{h}_1^\top \mathbf{h}_2)^2 - (\|\mathbf{h}_1\|^2 - 1)(\|\mathbf{h}_2\|^2 - 1)} \\ (\|\mathbf{h}_2\|^2 - 1) \\ \mathbf{h}_2^\top \mathbf{h}_3 + \epsilon_{13} \sqrt{(\mathbf{h}_2^\top \mathbf{h}_3)^2 - (\|\mathbf{h}_2\|^2 - 1)(\|\mathbf{h}_3\|^2 - 1)} \end{bmatrix} \quad (15)$$

and where  $\epsilon_{ij} = \text{sign}(M_{\mathbf{S}_{ij}})$ , the expression of which is, in this particular case:

$$\epsilon_{13} = \text{sign}(-\mathbf{h}_1^\top [\mathbf{I} + [\mathbf{h}_2]_\times^2] \mathbf{h}_3)$$

The expressions for the translation vector in the reference frame,  $\mathbf{t}_e^* = \mathbf{R}_e^\top \mathbf{t}_e$ , can be obtained after the given expressions of the normal vector:

$$\begin{aligned} \mathbf{t}_e^*(s_{11}) &= \frac{\|\mathbf{n}'_e(s_{11})\|}{2 s_{11}} \begin{bmatrix} s_{11} \\ s_{12} \mp \sqrt{M_{\mathbf{S}_{33}}} \\ s_{13} \mp \epsilon_{23} \sqrt{M_{\mathbf{S}_{22}}} \end{bmatrix} - \frac{\|\mathbf{t}_e\|^2}{2 \|\mathbf{n}'_e(s_{11})\|} \begin{bmatrix} s_{11} \\ s_{12} \pm \sqrt{M_{\mathbf{S}_{33}}} \\ s_{13} \pm \epsilon_{23} \sqrt{M_{\mathbf{S}_{22}}} \end{bmatrix} \\ \mathbf{t}_e^*(s_{22}) &= \frac{\|\mathbf{n}'_e(s_{22})\|}{2 s_{22}} \begin{bmatrix} s_{12} \mp \sqrt{M_{\mathbf{S}_{33}}} \\ s_{22} \\ s_{23} \pm \epsilon_{13} \sqrt{M_{\mathbf{S}_{11}}} \end{bmatrix} - \frac{\|\mathbf{t}_e\|^2}{2 \|\mathbf{n}'_e(s_{22})\|} \begin{bmatrix} s_{12} \pm \sqrt{M_{\mathbf{S}_{33}}} \\ s_{22} \\ s_{23} \mp \epsilon_{13} \sqrt{M_{\mathbf{S}_{11}}} \end{bmatrix} \\ \mathbf{t}_e^*(s_{33}) &= \frac{\|\mathbf{n}'_e(s_{33})\|}{2 s_{33}} \begin{bmatrix} s_{13} \mp \epsilon_{12} \sqrt{M_{\mathbf{S}_{22}}} \\ s_{23} \mp \sqrt{M_{\mathbf{S}_{11}}} \\ s_{33} \end{bmatrix} - \frac{\|\mathbf{t}_e\|^2}{2 \|\mathbf{n}'_e(s_{33})\|} \begin{bmatrix} s_{13} \pm \epsilon_{12} \sqrt{M_{\mathbf{S}_{22}}} \\ s_{23} \pm \sqrt{M_{\mathbf{S}_{11}}} \\ s_{33} \end{bmatrix} \end{aligned}$$

For  $e = a$  the upper operator in the symbols  $\pm, \mp$  must be chosen, for  $e = b$  choose the lower operator. The vector  $\mathbf{t}_e^*$  can also be given as a compact expression of  $\mathbf{n}_a$  and  $\mathbf{n}_b$ :

$$\mathbf{t}_a^*(s_{ii}) = \frac{\|\mathbf{t}_e\|}{2} [\epsilon_{s_{ii}} \rho \mathbf{n}_b(s_{ii}) - \|\mathbf{t}_e\| \mathbf{n}_a(s_{ii})] \quad (16)$$

$$\mathbf{t}_b^*(s_{ii}) = \frac{\|\mathbf{t}_e\|}{2} [\epsilon_{s_{ii}} \rho \mathbf{n}_a(s_{ii}) - \|\mathbf{t}_e\| \mathbf{n}_b(s_{ii})] \quad (17)$$

being

$$\epsilon_{s_{ii}} = \text{sign}(s_{ii})$$

$$\rho^2 = 2 + \text{trace}(\mathbf{S}) + \nu \quad (18)$$

$$\|\mathbf{t}_e\|^2 = 2 + \text{trace}(\mathbf{S}) - \nu \quad (19)$$

Where  $\nu$  can be obtained from:

$$\begin{aligned} \nu &= \sqrt{2 [(1 + \text{trace}(\mathbf{S}))^2 + 1 - \text{trace}(\mathbf{S}^2)]} \\ &= 2 \sqrt{1 + \text{trace}(\mathbf{S}) - M_{\mathbf{S}_{11}} - M_{\mathbf{S}_{22}} - M_{\mathbf{S}_{33}}} \end{aligned}$$

The expression for the rotation matrix is:

$$\mathbf{R}_e = \mathbf{H} \left( \mathbf{I} - \frac{2}{\nu} \mathbf{t}_e^* \mathbf{n}_e^\top \right) \quad (20)$$

Finally,  $\mathbf{t}_e$  can be obtained:

$$\mathbf{t}_e = \mathbf{R}_e \mathbf{t}_e^* \quad (21)$$

**Second method: computing the translation vector first**

A simpler set of expressions for  $\mathbf{t}_e$  can be obtained, starting from the following matrix,  $\mathbf{S}_r$ , instead of the previous  $\mathbf{S}$ :

$$\mathbf{S}_r = \mathbf{H}\mathbf{H}^\top - \mathbf{I} = \begin{bmatrix} s_{r11} & s_{r12} & s_{r13} \\ s_{r12} & s_{r22} & s_{r23} \\ s_{r13} & s_{r23} & s_{r33} \end{bmatrix}$$

The new relations for vector  $\mathbf{t}_e$  are:

$$\mathbf{t}_e(s_{r_{ii}}) = \|\mathbf{t}_e\| \frac{\mathbf{t}'_e(s_{r_{ii}})}{\|\mathbf{t}'_e(s_{r_{ii}})\|}; \quad e = \{a, b\}$$

Where  $\mathbf{t}_e(s_{r_{ii}})$  means for  $\mathbf{t}_e$  developed using  $s_{r_{ii}}$ . Then, the three possible cases are:

$$\mathbf{t}'_a(s_{r_{11}}) = \begin{bmatrix} s_{r11} \\ s_{r12} + \sqrt{M\mathbf{S}_{r33}} \\ s_{r13} + \epsilon_{r23}\sqrt{M\mathbf{S}_{r22}} \end{bmatrix}; \quad \mathbf{t}'_b(s_{r_{11}}) = \begin{bmatrix} s_{r11} \\ s_{r12} - \sqrt{M\mathbf{S}_{r33}} \\ s_{r13} - \epsilon_{r23}\sqrt{M\mathbf{S}_{r22}} \end{bmatrix} \quad (22)$$

$$\mathbf{t}'_a(s_{r_{22}}) = \begin{bmatrix} s_{r12} + \sqrt{M\mathbf{S}_{r33}} \\ s_{r22} \\ s_{r23} - \epsilon_{r13}\sqrt{M\mathbf{S}_{r11}} \end{bmatrix}; \quad \mathbf{t}'_b(s_{r_{22}}) = \begin{bmatrix} s_{r12} - \sqrt{M\mathbf{S}_{r33}} \\ s_{r22} \\ s_{r23} + \epsilon_{r13}\sqrt{M\mathbf{S}_{r11}} \end{bmatrix} \quad (23)$$

$$\mathbf{t}'_a(s_{r_{33}}) = \begin{bmatrix} s_{r13} + \epsilon_{r12}\sqrt{M\mathbf{S}_{r22}} \\ s_{r23} + \sqrt{M\mathbf{S}_{r11}} \\ s_{r33} \end{bmatrix}; \quad \mathbf{t}'_b(s_{r_{33}}) = \begin{bmatrix} s_{r13} - \epsilon_{r12}\sqrt{M\mathbf{S}_{r22}} \\ s_{r23} - \sqrt{M\mathbf{S}_{r11}} \\ s_{r33} \end{bmatrix} \quad (24)$$

where  $M\mathbf{S}_{r_{ii}}$  and  $\epsilon_{r_{ij}}$  have the same meaning as before, but referred to matrix  $\mathbf{S}_r$  instead of  $\mathbf{S}$ . Notice that the expression for  $\|\mathbf{t}_e\|$  is given in (19). In this case,  $s_{r_{ii}}$  becomes zero, for instance, when the  $i$ -th component of  $\mathbf{t}$  is null.

We can also write the expression of  $\mathbf{t}_e$  directly in terms of the rows of matrix  $\mathbf{H}$ :

$$\mathbf{H}^\top = [\mathbf{h}_{r1} \quad \mathbf{h}_{r2} \quad \mathbf{h}_{r3}]$$

We give, as an example, the result derived from  $s_{r22}$ :

$$\mathbf{t}'_a(s_{r22}) = \begin{bmatrix} \mathbf{h}_{r1}^\top \mathbf{h}_{r2} + \sqrt{(\mathbf{h}_{r1}^\top \mathbf{h}_{r2})^2 - (\|\mathbf{h}_{r1}\|^2 - 1)(\|\mathbf{h}_{r2}\|^2 - 1)} \\ (\|\mathbf{h}_{r2}\|^2 - 1) \\ \mathbf{h}_{r2}^\top \mathbf{h}_{r3} - \epsilon_{r13} \sqrt{(\mathbf{h}_{r2}^\top \mathbf{h}_{r3})^2 - (\|\mathbf{h}_{r2}\|^2 - 1)(\|\mathbf{h}_{r3}\|^2 - 1)} \end{bmatrix} \quad (25)$$

$$\mathbf{t}'_b(s_{r22}) = \begin{bmatrix} \mathbf{h}_{r1}^\top \mathbf{h}_{r2} - \sqrt{(\mathbf{h}_{r1}^\top \mathbf{h}_{r2})^2 - (\|\mathbf{h}_{r1}\|^2 - 1)(\|\mathbf{h}_{r2}\|^2 - 1)} \\ (\|\mathbf{h}_{r2}\|^2 - 1) \\ \mathbf{h}_{r2}^\top \mathbf{h}_{r3} + \epsilon_{r13} \sqrt{(\mathbf{h}_{r2}^\top \mathbf{h}_{r3})^2 - (\|\mathbf{h}_{r2}\|^2 - 1)(\|\mathbf{h}_{r3}\|^2 - 1)} \end{bmatrix} \quad (26)$$

being  $\epsilon_{r_{ij}} = \text{sign}(M_{\mathbf{S}_{r_{ij}}})$ , that can be written in this case as:

$$\epsilon_{r13} = \text{sign}(-\mathbf{h}_{r1}^\top [\mathbf{I} + [\mathbf{h}_{r2}]_{\times}^2] \mathbf{h}_{r3})$$

In the same way we obtained before the expressions for  $\mathbf{t}_e^* = \mathbf{R}_e^\top \mathbf{t}_e$  from the expressions of  $\mathbf{n}_e$ , we can obtain now the expressions for  $\mathbf{n}'_e = \mathbf{R}_e \mathbf{n}_e$ , from the given expressions of  $\mathbf{t}_e$ :

$$\mathbf{n}'_a(s_{r_{ii}}) = \frac{1}{2} \left[ \epsilon_{s_{r_{ii}}} \frac{\rho}{\|\mathbf{t}_e\|} \mathbf{t}_b(s_{r_{ii}}) - \mathbf{t}_a(s_{r_{ii}}) \right] \quad (27)$$

$$\mathbf{n}'_b(s_{r_{ii}}) = \frac{1}{2} \left[ \epsilon_{s_{r_{ii}}} \frac{\rho}{\|\mathbf{t}_e\|} \mathbf{t}_a(s_{r_{ii}}) - \mathbf{t}_b(s_{r_{ii}}) \right] \quad (28)$$

being

$$\epsilon_{s_{r_{ii}}} = \text{sign}(s_{r_{ii}})$$

The expression for the rotation matrix, analogous to (20), is:

$$\mathbf{R}_e = \left( \mathbf{I} - \frac{2}{\nu} \mathbf{t}_e \mathbf{n}_e'^\top \right) \mathbf{H}$$

Finally,  $\mathbf{n}_e$  can be obtained:

$$\mathbf{n}_e = \mathbf{R}_e^\top \mathbf{n}'_e$$

Of course, if we have directly the couple  $\mathbf{n}_e$  and  $\mathbf{t}_e$  corresponding to the same solution, we can get the rotation matrix as:

$$\mathbf{R}_e = \mathbf{H} - \mathbf{t}_e \mathbf{n}_e^\top$$

It must be noticed that if we combine the expressions for  $\mathbf{n}_e$  and  $\mathbf{t}_e$  (14)-(15) with (25)-(26) (or equivalently (11)-(13) with (22)-(24)), in order to set up the set of solutions, instead of deriving one from the other, we must be aware that, as expected,  $\mathbf{n}_a(s_{ii})$  not necessary will couple with  $\mathbf{t}_a(s_{r_{ii}})$ .

As it can be seen, contrarily to the numerical methods, in this case, we have the analytical expressions of the decomposition elements  $\{\mathbf{R}, \mathbf{t}, \mathbf{n}\}$ , in terms of the components of matrix  $\mathbf{H}$ .

## 4.2 Detailed development of the analytical decomposition

In this section, we present the detailed development that give rise to the set of analytical expressions summarized before. We will describe two alternative methods for the analytical decomposition. Using the first one, we will derive the set of formulas that allow us to compute the normal vector first, and after it, the translation vector and the rotation matrix. On the contrary, the second method allows to compute the translation vector first, and after it, the normal vector and the rotation matrix.

### 4.2.1 First method

In order to simplify the computations, we start defining the symmetric matrix,  $\mathbf{S}$ , obtained from the homography matrix as follows:

$$\mathbf{S} = \mathbf{H}^\top \mathbf{H} - \mathbf{I} = \begin{bmatrix} s_{11} & s_{12} & s_{13} \\ s_{12} & s_{22} & s_{23} \\ s_{13} & s_{23} & s_{33} \end{bmatrix} \quad (29)$$

The matrix  $\mathbf{S}$  is a singular matrix. That is:

$$\det(\mathbf{S}) = s_{11}s_{22}s_{33} - s_{11}s_{23}^2 - s_{22}s_{13}^2 - s_{33}s_{12}^2 + 2s_{12}s_{13}s_{23} = 0 \quad (30)$$

This means that we could write, for instance, element  $s_{33}$  as:

$$s_{33} = \frac{s_{11}s_{23}^2 + s_{22}s_{13}^2 - 2s_{12}s_{13}s_{23}}{s_{11}s_{22} - s_{12}^2} \quad (31)$$

We will denote the opposites of the two-dimension minors of this matrix as  $M_{\mathbf{S}_{ij}}$  (minor corresponding to element  $s_{ij}$ ). The opposites of the principal minors are:

$$M_{\mathbf{S}_{11}} = - \begin{vmatrix} s_{22} & s_{23} \\ s_{23} & s_{33} \end{vmatrix} = s_{23}^2 - s_{22}s_{33} \geq 0$$

$$M_{\mathbf{S}_{22}} = - \begin{vmatrix} s_{11} & s_{13} \\ s_{13} & s_{33} \end{vmatrix} = s_{13}^2 - s_{11}s_{33} \geq 0$$

$$M_{\mathbf{S}_{33}} = - \begin{vmatrix} s_{11} & s_{12} \\ s_{12} & s_{22} \end{vmatrix} = s_{12}^2 - s_{11}s_{22} \geq 0$$

all of them being non-negative (this property, that will be helpful afterwards, is proved in Appendix C.1). On the other hand, the opposites of the non-principal minors are:

$$M_{\mathbf{S}_{12}} = M_{\mathbf{S}_{21}} = - \begin{vmatrix} s_{12} & s_{13} \\ s_{23} & s_{33} \end{vmatrix} = s_{23}s_{13} - s_{12}s_{33}$$

$$M_{\mathbf{S}_{13}} = M_{\mathbf{S}_{31}} = - \begin{vmatrix} s_{12} & s_{13} \\ s_{22} & s_{23} \end{vmatrix} = s_{22}s_{13} - s_{12}s_{23}$$

$$M_{\mathbf{S}_{23}} = M_{\mathbf{S}_{32}} = - \begin{vmatrix} s_{11} & s_{13} \\ s_{12} & s_{23} \end{vmatrix} = s_{12}s_{13} - s_{11}s_{23}$$

There are some interesting geometrical aspects related to these minors, which are described in Appendix C.2. It can also be verified that the following relations between the principal and non-principal minors hold:

$$M_{\mathbf{S}_{12}}^2 = M_{\mathbf{S}_{11}} M_{\mathbf{S}_{22}} \quad (32)$$

$$M_{\mathbf{S}_{13}}^2 = M_{\mathbf{S}_{11}} M_{\mathbf{S}_{33}} \quad (33)$$

$$M_{\mathbf{S}_{23}}^2 = M_{\mathbf{S}_{22}} M_{\mathbf{S}_{33}} \quad (34)$$

This can be easily proved using the property of null determinant of  $\mathbf{S}$  and writing some diagonal element as done with  $s_{33}$  in (31) (alternatively, see Appendix C.1). These relations can be also written in another way:

$$M_{\mathbf{S}_{12}} = \epsilon_{12} \sqrt{M_{\mathbf{S}_{11}}} \sqrt{M_{\mathbf{S}_{22}}} \quad (35)$$

$$M_{\mathbf{S}_{13}} = \epsilon_{13} \sqrt{M_{\mathbf{S}_{11}}} \sqrt{M_{\mathbf{S}_{33}}} \quad (36)$$

$$M_{\mathbf{S}_{23}} = \epsilon_{23} \sqrt{M_{\mathbf{S}_{22}}} \sqrt{M_{\mathbf{S}_{33}}} \quad (37)$$

where

$$\epsilon_{ij} = \text{sign}(M_{\mathbf{S}_{ij}})$$

Condition (30) could also have been written using these determinants:

$$\det(\mathbf{S}) = -s_{11} M_{\mathbf{S}_{11}} - s_{12} M_{\mathbf{S}_{12}} - s_{13} M_{\mathbf{S}_{13}} = 0$$

If we denote by  $\mathbf{h}$ ,  $i = 1..3$  each column of matrix  $\mathbf{H}$ :

$$\mathbf{H} = [ \mathbf{h}_1 \quad \mathbf{h}_2 \quad \mathbf{h}_3 ]$$

matrix  $\mathbf{S}$  could be written as:

$$\mathbf{S} = \begin{bmatrix} \|\mathbf{h}_1\|^2 - 1 & \mathbf{h}_1^\top \mathbf{h}_2 & \mathbf{h}_1^\top \mathbf{h}_3 \\ \mathbf{h}_1^\top \mathbf{h}_2 & \|\mathbf{h}_2\|^2 - 1 & \mathbf{h}_2^\top \mathbf{h}_3 \\ \mathbf{h}_1^\top \mathbf{h}_3 & \mathbf{h}_2^\top \mathbf{h}_3 & \|\mathbf{h}_3\|^2 - 1 \end{bmatrix} \quad (38)$$

In a similar way, the opposites of the minors can be written as:

$$M_{\mathbf{S}_{11}} = (\mathbf{h}_2^\top \mathbf{h}_3)^2 - (\|\mathbf{h}_2\|^2 - 1)(\|\mathbf{h}_3\|^2 - 1) \quad (39)$$

$$M_{\mathbf{S}_{22}} = (\mathbf{h}_1^\top \mathbf{h}_3)^2 - (\|\mathbf{h}_1\|^2 - 1)(\|\mathbf{h}_3\|^2 - 1) \quad (40)$$

$$M_{\mathbf{S}_{33}} = (\mathbf{h}_1^\top \mathbf{h}_2)^2 - (\|\mathbf{h}_1\|^2 - 1)(\|\mathbf{h}_2\|^2 - 1) \quad (41)$$

$$M_{\mathbf{S}_{12}} = \mathbf{h}_1^\top (\mathbf{I} + [\mathbf{h}_3]_{\times}^2) \mathbf{h}_2 \quad (42)$$

$$M_{\mathbf{S}_{13}} = \mathbf{h}_1^\top (\mathbf{I} + [\mathbf{h}_2]_{\times}^2) \mathbf{h}_3 \quad (43)$$

$$M_{\mathbf{S}_{23}} = \mathbf{h}_2^\top (\mathbf{I} + [\mathbf{h}_1]_{\times}^2) \mathbf{h}_3 \quad (44)$$

Once the definition and properties of matrix  $\mathbf{S}$  have been stated, we start now the development that will allow us to extract the decomposition elements from this matrix. We will see that the interest of defining such a matrix is that it will allow us to eliminate the rotation matrix from the equations. Using (3) we can write  $\mathbf{S}$  in terms of  $\{\mathbf{R}, \mathbf{t}, \mathbf{n}\}$  in the following way:

$$\mathbf{S} = (\mathbf{R}^\top + \mathbf{n} \mathbf{t}^\top) (\mathbf{R} + \mathbf{t} \mathbf{n}^\top) - \mathbf{I} = \mathbf{R}^\top \mathbf{t} \mathbf{n}^\top + \mathbf{n} \mathbf{t}^\top \mathbf{R} + \mathbf{n} \mathbf{t}^\top \mathbf{t} \mathbf{n}^\top \quad (45)$$

If we introduce two new vectors,  $\mathbf{x}$  and  $\mathbf{y}$ , defined as:

$$\mathbf{x} = \frac{\mathbf{R}^\top \mathbf{t}}{\|\mathbf{R}^\top \mathbf{t}\|} = \frac{\mathbf{R}^\top \mathbf{t}}{\|\mathbf{t}\|} \quad (46)$$

$$\mathbf{y} = \frac{\mathbf{R}^\top \mathbf{t} \|\mathbf{n}\|}{\|\mathbf{R}^\top \mathbf{t}\| \|\mathbf{n}\|} = \frac{\mathbf{R}^\top \mathbf{t} \|\mathbf{n}\|}{\|\mathbf{t}\| \|\mathbf{n}\|} \quad (47)$$

$\mathbf{S}$  can be written as:

$$\mathbf{S} = \mathbf{x} \mathbf{y}^\top + \mathbf{y} \mathbf{x}^\top + \mathbf{y} \mathbf{y}^\top \quad (48)$$

It is clear that matrix  $\mathbf{S}$  is linear in  $\mathbf{x}$ :

$$\begin{bmatrix} y_1^2 + 2y_1x_1 & y_2x_1 + y_1x_2 + y_1y_2 & y_3x_1 + y_1x_3 + y_1y_3 \\ \cdot & y_2^2 + 2y_2x_2 & y_3x_2 + y_2x_3 + y_2y_3 \\ \cdot & \cdot & y_3^2 + 2y_3x_3 \end{bmatrix} = \begin{bmatrix} s_{11} & s_{12} & s_{13} \\ s_{12} & s_{22} & s_{23} \\ s_{13} & s_{23} & s_{33} \end{bmatrix} \quad (49)$$

From this, we can set up two systems of equations:

$$y_1^2 + 2y_1x_1 = s_{11} \quad (50)$$

$$y_2^2 + 2y_2x_2 = s_{22} \quad (51)$$

$$y_3^2 + 2y_3x_3 = s_{33} \quad (52)$$

$$y_2x_1 + y_1x_2 + y_1y_2 = s_{12} \quad (53)$$

$$y_3x_1 + y_1x_3 + y_1y_3 = s_{13} \quad (54)$$

$$y_3x_2 + y_2x_3 + y_2y_3 = s_{23} \quad (55)$$



Solving for  $\mathbf{x}$  from equations (50), (51) and (52):

$$x_1 = \frac{s_{11} - y_1^2}{2y_1} \quad (56)$$

$$x_2 = \frac{s_{22} - y_2^2}{2y_2} \quad (57)$$

$$x_3 = \frac{s_{33} - y_3^2}{2y_3} \quad (58)$$

Replacing this in equations (53), (54) and (55)

$$s_{22}y_1^2 - 2s_{12}y_1y_2 + s_{11}y_2^2 = 0 \quad (59)$$

$$s_{11}y_3^2 - 2s_{13}y_1y_3 + s_{33}y_1^2 = 0 \quad (60)$$

$$s_{33}y_2^2 - 2s_{23}y_2y_3 + s_{22}y_3^2 = 0 \quad (61)$$

Then, after setting

$$z_1 = \frac{y_1}{y_2} \quad (62)$$

$$z_2 = \frac{y_1}{y_3} \quad (63)$$

$$z_3 = \frac{y_3}{y_2} \quad (64)$$

we get three independent second-order equations in  $z_1, z_2, z_3$ , respectively:

$$s_{22}z_1^2 - 2s_{12}z_1 + s_{11} = 0 \quad (65)$$

$$s_{33}z_2^2 - 2s_{13}z_2 + s_{11} = 0 \quad (66)$$

$$s_{22}z_3^2 - 2s_{23}z_3 + s_{33} = 0 \quad (67)$$

the solutions of which are:

$$z_1 = \alpha_1 \pm \beta_1; \quad \alpha_1 = \frac{s_{12}}{s_{22}}; \quad \beta_1 = \frac{\sqrt{s_{12}^2 - s_{11}s_{22}}}{s_{22}} = \frac{\sqrt{M_{\mathbf{S}_{33}}}}{s_{22}} \quad (68)$$

$$z_2 = \alpha_2 \pm \beta_2; \quad \alpha_2 = \frac{s_{13}}{s_{33}}; \quad \beta_2 = \frac{\sqrt{s_{13}^2 - s_{11}s_{22}}}{s_{33}} = \frac{\sqrt{M_{\mathbf{S}_{22}}}}{s_{33}} \quad (69)$$

$$z_3 = \alpha_3 \pm \beta_3; \quad \alpha_3 = \frac{s_{23}}{s_{22}}; \quad \beta_3 = \frac{\sqrt{s_{23}^2 - s_{22}s_{33}}}{s_{22}} = \frac{\sqrt{M_{\mathbf{S}_{11}}}}{s_{22}} \quad (70)$$

where it has been assumed that  $s_{22}$  and  $s_{33}$  are different from 0 (we will see later that, in this case, the constraint on  $s_{33}$  can be removed). Note that thanks to the given property, related to the minors of  $\mathbf{S}$ ,  $z_i$  will always be real.

We impose now the constraint  $x_1^2 + x_2^2 + x_3^2 = 1$ :

$$x_1^2 + x_2^2 + x_3^2 = \frac{(s_{11} - y_1^2)^2}{4y_1^2} + \frac{(s_{22} - y_2^2)^2}{4y_2^2} + \frac{(s_{33} - y_3^2)^2}{4y_3^2} = 1$$

After setting  $w = y_2^2$ , and using  $y_1^2 = z_1^2 y_2^2$ ,  $y_3^2 = z_3^2 y_2^2$ ,

$$(s_{22} - w)^2 + \frac{(s_{11} - w z_1^2)^2}{z_1^2} + \frac{(s_{33} - z_3^2 w)^2}{z_3^2} - 4w = 0$$

Now, we can solve for  $w$  the following second-order equation:

$$a w^2 - 2 b w + c = 0$$

being the coefficients:

$$a = 1 + z_1^2 + z_3^2 \quad (71)$$

$$b = 2 + \text{trace}(\mathbf{S}) = 2 + s_{11} + s_{22} + s_{33} \quad (72)$$

$$c = s_{22}^2 + \frac{s_{11}^2}{z_1^2} + \frac{s_{33}^2}{z_3^2} \quad (73)$$

Then, the two possible solutions for  $w$  are:

$$w = \frac{w_{num}}{a} = \frac{b \pm \sqrt{b^2 - a c}}{a} \quad (74)$$

After this, the  $\mathbf{y}$  vector can be computed:

$$\mathbf{y} = \begin{bmatrix} z_1 \\ 1 \\ z_3 \end{bmatrix} \cdot y_2; \quad y_2 = \pm \sqrt{w} \quad (75)$$

Now, from (56)-(58), the  $\mathbf{x}$  vector could be obtained. It can be checked that the possible solutions for  $w$  are real and positive ( $w$  must be the square of a real number), guaranteeing that the components of vectors  $\mathbf{x}$  and  $\mathbf{y}$  are always real. This is proved in Appendix C.3.

As said before, the homography decomposition problem has, in general, eight different mathematical solutions. The eight possible solutions come out from two possible couples of  $\{z_1, z_3\}$ , two possible values of  $w$  for each one of these couples, and finally, two possible values of  $y_2$  from the plus/minus square root of  $w$ . Four of them correspond to the configuration of the reference object plane being in front of the camera, while the other four correspond to the non-realistic situation of the object plane being behind the camera. The latter set of solutions can be simply discarded when we are working with real images. In fact, we will prove now that, using the given formulation, the four valid solutions of the homography decomposition problem (verifying the reference-plane non-crossing constraint) are those corresponding to

the choice of the minus sign for  $w$  in (74). In Section 3.3.1, we stated that the reference-plane non-crossing constraint implies the following condition:

$$1 + \mathbf{n}^\top \mathbf{R}^\top \mathbf{t} > 0 \quad (76)$$

Then, we can choose the right four solutions writing this condition in terms of  $\mathbf{x}$  and  $\mathbf{y}$ :

$$1 + \mathbf{n}^\top \mathbf{R}^\top \mathbf{t} = 1 + \mathbf{y}^\top \mathbf{x} > 0$$

If we replace  $\mathbf{x}$  as a function of  $\mathbf{y}$  using (56)-(58),

$$[y_1 \ y_2 \ y_3] \begin{bmatrix} \frac{s_{11}-y_1^2}{2y_1} \\ \frac{s_{22}-y_2^2}{2y_2} \\ \frac{s_{33}-y_3^2}{2y_3} \end{bmatrix} = \frac{s_{11}-y_1^2}{2} + \frac{s_{22}-y_2^2}{2} + \frac{s_{33}-y_3^2}{2} \geq -1$$

This can also be written as

$$\text{trace}(\mathbf{S}) + 2 \geq \|\mathbf{y}\|^2 \quad (77)$$

Using (62)-(64) and (71), the squared norm of  $\mathbf{y}$  takes the form

$$\|\mathbf{y}\|^2 = y_1^2 + y_2^2 + y_3^2 = w(1 + z_1^2 + z_3^2) = w a = w_{num} \quad (78)$$

Then, the condition (77) becomes

$$b \geq w a$$

Let us check which one of the possible values of  $w$  verify this condition. These two values will be called:

$$w^+ = \frac{b + \sqrt{b^2 - a c}}{a} \quad (79)$$

$$w^- = \frac{b - \sqrt{b^2 - a c}}{a} \quad (80)$$

It is obvious that, according that  $w$  is real as stated before, only  $w = w^-$  will verify the required condition

$$b \geq w^- a$$

Then, we can conclude that, to get the four physically feasible solutions, it is sufficient to choose:

$$w = w^-$$

On the other hand, it is worth noticing that only  $z_1$  and  $z_3$  are in fact needed for computing the values of  $w$  and then the solutions of the problem. From the four possible couples we can set up for  $\{z_1, z_3\}$ :

$$\{z_{a_1}, z_{a_3}\}, \quad \{z_{a_1}, z_{b_3}\}, \quad \{z_{b_1}, z_{a_3}\}, \quad \{z_{b_1}, z_{b_3}\}$$

being

$$\begin{aligned} z_{a_1} &= \alpha_1 + \beta_1 \\ z_{b_1} &= \alpha_1 - \beta_1 \\ z_{a_3} &= \alpha_3 + \beta_3 \\ z_{b_3} &= \alpha_3 - \beta_3 \end{aligned}$$

only two are valid, these are those verifying:

$$z_2 = \frac{z_1}{z_3}$$

as they are related through (62)-(64). In other words, the couples  $\{z_1, z_3\}$  must verify equation (66), when  $z_2$  is replaced by  $z_1/z_3$ :

$$s_{33} \frac{z_1^2}{z_3^2} - 2s_{13} \frac{z_1}{z_3} + s_{11} = 0 \quad (81)$$

Hence, equation (66) is only needed as a way of discerning the two valid couples for  $z_1, z_3$ . We show now how to make the straightforward computation of the two valid couples  $\{z_1, z_3\}$ .

### Choosing the valid pairs $\{z_1, z_3\}$

When computing the couples  $\{z_1, z_3\}$  using (68) and (70), some inconvenience arises. It is derived from the fact that the right two couples  $\{z_1, z_3\}$  are not always the same, but they may swap among the four possibilities. In fact, the two valid couples are always complementary. That is, the only possibilities are:

$$\{\{z_{a_1}, z_{a_3}\}, \{z_{b_1}, z_{b_3}\}\}$$

or

$$\{\{z_{a_1}, z_{b_3}\}, \{z_{b_1}, z_{a_3}\}\}$$

This means that we need to check, each time, if the right pair complement of  $z_{a_1}$  is  $z_{a_3}$  or  $z_{b_3}$ , evaluating (81) in both cases. What it is intended here is to avoid the eventual swapping of the right pair complement of  $z_{a_1}$  between the two possibilities, forcing it to be always equal to one of them. This will provide a straight analytical computation for the eight homography decomposition solutions.

Replacing in (70)  $s_{33}$  according to (31) (or directly using (33)), will give a better insight into this swapping mechanism. In particular, we get a new expression for  $\beta_3$ :

$$\beta_3 = \frac{\sqrt{\frac{(s_{23}s_{12} - s_{22}s_{13})^2}{s_{12}^2 - s_{11}s_{22}}}}{s_{22}} = \frac{|s_{23}s_{12} - s_{22}s_{13}|}{s_{22}\sqrt{M_{\mathbf{S}_{33}}}}$$

The absolute value in the numerator of this expression is the cause of the eventual swapping between  $z_{a_3}$  and  $z_{b_3}$ . If we compute  $z_3$  using the following expressions, instead

$$z'_{a_3} = \alpha_3 + \beta'_3 \quad (82)$$

$$z'_{b_3} = \alpha_3 - \beta'_3 \quad (83)$$

being now

$$\beta'_3 = \frac{s_{23}s_{12} - s_{22}s_{13}}{s_{22}\sqrt{M_{\mathbf{S}_{33}}}} = \frac{-M_{\mathbf{S}_{13}}}{s_{22}\sqrt{M_{\mathbf{S}_{33}}}}$$

where the absolute value has been removed, we can verify that the right pair complement of  $z_{a_1}$  is  $z'_{a_3}$ . Therefore, the right couples are always the same:

$$\{\{z_{a_1}, z'_{a_3}\}, \{z_{b_1}, z'_{b_3}\}\}$$

This can be verified by simply replacing the expressions of  $z_{a_1}$  and  $z'_{a_3}$  (correspondingly with  $z_{b_1}$  and  $z'_{b_3}$ ) in (81) and checking the equality.

The procedure now is much simpler. We can completely ignore  $z_2$ , and forget about its computation and about the checking (81). Just compute  $z_1$  and  $z_3$  according to:

$$z_1 = \alpha_1 \pm \beta_1$$

$$z_3 = \alpha_3 \pm \beta'_3$$

The only problem of this alternative of computing  $z_3$  to avoid the above-mentioned swapping is that we introduce a division for  $\sqrt{M_{\mathbf{S}_{33}}}$  and, as a consequence, it could not be applied when this minor is null. We can obtain the same result, avoiding this inconvenience, by simply computing  $\beta'_3$  as:

$$\beta'_3 = \frac{-\epsilon_{13} \sqrt{M_{\mathbf{S}_{11}}}}{s_{22}}$$

where  $\epsilon_{13}$  is:

$$\epsilon_{13} = \text{sign}(M_{\mathbf{S}_{13}})$$

The four solutions we will achieve following the procedure will be denoted as:

$$Rtn_a = \{\mathbf{R}_a, \mathbf{t}_a, \mathbf{n}_a\}$$

$$Rtn_b = \{\mathbf{R}_b, \mathbf{t}_b, \mathbf{n}_b\}$$

$$Rtn_{a-} = \{\mathbf{R}_a, -\mathbf{t}_a, -\mathbf{n}_a\}$$

$$Rtn_{b-} = \{\mathbf{R}_b, -\mathbf{t}_b, -\mathbf{n}_b\}$$

as said before, these solutions are, in general, two completely different solutions and their opposites.

### Computation of the normal vector

Once we have seen how to avoid unrealistic solutions, we will now give the formulas to obtain the elements the homography decomposition  $\{\mathbf{R}, \mathbf{t}, \mathbf{n}\}$  directly as a functions of the components of matrix  $\mathbf{H}$ . We start with the normal vector. We have already determined the following expressions for the intermediary variables  $z_1$  and  $z_3$

$$\begin{aligned} z_{a_1} &= \frac{s_{12} + \sqrt{M_{\mathbf{S}_{33}}}}{s_{22}}; & z_{b_1} &= \frac{s_{12} - \sqrt{M_{\mathbf{S}_{33}}}}{s_{22}} \\ z_{a_3} &= \frac{s_{23} - \epsilon_{13} \sqrt{M_{\mathbf{S}_{11}}}}{s_{22}}; & z_{b_3} &= \frac{s_{23} + \epsilon_{13} \sqrt{M_{\mathbf{S}_{11}}}}{s_{22}} \end{aligned}$$

We also need to compute another intermediary variable,  $w$  (see (80)):

$$\begin{aligned} w_a &= \frac{b - \nu}{a_a} \\ w_b &= \frac{b - \nu}{a_b} \end{aligned}$$

where the coefficients  $a_e$ ,  $b$  are:

$$a_e = 1 + z_{e_1}^2 + z_{e_3}^2 \quad (84)$$

$$b = 2 + \text{trace}(\mathbf{S}) \quad (85)$$

where the subscript can be  $e = \{a, b\}$ . After some manipulations of the expressions of these coefficients,  $\nu$  can be written as a function of matrix  $\mathbf{S}$ :

$$\nu = \sqrt{2 [(1 + \text{trace}(\mathbf{S}))^2 + 1 - \text{trace}(\mathbf{S}^2)]} \quad (86)$$

or, alternatively:

$$\nu = 2 \sqrt{1 + \text{trace}(\mathbf{S}) - M_{\mathbf{S}_{11}} - M_{\mathbf{S}_{22}} - M_{\mathbf{S}_{33}}} \quad (87)$$

It can be proved (see Appendix C.4) that the coefficient  $\nu$  introduced in (84) is:

$$\nu = 2 (1 + \mathbf{n}^\top \mathbf{R}^\top \mathbf{t}) \quad (88)$$

Now, we can compute the four possible  $\mathbf{y}$  vectors:

$$\begin{aligned} \mathbf{y}_e &= \pm \sqrt{w_e} \begin{bmatrix} z_{e_1} \\ 1 \\ z_{e_3} \end{bmatrix} = \pm \sqrt{w_e} \mathbf{n}'_e \\ \mathbf{y}_e &= \pm \frac{\sqrt{b - \nu}}{\sqrt{a_e}} \mathbf{n}'_e = \pm \sqrt{b - \nu} \frac{\mathbf{n}'_e}{\|\mathbf{n}'_e\|} \end{aligned}$$

As  $\|\mathbf{y}_e\| = \|\mathbf{t}_e\|$ , from the previous expression, we can deduce the translation vector norm, which is the same for all the solutions:

$$\|\mathbf{t}_e\|^2 = w_{num} = 2 + \text{trace}(\mathbf{S}) - \nu \quad (89)$$

Dividing  $\mathbf{y}_e$  by this norm, we get the expression of the normal vector:

$$\mathbf{n}_e = \frac{\mathbf{n}'_e}{\|\mathbf{n}'_e\|}; \quad e = \{a, b\}$$

$$\mathbf{n}'_a = \begin{bmatrix} s_{12} + \sqrt{M_{\mathbf{S}_{33}}} \\ s_{22} \\ s_{23} - \epsilon_{13}\sqrt{M_{\mathbf{S}_{11}}} \end{bmatrix}; \quad \mathbf{n}'_b = \begin{bmatrix} s_{12} - \sqrt{M_{\mathbf{S}_{33}}} \\ s_{22} \\ s_{23} + \epsilon_{13}\sqrt{M_{\mathbf{S}_{11}}} \end{bmatrix} \quad (90)$$

being

$$\epsilon_{13} = \text{sign}(M_{\mathbf{S}_{13}})$$

In particular, the  $\text{sign}(\cdot)$  function in this case should be implemented like:

$$\text{sign}(a) = \begin{cases} 1 & \text{if } a \geq 0 \\ -1 & \text{otherwise} \end{cases}$$

in order to avoid problems in the cases when  $M_{\mathbf{S}_{ii}} = 0$ . To understand this, suppose that  $M_{\mathbf{S}_{33}} = 0$ , according to relations (36)-(37), also  $M_{\mathbf{S}_{13}} = 0$  and  $M_{\mathbf{S}_{23}} = 0$ . Then, with the typical  $\text{sign}(\cdot)$  function,  $\epsilon_{13} = \epsilon_{23} = 0$ , erroneously cancelling also the second addend of the third component of  $\mathbf{n}_{a,b}$  and providing a wrong result. Moreover, in order to avoid numerical problems, it is advisable to consider the parameter of the  $\text{sign}(\cdot)$  function equal to zero if its magnitude is under some precision value.

**The complete set of formulas.** The previous development started with the assumption that  $s_{22} \neq 0$ , as the expressions were developed dividing by  $s_{22}$ . In case  $s_{22} = 0$  (for instance when the second component of the object-plane normal is null), this formulas cannot be applied. In this situation, we can make a similar development, but dividing by  $s_{11}$  or  $s_{33}$ , instead. Suppose  $s_{22} = 0$  and we want to develop dividing by  $s_{11}$ . What we need to do is to define variables  $z_1, z_2, z_3$  in (62)-(64) in a different way. In particular, we will choose:

$$\begin{aligned} z_1 &= \frac{y_2}{y_1} \\ z_2 &= \frac{y_3}{y_1} \\ z_3 &= \frac{y_2}{y_3} \end{aligned}$$

The three new second-order equations in  $z_1, z_2, z_3$  are:

$$\begin{aligned} s_{11}z_1^2 - 2s_{12}z_1 + s_{22} &= 0 \\ s_{11}z_2^2 - 2s_{13}z_2 + s_{33} &= 0 \\ s_{33}z_3^2 - 2s_{23}z_3 + s_{22} &= 0 \end{aligned}$$

From this, we can follow a parallel development and we will find new expressions for  $\mathbf{n}_a$  and  $\mathbf{n}_b$ :

$$\mathbf{n}'_a(s_{11}) = \begin{bmatrix} s_{11} \\ s_{12} + \sqrt{M_{\mathbf{S}_{33}}} \\ s_{13} + \epsilon_{23} \sqrt{M_{\mathbf{S}_{22}}} \end{bmatrix}; \quad \mathbf{n}'_b(s_{11}) = \begin{bmatrix} s_{11} \\ s_{12} - \sqrt{M_{\mathbf{S}_{33}}} \\ s_{13} - \epsilon_{23} \sqrt{M_{\mathbf{S}_{22}}} \end{bmatrix} \quad (91)$$

with the notation  $\mathbf{n}_e(s_{ii})$  we mean:

*the expression of  $\mathbf{n}_e$  obtained using  $s_{ii}$  (i.e. dividing by  $s_{ii}$ ).*

The third alternative is developing the formulas dividing for  $s_{33}$ . From this case we will obtain:

$$\mathbf{n}'_a(s_{33}) = \begin{bmatrix} s_{13} + \epsilon_{12} \sqrt{M_{\mathbf{S}_{22}}} \\ s_{23} + \sqrt{M_{\mathbf{S}_{11}}} \\ s_{33} \end{bmatrix}; \quad \mathbf{n}'_b(s_{33}) = \begin{bmatrix} s_{13} - \epsilon_{12} \sqrt{M_{\mathbf{S}_{22}}} \\ s_{23} - \sqrt{M_{\mathbf{S}_{11}}} \\ s_{33} \end{bmatrix}$$

On the other hand, we may prefer to write the expressions of  $\mathbf{n}_e$  directly in terms of the column vectors of the  $\mathbf{H}$  matrix,  $\mathbf{h}_i$ :

$$\mathbf{H} = [ \mathbf{h}_1 \quad \mathbf{h}_2 \quad \mathbf{h}_3 ]$$

We give, as an example, the result derived from  $s_{22}$ :

$$\mathbf{n}'_a(s_{22}) = \begin{bmatrix} \mathbf{h}_1^\top \mathbf{h}_2 + \sqrt{(\mathbf{h}_1^\top \mathbf{h}_2)^2 - (\|\mathbf{h}_1\|^2 - 1)(\|\mathbf{h}_2\|^2 - 1)} \\ (\|\mathbf{h}_2\|^2 - 1) \\ \mathbf{h}_2^\top \mathbf{h}_3 - \epsilon_{13} \sqrt{(\mathbf{h}_2^\top \mathbf{h}_3)^2 - (\|\mathbf{h}_2\|^2 - 1)(\|\mathbf{h}_3\|^2 - 1)} \end{bmatrix} \quad (92)$$

$$\mathbf{n}'_b(s_{22}) = \begin{bmatrix} \mathbf{h}_1^\top \mathbf{h}_2 - \sqrt{(\mathbf{h}_1^\top \mathbf{h}_2)^2 - (\|\mathbf{h}_1\|^2 - 1)(\|\mathbf{h}_2\|^2 - 1)} \\ (\|\mathbf{h}_2\|^2 - 1) \\ \mathbf{h}_2^\top \mathbf{h}_3 + \epsilon_{13} \sqrt{(\mathbf{h}_2^\top \mathbf{h}_3)^2 - (\|\mathbf{h}_2\|^2 - 1)(\|\mathbf{h}_3\|^2 - 1)} \end{bmatrix} \quad (93)$$

being  $\epsilon_{13} = \text{sign}(M_{\mathbf{S}_{13}})$ , that can be written as:

$$\epsilon_{13} = \text{sign} \left( -\mathbf{h}_1^\top [\mathbf{I} + [\mathbf{h}_2]_{\times}^2] \mathbf{h}_3 \right)$$



### Computation of the translation vector

Next, we want to obtain the expression for the translation vector. From (56)-(58), the  $\mathbf{x}$  vector could be computed as:

$$\mathbf{x}_e = \begin{bmatrix} x_{e1} \\ x_{e2} \\ x_{e3} \end{bmatrix}; \quad x_{ei} = \frac{s_{ii} - y_{ei}^2}{2y_{ei}}; \quad i = 1..3$$

We can rewrite this expression in terms of the translation and normal vectors, using (46)-(47). In particular, we consider here the translation vector in the reference frame  $\mathbf{t}_e^* = \mathbf{R}_e^\top \mathbf{t}_e$ ,

$$\mathbf{t}_e^* = \frac{1}{2} \begin{bmatrix} \frac{s_{11}}{n_{e1}} \\ \frac{s_{22}}{n_{e2}} \\ \frac{s_{33}}{n_{e3}} \end{bmatrix} - \frac{\|\mathbf{t}_e\|^2}{2} \mathbf{n}_e; \quad e = \{a, b\}$$

This formula cannot be applied as such when any of the components of the normal vector are null. In those cases, we get an indetermination, as  $n_i = 0 \implies s_{ii} = 0$ . In order to avoid this, we make a simple operation that allows us to cancel out  $s_{ii}$  from  $n_{ei}$ . Consider, for instance, the ratio  $s_{11}/n_{a1}$ :

$$\frac{s_{11}}{n_{a1}} = \|\mathbf{n}'_a\| \frac{s_{11}}{n'_{a1}} = \|\mathbf{n}'_a\| \frac{s_{11}}{s_{12} + \sqrt{M_{\mathbf{S}_{33}}}}$$

multiplying and dividing by  $(s_{12} - \sqrt{M_{\mathbf{S}_{33}}})$ , we obtain:

$$\frac{s_{11}}{n_{a1}} = \frac{s_{12} - \sqrt{M_{\mathbf{S}_{33}}}}{s_{22}}$$

with a similar operation in the other components, we get:

$$\mathbf{t}_a^* = \frac{\|\mathbf{n}'_a\|}{2 s_{22}} \begin{bmatrix} s_{12} - \sqrt{M_{\mathbf{S}_{33}}} \\ s_{22} \\ s_{23} + \epsilon_{13} \sqrt{M_{\mathbf{S}_{11}}} \end{bmatrix} - \frac{\|\mathbf{t}_e\|^2}{2 \|\mathbf{n}'_a\|} \begin{bmatrix} s_{12} + \sqrt{M_{\mathbf{S}_{33}}} \\ s_{22} \\ s_{23} - \epsilon_{13} \sqrt{M_{\mathbf{S}_{11}}} \end{bmatrix} \quad (94)$$

$$\mathbf{t}_b^* = \frac{\|\mathbf{n}'_b\|}{2 s_{22}} \begin{bmatrix} s_{12} + \sqrt{M_{\mathbf{S}_{33}}} \\ s_{22} \\ s_{23} - \epsilon_{13} \sqrt{M_{\mathbf{S}_{11}}} \end{bmatrix} - \frac{\|\mathbf{t}_e\|^2}{2 \|\mathbf{n}'_b\|} \begin{bmatrix} s_{12} - \sqrt{M_{\mathbf{S}_{33}}} \\ s_{22} \\ s_{23} + \epsilon_{13} \sqrt{M_{\mathbf{S}_{11}}} \end{bmatrix} \quad (95)$$

Comparing with (90), it is clear that the translation vector can be obtained from the normals:

$$\begin{aligned} \mathbf{t}_a^* &= \frac{\|\mathbf{n}'_a\|}{2 s_{22}} \mathbf{n}'_b - \frac{\|\mathbf{t}_e\|^2}{2} \mathbf{n}_a \\ \mathbf{t}_b^* &= \frac{\|\mathbf{n}'_b\|}{2 s_{22}} \mathbf{n}'_a - \frac{\|\mathbf{t}_e\|^2}{2} \mathbf{n}_b \end{aligned}$$

In order to avoid dependencies from the non-unitary vectors  $\mathbf{n}'_e$ , we write:

$$\begin{aligned}\mathbf{t}_a^* &= \frac{\|\mathbf{n}'_a\| \|\mathbf{n}'_b\|}{2 s_{22}} \mathbf{n}_b - \frac{\|\mathbf{t}_e\|^2}{2} \mathbf{n}_a \\ \mathbf{t}_b^* &= \frac{\|\mathbf{n}'_b\| \|\mathbf{n}'_a\|}{2 s_{22}} \mathbf{n}_a - \frac{\|\mathbf{t}_e\|^2}{2} \mathbf{n}_b\end{aligned}$$

it can be verified that the scalar quotient appearing in the first term of both equations is the same value for all the solutions, in fact we can write it as:

$$\frac{\|\mathbf{n}'_a\| \|\mathbf{n}'_b\|}{|s_{22}|} = \rho \|\mathbf{t}_e\|$$

being  $\rho$ :

$$\rho^2 = b + \nu \implies \rho^2 = 2 + \text{trace}(\mathbf{S}) + \nu = \|\mathbf{t}_e\|^2 + 2\nu \quad (96)$$

where  $\nu$  was given in (86). Finally, we can write compact expressions for  $\mathbf{t}_e^*$  from  $\mathbf{n}_e$ :

$$\mathbf{t}_a^* = \frac{\|\mathbf{t}_e\|}{2} (\epsilon_{s_{22}} \rho \mathbf{n}_b - \|\mathbf{t}_e\| \mathbf{n}_a) \quad (97)$$

$$\mathbf{t}_b^* = \frac{\|\mathbf{t}_e\|}{2} (\epsilon_{s_{22}} \rho \mathbf{n}_a - \|\mathbf{t}_e\| \mathbf{n}_b) \quad (98)$$

being

$$\epsilon_{s_{22}} = \text{sign}(s_{22})$$

In this case, for the  $\text{sign}(\cdot)$  function we don't have the same problem as for  $\epsilon_{13}$  in (90), as we assumed  $s_{22} \neq 0$ . This means that we can use the typical  $\text{sign}(\cdot)$  function ( $\text{sign}(0) = 0$ ) for  $\epsilon_{s_{22}}$ .

In order to find the translation vector in the current frame,  $\mathbf{t}_e$ , we need to compute the rotation matrix in advance.

**The complete set of formulas.** Again, we need a complete set of formulas, that makes possible the computation of the translation vector even if some  $s_{ii}$  are null. In particular, relation (91) was obtained by dividing by  $s_{11}$ . The translation vector derived from that is:

$$\begin{aligned}\mathbf{t}_a^*(s_{11}) &= \frac{\|\mathbf{n}'_a(s_{11})\|}{2 s_{11}} \begin{bmatrix} s_{11} \\ s_{12} - \sqrt{M_{\mathbf{S}_{33}}} \\ s_{13} - \epsilon_{23} \sqrt{M_{\mathbf{S}_{22}}} \end{bmatrix} - \frac{\|\mathbf{t}_e\|^2}{2 \|\mathbf{n}'_a(s_{11})\|} \begin{bmatrix} s_{11} \\ s_{12} + \sqrt{M_{\mathbf{S}_{33}}} \\ s_{13} + \epsilon_{23} \sqrt{M_{\mathbf{S}_{22}}} \end{bmatrix} \\ \mathbf{t}_b^*(s_{11}) &= \frac{\|\mathbf{n}'_b(s_{11})\|}{2 s_{11}} \begin{bmatrix} s_{11} \\ s_{12} + \sqrt{M_{\mathbf{S}_{33}}} \\ s_{13} + \epsilon_{23} \sqrt{M_{\mathbf{S}_{22}}} \end{bmatrix} - \frac{\|\mathbf{t}_e\|^2}{2 \|\mathbf{n}'_b(s_{11})\|} \begin{bmatrix} s_{11} \\ s_{12} - \sqrt{M_{\mathbf{S}_{33}}} \\ s_{13} - \epsilon_{23} \sqrt{M_{\mathbf{S}_{22}}} \end{bmatrix}\end{aligned}$$

We can also write the expressions directly in terms of  $\mathbf{n}_a(s_{11})$  and  $\mathbf{n}_b(s_{11})$ :

$$\begin{aligned}\mathbf{t}_a^*(s_{11}) &= \frac{\|\mathbf{t}_e\|}{2} (\epsilon_{s_{11}} \rho \mathbf{n}_b(s_{11}) - \|\mathbf{t}_e\| \mathbf{n}_a(s_{11})) \\ \mathbf{t}_b^*(s_{11}) &= \frac{\|\mathbf{t}_e\|}{2} (\epsilon_{s_{11}} \rho \mathbf{n}_a(s_{11}) - \|\mathbf{t}_e\| \mathbf{n}_b(s_{11}))\end{aligned}$$

The third alternative is developing the formulas dividing for  $s_{33}$ . In this case we obtain:

$$\begin{aligned}\mathbf{t}_a^*(s_{33}) &= \frac{\|\mathbf{n}'_a(s_{33})\|}{2 s_{33}} \begin{bmatrix} s_{13} - \epsilon_{12} \sqrt{M \mathbf{S}_{22}} \\ s_{23} - \sqrt{M \mathbf{S}_{11}} \\ s_{33} \end{bmatrix} - \frac{\|\mathbf{t}_e\|^2}{2 \|\mathbf{n}'_a(s_{33})\|} \begin{bmatrix} s_{13} + \epsilon_{12} \sqrt{M \mathbf{S}_{22}} \\ s_{23} + \sqrt{M \mathbf{S}_{11}} \\ s_{33} \end{bmatrix} \\ \mathbf{t}_b^*(s_{33}) &= \frac{\|\mathbf{n}'_a(s_{33})\|}{2 s_{33}} \begin{bmatrix} s_{13} + \epsilon_{12} \sqrt{M \mathbf{S}_{22}} \\ s_{23} + \sqrt{M \mathbf{S}_{11}} \\ s_{33} \end{bmatrix} - \frac{\|\mathbf{t}_e\|^2}{2 \|\mathbf{n}'_a(s_{33})\|} \begin{bmatrix} s_{13} - \epsilon_{12} \sqrt{M \mathbf{S}_{22}} \\ s_{23} - \sqrt{M \mathbf{S}_{11}} \\ s_{33} \end{bmatrix}\end{aligned}$$

The alternative expression of the translation vector directly from  $\mathbf{n}_a(s_{33})$  and  $\mathbf{n}_b(s_{33})$  is, as expected:

$$\begin{aligned}\mathbf{t}_a^*(s_{33}) &= \frac{\|\mathbf{t}_e\|}{2} (\epsilon_{s_{33}} \rho \mathbf{n}_b(s_{33}) - \|\mathbf{t}_e\| \mathbf{n}_a(s_{33})) \\ \mathbf{t}_b^*(s_{33}) &= \frac{\|\mathbf{t}_e\|}{2} (\epsilon_{s_{33}} \rho \mathbf{n}_a(s_{33}) - \|\mathbf{t}_e\| \mathbf{n}_b(s_{33}))\end{aligned}$$

From the previous expressions, we see that the formulas we could write for  $\mathbf{t}_e^*$  in terms of the columns of matrix  $\mathbf{H}$  will not be as simple as those given in (92)-(93) for the normal vector. On top of this, we need to multiply by matrix  $\mathbf{R}_e^\top$  in order to get  $\mathbf{t}_e$ . In the next subsection, we will propose a different starting point for the development, such that, the expressions obtained for  $\mathbf{t}_e$  will be exactly as simple as those already obtained for  $\mathbf{n}_e$  (90), (92) and (93). However, it must be noticed that, computing the normal and translation vectors using the previous set of formulas, we always get the right couples. That means that, for instance,  $\mathbf{t}_a$  (and not  $-\mathbf{t}_a$  nor  $\mathbf{t}_b$  nor  $-\mathbf{t}_b$ ) is always the right couple for  $\mathbf{n}_a$ , without requiring any additional checking.

### Computation of the rotation matrix

The rotation matrix could be obtained from  $\mathbf{x}$  and  $\mathbf{y}$ , using the definition of homography matrix and the relations (46)-(47):

$$\mathbf{H} = \mathbf{R} + \mathbf{t} \mathbf{n}^\top = \mathbf{R} (\mathbf{I} + \mathbf{x} \mathbf{y}^\top)$$

as:

$$\mathbf{R} = \mathbf{H} (\mathbf{I} + \mathbf{x} \mathbf{y}^\top)^{-1}$$

The required inverse matrix can be computed making use of the following relation:

$$(\mathbf{I} + \mathbf{x}\mathbf{y}^\top)^{-1} = \mathbf{I} - \frac{1}{1 + \mathbf{x}^\top\mathbf{y}} \mathbf{x}\mathbf{y}^\top$$

Then, the rotation matrix can be written as:

$$\mathbf{R}_e = \mathbf{H} \left( \mathbf{I} - \frac{1}{1 + \mathbf{x}_e^\top\mathbf{y}_e} \mathbf{x}_e\mathbf{y}_e^\top \right)$$

Alternatively, we can express the rotation matrix directly in terms of  $\mathbf{n}_e$  and  $\mathbf{t}_e^*$ :

$$\mathbf{R}_e = \mathbf{H} \left( \mathbf{I} - \frac{1}{1 + \mathbf{n}_e^\top\mathbf{t}_e^*} \mathbf{t}_e^*\mathbf{n}_e^\top \right) = \mathbf{H} \left( \mathbf{I} - \frac{2}{\nu} \mathbf{t}_e^*\mathbf{n}_e^\top \right) \quad (99)$$

#### 4.2.2 Second method

Even if we consider that, for the analytical computation of the translation vector, the given formulas (94)-(95) or (97)-(98) are good enough, it maybe sometimes convenient to have a closer form for obtaining this vector. For instance, if we want to study the effects of camera-calibration errors on the translation vector derived from homography decomposition, having a pair of formulas for it similar to (92) and (93), directly in terms of the elements of matrix  $\mathbf{H}$ , would greatly simplify the analysis. In this subsection, we will derive such a more compact expression for  $\mathbf{t}_e$ .

#### Computation of the translation vector

The symmetry of the problem suggest that, instead of (45), we could have started defining the matrix:

$$\mathbf{S}_r = \mathbf{H}\mathbf{H}^\top - \mathbf{I} = (\mathbf{R} + \mathbf{t}\mathbf{n}^\top)(\mathbf{R}^\top + \mathbf{n}\mathbf{t}^\top) - \mathbf{I} = \mathbf{R}\mathbf{n}\mathbf{t}^\top + \mathbf{t}\mathbf{n}^\top\mathbf{R}^\top + \mathbf{t}\mathbf{t}^\top$$

We also redefine vectors  $\mathbf{x}$  and  $\mathbf{y}$  as:

$$\begin{aligned} \mathbf{x} &= \mathbf{R}\mathbf{n} \\ \mathbf{y} &= \mathbf{t} \end{aligned}$$

Then,  $\mathbf{S}_r$  can be written as:

$$\mathbf{S}_r = \mathbf{x}\mathbf{y}^\top + \mathbf{y}\mathbf{x}^\top + \mathbf{y}\mathbf{y}^\top = \begin{bmatrix} s_{r11} & s_{r12} & s_{r13} \\ s_{r12} & s_{r22} & s_{r23} \\ s_{r13} & s_{r23} & s_{r33} \end{bmatrix}$$

It can be easily verified that:

$$\begin{aligned} \text{trace}(\mathbf{S}_r) &= \text{trace}(\mathbf{S}) \\ \text{trace}(\mathbf{S}_r^2) &= \text{trace}(\mathbf{S}^2) \\ M_{\mathbf{S}_{r_{11}}} + M_{\mathbf{S}_{r_{11}}} + M_{\mathbf{S}_{r_{11}}} &= M_{\mathbf{S}_{11}} + M_{\mathbf{S}_{11}} + M_{\mathbf{S}_{11}} \end{aligned}$$

Matrix  $\mathbf{S}_r$  has exactly the same form as  $\mathbf{S}$  in (48), but now, with a different definition of vectors  $\mathbf{x}$  and  $\mathbf{y}$ . This means that we can use the same results we had before, with the only difference that the first elements we derive now with the expressions equivalent to those given in (90) are vectors parallel to  $\mathbf{t}_e$ , instead of vectors parallel to  $\mathbf{n}_e$ . Then, we can obtain the new relations for vector  $\mathbf{t}_e$ :

$$\mathbf{t}'_a = \begin{bmatrix} s_{r12} + \sqrt{M\mathbf{S}_{r33}} \\ s_{r22} \\ s_{r23} - \epsilon_{r13}\sqrt{M\mathbf{S}_{r11}} \end{bmatrix}; \quad \mathbf{t}'_b = \begin{bmatrix} s_{r12} - \sqrt{M\mathbf{S}_{r33}} \\ s_{r22} \\ s_{r23} + \epsilon_{r13}\sqrt{M\mathbf{S}_{r11}} \end{bmatrix} \quad (100)$$

where  $M\mathbf{S}_{r_{ii}}$  and  $\epsilon_{r_{ij}}$  have the same meaning as before, but referred to matrix  $\mathbf{S}_r$  instead of  $\mathbf{S}$ . From (100), we compute the translation vector with the right norm:

$$\mathbf{t}_e = \|\mathbf{t}_e\| \frac{\mathbf{t}'_e}{\|\mathbf{t}'_e\|}$$

Where we need the expression for  $\|\mathbf{t}_e\|$ :

$$\begin{aligned} \|\mathbf{t}_e\| &= 2 + \text{trace}(\mathbf{S}_r) - \nu \\ \|\mathbf{t}_e\| &= 2 + \text{trace}(\mathbf{S}) - \nu \end{aligned}$$

and  $\nu$  can be computed using (86) or (87), using either of them,  $\mathbf{S}$  or  $\mathbf{S}_r$ .

On the other hand, notice that, in a similar way to (38),  $\mathbf{S}_r$  can be written as:

$$\mathbf{S}_r = \begin{bmatrix} \|\mathbf{h}_{r1}\|^2 - 1 & \mathbf{h}_{r1}^\top \mathbf{h}_{r2} & \mathbf{h}_{r1}^\top \mathbf{h}_{r3} \\ \mathbf{h}_{r1}^\top \mathbf{h}_{r2} & \|\mathbf{h}_{r2}\|^2 - 1 & \mathbf{h}_{r2}^\top \mathbf{h}_{r3} \\ \mathbf{h}_{r1}^\top \mathbf{h}_{r3} & \mathbf{h}_{r2}^\top \mathbf{h}_{r3} & \|\mathbf{h}_{r3}\|^2 - 1 \end{bmatrix} \quad (101)$$

where  $\mathbf{h}_{ri}^\top$ ,  $i = 1..3$  means for each row of matrix  $\mathbf{H}$ :

$$\mathbf{H} = \begin{bmatrix} \mathbf{h}_{r1}^\top \\ \mathbf{h}_{r2}^\top \\ \mathbf{h}_{r3}^\top \end{bmatrix}$$

This is why the new  $\mathbf{S}_r$  matrix was named with subindex  $r$ : because it can be written in terms of the rows of  $\mathbf{H}$ , instead of its columns, as for  $\mathbf{S}$ . Finally, we write the expression of

$\mathbf{t}_e$  in terms of the components of matrix  $\mathbf{H}$ , as intended:

$$\mathbf{t}'_a = \begin{bmatrix} \mathbf{h}_{r_1}^\top \mathbf{h}_{r_2} + \sqrt{(\mathbf{h}_{r_1}^\top \mathbf{h}_{r_2})^2 - (\|\mathbf{h}_{r_1}\|^2 - 1)(\|\mathbf{h}_{r_2}\|^2 - 1)} \\ (\|\mathbf{h}_{r_2}\|^2 - 1) \\ \mathbf{h}_{r_2}^\top \mathbf{h}_{r_3} - \epsilon_{r_{13}} \sqrt{(\mathbf{h}_{r_2}^\top \mathbf{h}_{r_3})^2 - (\|\mathbf{h}_{r_2}\|^2 - 1)(\|\mathbf{h}_{r_3}\|^2 - 1)} \end{bmatrix}$$

$$\mathbf{t}'_b = \begin{bmatrix} \mathbf{h}_{r_1}^\top \mathbf{h}_{r_2} - \sqrt{(\mathbf{h}_{r_1}^\top \mathbf{h}_{r_2})^2 - (\|\mathbf{h}_{r_1}\|^2 - 1)(\|\mathbf{h}_{r_2}\|^2 - 1)} \\ (\|\mathbf{h}_{r_2}\|^2 - 1) \\ \mathbf{h}_{r_2}^\top \mathbf{h}_{r_3} + \epsilon_{r_{13}} \sqrt{(\mathbf{h}_{r_2}^\top \mathbf{h}_{r_3})^2 - (\|\mathbf{h}_{r_2}\|^2 - 1)(\|\mathbf{h}_{r_3}\|^2 - 1)} \end{bmatrix}$$

being  $\epsilon_{r_{13}} = \text{sign}(M_{\mathbf{S}_{r_{13}}})$ , that can be written as:

$$\epsilon_{r_{13}} = \text{sign}(-\mathbf{h}_{r_1}^\top [\mathbf{I} + [\mathbf{h}_{r_2}]_{\times}^2] \mathbf{h}_{r_3})$$

The vectors  $\mathbf{t}_e$  (with  $e = a, b$ ) computed in this way are actually  $\mathbf{t}_e(s_{22})$ . The complete set of formulas, including  $\mathbf{t}_e(s_{11})$  and  $\mathbf{t}_e(s_{33})$  are given in the summary.

### Computation of the normal vector

In Section 4.2.1, we computed  $\mathbf{t}_e^* = \mathbf{R}_e^\top \mathbf{t}_e$  from the expressions of  $\mathbf{n}_e$ . Following a symmetric development, we can obtain now the expressions for  $\mathbf{n}'_e = \mathbf{R}_e \mathbf{n}_e$ , from the given expressions of  $\mathbf{t}_e$ . These are:

$$\mathbf{n}'_a(s_{r_{ii}}) = \frac{1}{2} \left[ \epsilon_{s_{r_{ii}}} \frac{\rho}{\|\mathbf{t}_e\|} \mathbf{t}_b(s_{r_{ii}}) - \mathbf{t}_a(s_{r_{ii}}) \right]$$

$$\mathbf{n}'_b(s_{r_{ii}}) = \frac{1}{2} \left[ \epsilon_{s_{r_{ii}}} \frac{\rho}{\|\mathbf{t}_e\|} \mathbf{t}_a(s_{r_{ii}}) - \mathbf{t}_b(s_{r_{ii}}) \right]$$

being

$$\epsilon_{s_{r_{ii}}} = \text{sign}(s_{r_{ii}})$$

### Computation of the rotation matrix

An expression for the rotation matrix, analogous to (99), can also be obtained:

$$\mathbf{R}_e^\top = \mathbf{H}^\top \left( \mathbf{I} - \frac{2}{\nu} \mathbf{n}'_e \mathbf{t}_e^\top \right)$$

or, what is the same:

$$\mathbf{R}_e = \left( \mathbf{I} - \frac{2}{\nu} \mathbf{t}_e \mathbf{n}_e^\top \right) \mathbf{H}$$

## 5 Relations among the possible solutions

The purpose of this section can be easily understood posing the following question: suppose we have one of the four solutions referred in (7)-(10) of the homography decomposition for a given homography matrix. Is it possible to find any expressions that allow us to compute the other three possible solutions? The answer is yes and these expressions will be given in this section. In particular, we need to find the expressions of one of the solutions in terms of the other one:

$$\begin{aligned} Rtn_b &= f(Rtn_a) \\ Rtn_a &= f(Rtn_b) \end{aligned}$$

We will take advantage of the described analytical decomposition procedure in order to get these relations. Again, we first introduce the expressions relating the solutions, and then proceed with the detailed description.

### 5.1 Summary of the relations among the possible solutions

We summarize here the final achieved expressions. Suppose we have one solution and we call it:  $Rtn_a = \{\mathbf{R}_a, \mathbf{t}_a, \mathbf{n}_a\}$ . Then, the other solutions can be denoted by:

$$\begin{aligned} Rtn_b &= \{\mathbf{R}_b, \mathbf{t}_b, \mathbf{n}_b\} \\ Rtn_{a-} &= \{\mathbf{R}_a, -\mathbf{t}_a, -\mathbf{n}_a\} \\ Rtn_{b-} &= \{\mathbf{R}_b, -\mathbf{t}_b, -\mathbf{n}_b\} \end{aligned}$$

where the elements  $\mathbf{R}_b$ ,  $\mathbf{t}_b$  and  $\mathbf{n}_b$  can be obtained as:

$$\mathbf{t}_b = \frac{\|\mathbf{t}_a\|}{\rho} \mathbf{R}_a (2\mathbf{n}_a + \mathbf{R}_a^\top \mathbf{t}_a) \quad (102)$$

$$\mathbf{n}_b = \frac{1}{\rho} \left( \|\mathbf{t}_a\| \mathbf{n}_a + \frac{2}{\|\mathbf{t}_a\|} \mathbf{R}_a^\top \mathbf{t}_a \right) \quad (103)$$

$$\mathbf{R}_b = \mathbf{R}_a + \frac{2}{\rho^2} [\nu \mathbf{t}_a \mathbf{n}_a^\top - \mathbf{t}_a \mathbf{t}_a^\top \mathbf{R}_a - \|\mathbf{t}_a\|^2 \mathbf{R}_a \mathbf{n}_a \mathbf{n}_a^\top - 2 \mathbf{R}_a \mathbf{n}_a \mathbf{t}_a^\top \mathbf{R}_a] \quad (104)$$

In these relations the subindexes  $a$  and  $b$  can be exchanged. The coefficients  $\rho$  and  $\nu$  are:

$$\rho = \|\mathbf{2n}_e + \mathbf{R}_e^\top \mathbf{t}_e\| > 1; \quad e = \{a, b\} \quad (105)$$

$$\nu = 2(\mathbf{n}_e^\top \mathbf{R}_e^\top \mathbf{t}_e + 1) > 0 \quad (106)$$

$$\rho^2 = \|\mathbf{t}_e\|^2 + 2\nu \quad (107)$$



For the rotation axes and angles:

$$\mathbf{r}_b = \frac{[(2 - \mathbf{n}_a^\top \mathbf{t}_a) \mathbf{I} + \mathbf{t}_a \mathbf{n}_a^\top + \mathbf{n}_a \mathbf{t}_a^\top] \mathbf{r}_a + (\mathbf{n}_a \times \mathbf{t}_a)}{2 + \mathbf{n}_a^\top \mathbf{t}_a + \mathbf{r}_a^\top (\mathbf{n}_a \times \mathbf{t}_a)} \quad (108)$$

being  $\mathbf{r}_e$  the chosen parametrization for a rotation of an angle  $\theta_e$  about an axis  $\mathbf{u}_e$ :

$$\mathbf{r}_e = \tan\left(\frac{\theta_e}{2}\right) \mathbf{u}_e; \quad e = \{a, b\}$$

It must be pointed out that, in the usual case when two solutions verify the visibility constraint according to the given set of image points, if we suppose that one of them is  $Rtn_a$ , the other one can be either  $Rtn_b$  or  $Rtn_{b^-}$ , according to the formulation given.

### Special cases

It is worth noticing that these expressions have two singular situations on which they cannot be used. One of them occurs when  $\rho = 0$ , what we already know is physically impossible to happen. Anyway, we will do a geometric interpretation of this situation, in which:

$$\mathbf{t}_a = -\mathbf{R}_a \mathbf{n}_a \|\mathbf{t}_a\| \quad \text{and} \quad \|\mathbf{t}_a\| = 2 \quad \implies \quad \rho = 0$$

This means that the required motion for the camera going from  $\{\mathcal{F}^*\}$  to  $\{\mathcal{F}\}$  implies a displacement towards the reference plane following the direction of the normal and after crossing this plane, situating at the same distance it was at the beginning. This is clearly understood if we write the relation:

$$\mathbf{t}_a^* = \mathbf{R}_a^\top \mathbf{t}_a = -2 \mathbf{n}_a$$

Where  $\mathbf{t}_a^*$  is the translation vector expressed in the reference frame. Also as the translation is normalized with the depth to the plane  $d^*$ , we will write instead:

$$\mathbf{t}_a^* = 2 d^* \mathbf{n}_a; \quad \mathbf{t}_a^* = -\mathbf{R}_a^\top \mathbf{t}_a$$

As  $d^*$  is measured from the reference frame, we have also changed the displacement vector to see it as the displacement from the reference frame to the current frame.

The second singular situation for the formulas relating both solutions is when we are in the pure rotation case. This corresponds to the degenerate case of all the singular values of the homography matrix being equal to 1. In this case, no formulas are needed to obtain one solution from the other as both solutions are the same:

$$\mathbf{t}_b = \mathbf{t}_a = 0; \quad \mathbf{R}_a = \mathbf{R}_b$$

while the normal is not defined.

## 5.2 Preliminary relations

First, we look for the relation between vectors  $\mathbf{y}$  and  $\mathbf{x}$  in both solutions,  $Rtn_a$  and  $Rtn_b$ . From (75), we had:

$$\mathbf{y}_a = \mathbf{z}_a y_{a_2}; \quad \mathbf{y}_b = \mathbf{z}_b y_{b_2}$$

being:

$$\mathbf{z}_e = \begin{bmatrix} z_{e_1} \\ 1 \\ z_{e_3} \end{bmatrix}; \quad e = \{a, b\}$$

A matrix can be introduced as a multiplicative transformation from one to the other:

$$\mathbf{y}_b = \mathbf{T}_y \mathbf{y}_a; \quad \mathbf{T}_y = r_{y_2} \begin{bmatrix} r_{z_1} & 0 & 0 \\ 0 & 1 & 0 \\ 0 & 0 & r_{z_3} \end{bmatrix} \quad (109)$$

Where  $r_{z_1}$ ,  $r_{z_3}$  and  $r_{y_2}$  are the corresponding ratios:

$$r_{z_1} = \frac{z_{b_1}}{z_{a_1}}; \quad r_{z_3} = \frac{z_{b_3}}{z_{a_3}}; \quad r_{y_2} = \frac{y_{b_2}}{y_{a_2}}$$

If we start from the expression of the  $\mathbf{S}$  matrix as a function of the first solution:

$$\mathbf{S} = \mathbf{x}_a \mathbf{y}_a^\top + \mathbf{y}_a \mathbf{x}_a^\top + \mathbf{y}_a \mathbf{y}_a^\top$$

which has the form shown in (49) which is reproduced here for convenience:

$$\mathbf{S} = \begin{bmatrix} y_1^2 + 2y_1x_1 & y_2x_1 + y_1x_2 + y_1y_2 & y_3x_1 + y_1x_3 + y_1y_3 \\ \cdot & y_2^2 + 2y_2x_2 & y_3x_2 + y_2x_3 + y_2y_3 \\ \cdot & \cdot & y_3^2 + 2y_3x_3 \end{bmatrix} \quad (110)$$

and where for notation simplicity  $x_i$  and  $y_i$  are used instead of  $x_{a_i}$   $y_{a_i}$ . If we compute  $z_1$  and  $z_3$  using this form of the components of matrix  $\mathbf{S}$ , we get:

$$\begin{aligned} z_{a_1} &= \frac{(1 + \epsilon) x_1 y_2 + (1 - \epsilon) x_2 y_1 + y_1 y_2}{y_2(2x_2 + y_2)} \\ z_{b_1} &= \frac{(1 - \epsilon) x_1 y_2 + (1 + \epsilon) x_2 y_1 + y_1 y_2}{y_2(2x_2 + y_2)} \\ z_{a_3} &= \frac{(1 + \epsilon) x_3 y_2 + (1 - \epsilon) x_2 y_3 + y_3 y_2}{y_2(2x_2 + y_2)} \\ z_{b_3} &= \frac{(1 - \epsilon) x_3 y_2 + (1 + \epsilon) x_2 y_3 + y_3 y_2}{y_2(2x_2 + y_2)} \end{aligned}$$

where

$$\epsilon = \text{sign}(x_1 y_2 - x_2 y_1)$$

Then, if  $\epsilon = -1$ , we get:

$$\begin{aligned} z_{a_1} &= \frac{y_1}{y_2}, & z_{a_3} &= \frac{y_3}{y_2} \\ z_{b_1} &= \frac{2x_1 + y_1}{2x_2 + y_2}, & z_{b_3} &= \frac{2x_3 + y_3}{2x_2 + y_2} \end{aligned}$$

and, in case  $\epsilon = +1$ , the solutions are swapped

$$\begin{aligned} z_{a_1} &= \frac{2x_1 + y_1}{2x_2 + y_2}, & z_{a_3} &= \frac{2x_3 + y_3}{2x_2 + y_2} \\ z_{b_1} &= \frac{y_1}{y_2}, & z_{b_3} &= \frac{y_3}{y_2} \end{aligned}$$

We will assume the first case, so the first solution is the trivial one, that is, that one from which we wrote  $\mathbf{S}$ . Otherwise, the value  $\epsilon = +1$  will lead us to the same result of how getting a solution from the other, the only difference is that these two solutions have been swapped, what does not need to be considered. Then, we assume  $\epsilon = -1$  and proceed computing the ratios:

$$\begin{aligned} r_{z_1} &= \frac{z_{b_1}}{z_{a_1}} = \frac{y_2(2x_1 + y_1)}{y_1(2x_2 + y_2)} \\ r_{z_3} &= \frac{z_{b_3}}{z_{a_3}} = \frac{y_2(2x_3 + y_3)}{y_3(2x_2 + y_2)} \end{aligned}$$

In order to get the ratio  $r_{y_2}$ , we first compute

$$\frac{w_b}{w_a} = \frac{(b - \nu)/a_b}{(b - \nu)/a_a} = \frac{a_a}{a_b} = \frac{(2x_2 + y_2)^2 \|\mathbf{y}\|^2}{y_2^2 (\|\mathbf{y}\|^2 + 4 \mathbf{x}^\top \mathbf{y} + 4)}$$

From this, the third ratio is

$$r_{y_2} = \frac{\sqrt{w_b}}{\sqrt{w_a}} = \frac{(2x_2 + y_2) \|\mathbf{y}\|}{y_2 \sqrt{\|\mathbf{y}\|^2 + 4 \mathbf{x}^\top \mathbf{y} + 4}} \quad (111)$$

Then, matrix  $\mathbf{T}_y$  can be constructed:

$$\mathbf{T}_y = \frac{\|\mathbf{y}\|}{\sqrt{\|\mathbf{y}\|^2 + 4 \mathbf{x}^\top \mathbf{y} + 4}} \begin{bmatrix} \frac{2x_1 + y_1}{y_1} & 0 & 0 \\ 0 & \frac{2x_2 + y_2}{y_2} & 0 \\ 0 & 0 & \frac{2x_3 + y_3}{y_3} \end{bmatrix}$$

Replacing this in (109), gives a very simple expression for computing  $\mathbf{y}_b$  from  $\mathbf{y}_a$  and  $\mathbf{x}_a$

$$\mathbf{y}_b = \pm \frac{\|\mathbf{y}_a\|}{\rho} (\mathbf{y}_a + 2\mathbf{x}_a) \quad (112)$$

the plus/minus ambiguity is due to the two possible values of the square root in (111). The coefficient  $\rho$  is

$$\rho = \sqrt{\|\mathbf{y}_e\|^2 + 4\mathbf{x}_e^\top \mathbf{y}_e + 4} = \sqrt{\|\mathbf{x}_e \times \mathbf{y}_e\|^2 + (\mathbf{x}_e^\top \mathbf{y}_e + 2)^2}; \quad e = \{a, b\}$$

No subscript is added to this coefficient as it is equal for every solution. Analogously, the first solution could be computed from the second one:

$$\mathbf{y}_a = \pm \frac{\|\mathbf{y}_b\|}{\rho} (\mathbf{y}_b + 2\mathbf{x}_b)$$

Now, the relation between the  $\mathbf{x}$  vectors is being obtained using (56)-(58) and the form of  $s_{11}$ ,  $s_{22}$  and  $s_{33}$  from (110), providing

$$\begin{aligned} \mathbf{x}_b &= \frac{1}{\rho} \left( \frac{\nu}{\|\mathbf{y}_a\|} \mathbf{y}_a - \|\mathbf{y}_a\| \mathbf{x}_a \right) \\ \mathbf{x}_a &= \frac{1}{\rho} \left( \frac{\nu}{\|\mathbf{y}_b\|} \mathbf{y}_b - \|\mathbf{y}_b\| \mathbf{x}_b \right) \end{aligned} \quad (113)$$

being the coefficient  $\nu$

$$\nu = 2(\mathbf{x}_e^\top \mathbf{y}_e + 1); \quad e = \{a, b\} \quad (114)$$

### 5.3 Relations for the rotation matrices

Next, we try to find the relations between  $\mathbf{R}_a$  and  $\mathbf{R}_b$ . We can start this development from the following expression:

$$\mathbf{H} = \mathbf{R}_a + \mathbf{t}_a \mathbf{n}_a^\top = \mathbf{R}_b + \mathbf{t}_b \mathbf{n}_b^\top = \mathbf{R}_b (\mathbf{I} + \mathbf{R}_b^\top \mathbf{t}_b \mathbf{n}_b^\top)$$

Then,  $\mathbf{R}_b$  is

$$\mathbf{R}_b = (\mathbf{R}_a + \mathbf{t}_a \mathbf{n}_a^\top) (\mathbf{I} + \mathbf{R}_b^\top \mathbf{t}_b \mathbf{n}_b^\top)^{-1}$$

We can write  $\mathbf{R}_b$  as the product of  $\mathbf{R}_a$  times another rotation matrix:

$$\mathbf{R}_b = \mathbf{R}_a \mathbf{R}_{ab} \quad (115)$$

This rotation matrix is:

$$\mathbf{R}_{ab} = (\mathbf{I} + \mathbf{R}_a^\top \mathbf{t}_a \mathbf{n}_a^\top) (\mathbf{I} + \mathbf{R}_b^\top \mathbf{t}_b \mathbf{n}_b^\top)^{-1}$$

Which can be written in a more compact form as a function of  $\mathbf{x}_a, \mathbf{y}_a$  and  $\mathbf{x}_b, \mathbf{y}_b$ :

$$\mathbf{R}_{ab} = (\mathbf{I} + \mathbf{x}_a \mathbf{y}_a^\top) (\mathbf{I} + \mathbf{x}_b \mathbf{y}_b^\top)^{-1}$$

The required matrix inversion can be avoided, making use of the following relation:

$$(\mathbf{I} + \mathbf{x}_b \mathbf{y}_b^\top)^{-1} = \mathbf{I} - \frac{1}{1 + \mathbf{x}_b^\top \mathbf{y}_b} \mathbf{x}_b \mathbf{y}_b^\top$$

As already said,  $\mathbf{x}_b^\top \mathbf{y}_b = \mathbf{x}_a^\top \mathbf{y}_a$ , giving:

$$\mathbf{R}_{ab} = (\mathbf{I} + \mathbf{x}_a \mathbf{y}_a^\top) \left( \mathbf{I} - \frac{2}{\nu} \mathbf{x}_b \mathbf{y}_b^\top \right)$$

where the expression of  $\nu$  (114) have been used. Replacing  $\mathbf{y}_b$  and  $\mathbf{x}_b$  by its expressions (112) and (113), respectively, and after some manipulations, another form of  $\mathbf{R}_{ab}$  is obtained:

$$\mathbf{R}_{ab} = \mathbf{I} + \frac{2}{\rho^2} [\nu \mathbf{x}_a \mathbf{y}_a^\top - \|\mathbf{y}_a\|^2 \mathbf{x}_a \mathbf{x}_a^\top - \mathbf{y}_a \mathbf{y}_a^\top - 2 \mathbf{y}_a \mathbf{x}_a^\top] \quad (116)$$

Finally,  $\mathbf{R}_b$  can be written as a function of the elements in  $Rtn_a$ :

$$\mathbf{R}_b = \mathbf{R}_a + \frac{2}{\rho^2} [\nu \mathbf{t}_a \mathbf{n}_a^\top - \mathbf{t}_a \mathbf{t}_a^\top \mathbf{R}_a - \|\mathbf{t}_a\|^2 \mathbf{R}_a \mathbf{n}_a \mathbf{n}_a^\top - 2 \mathbf{R}_a \mathbf{n}_a \mathbf{t}_a^\top \mathbf{R}_a]$$

### 5.3.1 Relations for the rotation axes and angles

Now we want to find the expression of the rotation axis and angle of  $\mathbf{R}_b$  as a direct function of the axis and angle corresponding to  $\mathbf{R}_a$ . The following well-known relations will be useful in the developments. Being  $\mathbf{R}$  a general rotation matrix, its corresponding rotation axis  $\mathbf{u}$  and rotation angle  $\theta$  can be retrieved from:

$$\begin{aligned} \cos(\theta) &= \frac{\text{trace}(\mathbf{R}) - 1}{2} \\ [\mathbf{u}]_\times &= \frac{\mathbf{R} - \mathbf{R}^\top}{2 \sin(\theta)} \\ \mathbf{u} &= \frac{\mathbf{k}'}{\|\mathbf{k}'\|}; \quad \mathbf{k}' = \begin{bmatrix} r_{32} - r_{23} \\ r_{13} - r_{31} \\ r_{21} - r_{12} \end{bmatrix} \end{aligned} \quad (117)$$

where  $r_{ij}$  are components of the rotation matrix. In order to avoid the ambiguity due to the double solution:  $\{\mathbf{u}, \theta\}$  and  $\{-\mathbf{u}, -\theta\}$ , we have assumed that the positive angle is always chosen. In the case of the rotation matrix  $\mathbf{R}_{ab}$  of the form (116), the corresponding angle  $\theta_{ab}$  is:

$$\cos(\theta_{ab}) = \frac{(\mathbf{x}_a^\top \mathbf{y}_a + 2)^2 - \|\mathbf{x}_a \times \mathbf{y}_a\|^2}{(\mathbf{x}_a^\top \mathbf{y}_a + 2)^2 + \|\mathbf{x}_a \times \mathbf{y}_a\|^2}$$

As  $(\mathbf{x}_a^\top \mathbf{y}_a + 2)$  is always strictly positive, we can divide by its square in order to get a more compact form for the trigonometric functions of this angle:

$$\begin{aligned}\cos(\theta_{ab}) &= \frac{1 - \eta^2}{1 + \eta^2} \\ \sin(\theta_{ab}) &= \frac{2\eta}{1 + \eta^2} \\ \tan(\theta_{ab}) &= \frac{2\eta}{1 - \eta^2} \\ \tan \frac{\theta_{ab}}{2} &= \eta\end{aligned}$$

Being  $\eta$ :

$$\eta = \frac{\|\mathbf{x}_a \times \mathbf{y}_a\|}{(\mathbf{x}_a^\top \mathbf{y}_a + 2)} \quad (118)$$

The rotation axis  $\mathbf{u}_{ab}$  is obtained from the vector  $\mathbf{k}'$  in (117) which, for the case at hand, can be written as:

$$\mathbf{k}' = \begin{bmatrix} r_{32} - r_{23} \\ r_{13} - r_{31} \\ r_{21} - r_{12} \end{bmatrix} = \frac{4}{\rho^2} (\mathbf{y}_a^\top \mathbf{x}_a + 2) (\mathbf{y}_a \times \mathbf{x}_a)$$

As the norm of this vector results:

$$\|\mathbf{k}'\| = \frac{4}{\rho^2} (\mathbf{y}_a^\top \mathbf{x}_a + 2) \|\mathbf{y}_a \times \mathbf{x}_a\|$$

the unitary  $\mathbf{u}_{ab}$  vector will be:

$$\mathbf{u}_{ab} = \frac{\mathbf{y}_a \times \mathbf{x}_a}{\|\mathbf{y}_a \times \mathbf{x}_a\|}$$

This means that we already have the axis and angle corresponding to the "incremental" rotation  $\mathbf{R}_{ab}$  as a function of  $Rtn_a$ :

$$\tan \frac{\theta_{ab}}{2} = \frac{\|\mathbf{n}_a \times \mathbf{R}_a^\top \mathbf{t}_a\|}{(\mathbf{n}_a^\top \mathbf{R}_a^\top \mathbf{t}_a + 2)} \quad (119)$$

$$\mathbf{u}_{ab} = \frac{\mathbf{n}_a \times \mathbf{R}_a^\top \mathbf{t}_a}{\|\mathbf{n}_a \times \mathbf{R}_a^\top \mathbf{t}_a\|} \quad (120)$$

As  $\mathbf{R}_{ba} = \mathbf{R}_{ab}^\top$ , and as we always select the positive rotation angle from any rotation matrix, it is clear that:

$$\begin{aligned}\theta_{ba} &= \theta_{ab} \\ \mathbf{u}_{ba} &= -\mathbf{u}_{ab}\end{aligned}$$

In order to get a suitable relation between the axes and angles of rotation, we will use now the relations for the composition of two rotations from the quaternion product.

### Making use of the definition of quaternion product

A generic quaternion has a real part and a pure part:

$$\mathring{\mathbf{q}} = \begin{bmatrix} \alpha \\ \boldsymbol{\beta} \end{bmatrix}$$

Any given rotation,  $\mathbf{R}$ , can be expressed by the three parameters given by a unitary quaternion:

$$\alpha = \cos \frac{\theta}{2}; \quad \boldsymbol{\beta} = \sin \frac{\theta}{2} \mathbf{u}$$

being,  $\theta$  and  $\mathbf{u}$ , as usual, the angle and axis corresponding to the rotation matrix  $\mathbf{R}$ . Consider again our rotation matrix  $\mathbf{R}_b$ , which is the composition of the rotations  $\mathbf{R}_a$  and  $\mathbf{R}_{ab}$ :

$$\mathbf{R}_b = \mathbf{R}_a \mathbf{R}_{ab}$$

The angles and axes of a composition of two rotations are related as follows, according to the quaternion composition rule:

$$\begin{aligned} \mathring{\mathbf{q}}_b &= \mathring{\mathbf{q}}_a \circ \mathring{\mathbf{q}}_{ab} \\ \alpha_b &= \alpha_a \alpha_{ab} - \boldsymbol{\beta}_a^\top \boldsymbol{\beta}_{ab} \\ \boldsymbol{\beta}_b &= \boldsymbol{\beta}_a \times \boldsymbol{\beta}_{ab} + \alpha_a \boldsymbol{\beta}_{ab} + \alpha_{ab} \boldsymbol{\beta}_a \end{aligned}$$

Hence, the following relations hold:

$$\begin{aligned} \cos \frac{\theta_b}{2} &= \cos \frac{\theta_a}{2} \cos \frac{\theta_{ab}}{2} - \sin \frac{\theta_a}{2} \sin \frac{\theta_{ab}}{2} \mathbf{u}_a^\top \mathbf{u}_{ab} \\ \sin \frac{\theta_b}{2} \mathbf{u}_b &= \cos \frac{\theta_{ab}}{2} \sin \frac{\theta_a}{2} \mathbf{u}_a + \cos \frac{\theta_a}{2} \sin \frac{\theta_{ab}}{2} \mathbf{u}_{ab} + \sin \frac{\theta_a}{2} \sin \frac{\theta_{ab}}{2} (\mathbf{u}_a \times \mathbf{u}_{ab}) \end{aligned}$$

From these relations, we can derive two particular cases, that may be helpful for future works:

- When the axis of rotation,  $\mathbf{u}_a$ , is normal to the plane defined by  $\mathbf{t}_a$  and  $\mathbf{n}_a$ . In this case,  $\mathbf{R}_a^\top \mathbf{t}_a$  is also on this same plane and, since  $\mathbf{u}_{ab}$  was defined (see (120)) as

$$\mathbf{u}_{ab} = \frac{\mathbf{k}_a}{\|\mathbf{k}_a\|}; \quad \mathbf{k}_a = \mathbf{y}_a \times \mathbf{x}_a = \mathbf{n}_a \times \mathbf{R}_a^\top \mathbf{t}_a$$

verifying the following relations:

$$\mathbf{u}_a^\top \mathbf{u}_{ab} = 1; \quad \mathbf{u}_a \times \mathbf{u}_{ab} = \mathbf{0}$$

what means that  $\mathbf{u}_{ab} = \mathbf{u}_a$

- Another particular case is when  $\mathbf{u}_a = \pm \mathbf{n}_a$ . In this case (among others), the conditions verified are:

$$\mathbf{u}_a^\top \mathbf{u}_{ab} = 0; \quad \|\mathbf{u}_a \times \mathbf{u}_{ab}\| = 1$$

what means that  $\mathbf{u}_{ab} \perp \mathbf{u}_a$ .

Resuming our analysis after these comments on particular cases, simpler relations can be obtained if we transform the relations into tangent-dependent relations, dividing both by  $\cos \frac{\theta_a}{2} \cos \frac{\theta_{ab}}{2}$ :

$$\begin{aligned} \frac{\cos \frac{\theta_b}{2}}{\cos \frac{\theta_a}{2} \cos \frac{\theta_{ab}}{2}} &= 1 - \tan \frac{\theta_a}{2} \tan \frac{\theta_{ab}}{2} \mathbf{u}_a^\top \mathbf{u}_{ab} \\ \frac{\sin \frac{\theta_b}{2}}{\cos \frac{\theta_a}{2} \cos \frac{\theta_{ab}}{2}} \mathbf{u}_b &= \tan \frac{\theta_a}{2} \mathbf{u}_a + \tan \frac{\theta_{ab}}{2} \mathbf{u}_{ab} + \tan \frac{\theta_a}{2} \tan \frac{\theta_{ab}}{2} (\mathbf{u}_a \times \mathbf{u}_{ab}) \end{aligned}$$

Dividing again the second one by the first one:

$$\mathbf{r}_b = \frac{\mathbf{r}_a + \mathbf{r}_{ab} + \mathbf{r}_a \times \mathbf{r}_{ab}}{1 - \mathbf{r}_a^\top \mathbf{r}_{ab}} \quad (121)$$

where we are combining axis and angle of rotation in the following parametrization:

$$\mathbf{r}_e = \tan \frac{\theta_e}{2} \mathbf{u}_e; \quad e = \{a, b, ab\} \quad (122)$$

From (119) and (120), we knew that:

$$\mathbf{r}_{ab} = \frac{\mathbf{n}_a \times \mathbf{R}_a^\top \mathbf{t}_a}{(\mathbf{n}_a^\top \mathbf{R}_a^\top \mathbf{t}_a + 2)} \quad (123)$$

We could also write the expression of  $\mathbf{r}_a$  in terms of  $\mathbf{r}_b$  and  $\mathbf{r}_{ab}$ :

$$\mathbf{r}_a = \frac{\mathbf{r}_b - \mathbf{r}_{ab} - \mathbf{r}_b \times \mathbf{r}_{ab}}{1 + \mathbf{r}_b^\top \mathbf{r}_{ab}}$$

which comes straightaway from (121), using the fact that  $\mathbf{r}_{ba} = -\mathbf{r}_{ab}$ . Finally, it is interesting to write  $\mathbf{R}_e$  in terms of  $\mathbf{r}_e$ . This is easily done starting from Rodrigues' expression of the rotation matrix:

$$\mathbf{R}_e = \mathbf{I} + \sin(\theta_e)[\mathbf{u}_e]_\times + (1 - \cos(\theta_e))[\mathbf{u}_e]_\times^2$$

Expanding the sine and cosine as functions of the half angle, and dividing by  $\cos^2(\theta_e/2)$ ,

$$\mathbf{R}_e = \mathbf{I} + 2 \cos^2 \frac{\theta_e}{2} ([\mathbf{r}_e]_\times^2 + [\mathbf{r}_e]_\times)$$

As  $\cos^2(\theta_e/2)$  can be written as a function of the tangent:

$$\cos^2 \frac{\theta_e}{2} = \frac{1}{1 + \tan^2 \frac{\theta_e}{2}} = \frac{1}{1 + \|\mathbf{r}_e\|^2}$$

The final expression is then:

$$\mathbf{R}_e = \mathbf{I} + \frac{2}{1 + \|\mathbf{r}_e\|^2} ([\mathbf{r}_e]_\times^2 + [\mathbf{r}_e]_\times) \quad (124)$$



and for the inverse rotation:

$$\mathbf{R}_e^\top = \mathbf{I} + \frac{2}{1 + \|\mathbf{r}_e\|^2} ([\mathbf{r}_e]_\times^2 - [\mathbf{r}_e]_\times) \quad (125)$$

Another equivalent form is:

$$\begin{aligned} \mathbf{R}_e &= \frac{1}{1 + \|\mathbf{r}_e\|^2} ((1 - \|\mathbf{r}_e\|^2) \mathbf{I} + 2[\mathbf{r}_e]_\times + 2\mathbf{r}_e \mathbf{r}_e^\top) \\ \mathbf{R}_e^\top &= \frac{1}{1 + \|\mathbf{r}_e\|^2} ((1 - \|\mathbf{r}_e\|^2) \mathbf{I} - 2[\mathbf{r}_e]_\times + 2\mathbf{r}_e \mathbf{r}_e^\top) \end{aligned}$$

As a collateral result, our rotation parametrization allows us to write:

$$\begin{aligned} (\mathbf{I} + \mathbf{R}_e)^{-1} &= \frac{1}{2} (\mathbf{I} - [\mathbf{r}_e]_\times) \\ (\mathbf{I} + \mathbf{R}_e^\top)^{-1} &= \frac{1}{2} (\mathbf{I} + [\mathbf{r}_e]_\times) \end{aligned} \quad (126)$$

Using the form given in (125) for  $\mathbf{R}_a^\top$  in (123) and replacing the resulting expression of  $\mathbf{r}_{ab}$  in (121), the following relation can be found:

$$\mathbf{r}_b = \frac{\mathbf{n}_a \times (\mathbf{t}_a \times \mathbf{r}_a) + 2\mathbf{r}_a + \mathbf{n}_a (\mathbf{t}_a^\top \mathbf{r}_a) + (\mathbf{n}_a \times \mathbf{t}_a)}{2 + \mathbf{n}_a^\top \mathbf{t}_a + \mathbf{r}_a^\top (\mathbf{n}_a \times \mathbf{t}_a)}$$

This relation can also be written as:

$$\mathbf{r}_b = \frac{[(2 - \mathbf{n}_a^\top \mathbf{t}_a) \mathbf{I} + \mathbf{t}_a \mathbf{n}_a^\top + \mathbf{n}_a \mathbf{t}_a^\top] \mathbf{r}_a + [\mathbf{n}_a]_\times \mathbf{t}_a}{2 + \mathbf{n}_a^\top \mathbf{t}_a + \mathbf{n}_a^\top [\mathbf{t}_a]_\times \mathbf{r}_a}$$

In the particular case of pure translation, the false solution has the form:

$$\mathbf{r}_a = \mathbf{0} \implies \mathbf{r}_b = \frac{\mathbf{n}_a \times \mathbf{t}_a}{2 + \mathbf{n}_a^\top \mathbf{t}_a}$$

## 5.4 Relations for translation and normal vectors

We will derive now the relations between translation vectors and normal vectors corresponding to the different solutions, starting from the relations among the  $\mathbf{y}$  and  $\mathbf{x}$  given in Section 5.2. By simple substitution of (46) and (47) in (112) we can write

$$\mathbf{n}_b = \frac{1}{\rho} \left( \|\mathbf{t}_a\| \mathbf{n}_a + \frac{2}{\|\mathbf{t}_a\|} \mathbf{R}_a^\top \mathbf{t}_a \right)$$

Again, the subindexes  $a$  and  $b$  are exchangeable in this expression. Doing the same substitution in (113) we get

$$\mathbf{t}_b = \frac{\|\mathbf{t}_a\|}{\rho} \mathbf{R}_b (\nu \mathbf{n}_a - \mathbf{R}_a^\top \mathbf{t}_a) \quad (127)$$

The coefficients  $\rho$  and  $\nu$  can be written directly as functions of  $Rtn$

$$\rho = \sqrt{\|\mathbf{n}_e \times \mathbf{R}_e^\top \mathbf{t}_e\|^2 + (\mathbf{n}_e^\top \mathbf{R}_e^\top \mathbf{t}_e + 2)^2} = \sqrt{\|\mathbf{t}_e\|^2 + 4\mathbf{n}_e^\top \mathbf{R}_e^\top \mathbf{t}_e + 4} = \sqrt{\|2\mathbf{R}_e \mathbf{n}_e + \mathbf{t}_e\|^2}; \quad e = \{a, b\}$$

that can be written in a more closed form as:

$$\begin{aligned} \rho &= \|\mathbf{t}_e\| > 1; & e &= \{a, b\} \\ \nu &= 2(\mathbf{n}_e^\top \mathbf{R}_e^\top \mathbf{t}_e + 1) > 0 \end{aligned}$$

The condition  $\nu > 0$  is evident from (76). On the other hand, the less evident condition  $\rho > 1$ , is proved in Appendix C.5. The expression of  $\mathbf{t}$  depends not only on  $\mathbf{R}_a$ , but also on  $\mathbf{R}_b$ . Recalling that  $\mathbf{R}_b$  could be written as:

$$\mathbf{R}_b = \mathbf{R}_a \mathbf{R}_{ab}$$

being  $\mathbf{R}_{ab}$  given by (116), and substituting in (127), we get, after some manipulations:

$$\mathbf{t}_b = \frac{1}{\rho} \mathbf{R}_a (\|\mathbf{y}_a\|^2 \mathbf{x}_a + 2 \mathbf{y}_a)$$

From this, a more compact relation between the two translation vectors is obtained:

$$\mathbf{t}_b = \frac{\|\mathbf{t}_a\|}{\rho} \mathbf{R}_a (2 \mathbf{n}_a + \mathbf{R}_a^\top \mathbf{t}_a)$$

In view of this, we can rewrite the expression for  $\mathbf{n}_b$  previously given in a way more similar to that of  $\mathbf{t}_b$ :

$$\mathbf{n}_b = \frac{1}{\rho} \left( \frac{\|\mathbf{t}_a\|}{2} 2 \mathbf{n}_a + \frac{2}{\|\mathbf{t}_a\|} \mathbf{R}_a^\top \mathbf{t}_a \right)$$

This expression makes evident a particularity in the relation of both solutions of the homography decomposition, when  $\|\mathbf{t}_e\| = 2$ . If this is the case, both solutions are coupled in a peculiar way:

$$\|\mathbf{t}_e\| = 2 \implies \begin{cases} \mathbf{n}_b = \frac{\mathbf{R}_a^\top \mathbf{t}_b}{\|\mathbf{t}_b\|} \\ \mathbf{n}_a = \frac{\mathbf{R}_b^\top \mathbf{t}_a}{\|\mathbf{t}_a\|} \end{cases}$$

If we want to infer a geometric interpretation of this fact, it must be taken into account that we are using a normalized homography matrix, this means that the distances are normalized up to  $d^*$ , the distance of the plane to the origin of the reference coordinate system. Hence,  $\|\mathbf{t}_e\| = 2$  has to be understood as the magnitude of the translation being double the distance  $d^*$ . This means that we can retrieve the unknown scale factor  $d^*$  with a very simple experiment: put the camera in front of the object, move the camera backwards until you detect that the previous equality becomes true, then the scale factor  $d^*$  is equal to half the displacement made. It may be worth considering the interest of the previous relation for self-calibration purposes in future works.

## 6 Position-based visual servoing based on analytical decomposition

We develop in this section a new vision-based control method for positioning a camera with respect to an unknown planar object as an application of the analytic homography decomposition, introduced in the previous sections. Standard methods use non-linear state observers based on homography decomposition. In the general case, there are two possible solutions to the decomposition problem, as we have already seen. Thus, some additional “a priori” information must be used. In this section, we propose to use the analytical decomposition of the homography matrix in order to define a new control objective that allows to discard the false solution without any “a priori” information. The stability of the proposed control law has been proved.

### 6.1 Introduction

Visual servoing can be stated as a non-linear output regulation problem [2]. The output is the image acquired by a camera mounted on a dynamic system. The state of the camera is thus accessible via a non-linear map. For this reason, positioning tasks have been defined using the so-called teach-by-showing technique [2]. The camera is moved to a reference position and the corresponding reference image is stored. Then, starting from a different camera position the control objective is to move the camera such that the current image will coincide to the reference one. In our work, we suppose that the observed object is a plane in the Cartesian space. One solution to the control problem is to build a non-linear observer of the state. This can be done using several output measurements. The problem is that, when considering real-time applications, we should process as few observations as possible. In [3, 4, 6, 5] the authors have built a non-linear state observer using additional information (the normal to the plane, vanishing points, ...). In this case only the current and the reference observations are needed. In this paper, we intend to perform vision-based control without knowing any a priori information. To do this we need more observations. This can be done by moving the camera. If we move the camera and the state is not observable we may have some problems. For this reason, we propose in this section a different approach. We define a new control objective in order to move the camera by keeping a bounded error and in order to obtain the necessary information for the state observer [9].

### 6.2 Vision-based control

We consider the control of the following nonlinear system:

$$\dot{\mathbf{x}} = \mathbf{g}(\mathbf{x}, \mathbf{v}) \quad (128)$$

$$\mathbf{y} = \mathbf{h}(\mathbf{x}, \boldsymbol{\mu}) \quad (129)$$

where  $\mathbf{x} \in \mathbb{SE}(3)$  is the state (i.e. the camera pose),  $\mathbf{y}$  is the output of the camera and  $\mathbf{v}$  is the control input (i.e. the camera velocity). The output of the camera depends on the state and on some parameters  $\boldsymbol{\mu}$  (e.g. the normal of the plane, ...). Let  $\mathbf{x}^*$  be the reference state of the camera. Without loss of generality one can choose  $\mathbf{x}^* = e$ , where  $e$  is the identity element of  $\mathbb{SE}(3)$ . Then, the reference output is  $\mathbf{y}^* = \mathbf{h}(\mathbf{x}^*, \boldsymbol{\mu})$ . If we suppose that the camera displacement is not too big, we can choose a state vector:

$$\mathbf{x} = \begin{bmatrix} \mathbf{t} \\ \mathbf{r} \end{bmatrix}$$

where  $\mathbf{t}$  is the translation vector and  $\mathbf{r}$  is:

$$\mathbf{r} = \tan\left(\frac{\theta}{2}\right) \mathbf{u}$$

according to the chosen rotation parametrization ( $\mathbf{u}$  and  $\theta$  are the axis and angle of rotation, respectively). On the other hand, the control input is a velocity screw of the form:

$$\mathbf{v} = \begin{bmatrix} \mathbf{v} \\ \boldsymbol{\omega} \end{bmatrix}$$

being  $\mathbf{v}$  and  $\boldsymbol{\omega}$  the specified linear and angular velocities, respectively. In other words, the open-loop system under consideration is a velocity-driven robot, whose dynamics is neglected, together with a visual sensor providing some reference points in the image  $\mathbf{p}_i$ . The input signal is a velocity setpoint and it is assumed that the robot instantaneously reaches the commanded velocity. Then, the system can be viewed as a pure integrator in Cartesian space plus a non-linear transformation from Cartesian space to image space: From this, the position and orientation derivatives of the desired camera pose, respect to

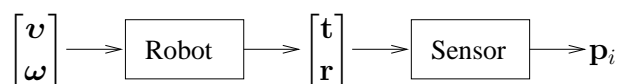


Figure 4: System's inputs and outputs

the current one, are:

$$\dot{\mathbf{x}} = \begin{bmatrix} \dot{\mathbf{t}} \\ \dot{\mathbf{r}} \end{bmatrix} = \begin{bmatrix} \mathbf{I} & -[\mathbf{t}]_{\times} \\ \mathbf{0} & \mathbf{J}_{\omega} \end{bmatrix} \begin{bmatrix} \mathbf{v} \\ \boldsymbol{\omega} \end{bmatrix} \quad (130)$$

where  $\mathbf{J}_{\omega}$  is the Jacobian relating the derivative of the chosen rotation parametrization to the angular velocity commanded to the system:

$$\dot{\mathbf{r}} = \mathbf{J}_{\omega} \boldsymbol{\omega}$$

### 6.2.1 Homography-based state observer with full information

The state observation is intended to be made from the homography decomposition. In [6] a new class of visual servoing methods has been proposed, based on the estimation of the homography matrix  $\mathbf{H}$ . An efficient real-time algorithm for estimating the homography from raw images has been proposed in [7]:

$$\mathbf{H} = \operatorname{argmin} \|\mathbf{y}(\mathbf{H}) - \mathbf{y}^*\|$$

We already know that there exist 4 solutions, in the general case, for the homography decomposition problem, two of them being the "opposites" of the other two.

$$Rtn_a = \{\mathbf{R}_a, \mathbf{t}_a, \mathbf{n}_a\}; \quad Rtn_{a-} = \{\mathbf{R}_a, -\mathbf{t}_a, -\mathbf{n}_a\} \quad (131)$$

$$Rtn_b = \{\mathbf{R}_b, \mathbf{t}_b, \mathbf{n}_b\}; \quad Rtn_{b-} = \{\mathbf{R}_b, -\mathbf{t}_b, -\mathbf{n}_b\} \quad (132)$$

These can be reduced to only two solutions applying the constraint that all the reference points must be visible from the camera (*visibility constraint*). We will assume along the development that the two solutions verifying this constraint are  $Rtn_a$  and  $Rtn_b$  and that, among them,  $Rtn_a$  is the "true" solution. These solutions are related according to (102)-(104). In practice, in order to determine which one is the good solution, we can use an approximation of the normal  $\mathbf{n}^*$ . Thus, having an approximated parameter vector  $\hat{\boldsymbol{\mu}}$  we build a non-linear state observer:

$$\hat{\mathbf{x}} = \varphi(\mathbf{y}(\mathbf{x}), \mathbf{y}^*, \hat{\boldsymbol{\mu}})$$

### 6.3 A modified control objective

A control law based on the Cartesian error on position and orientation is being developed. The error between the current relative camera pose and the desired one is obtained from the homography decomposition. However, we assume that we are not able to discard one of the two possible solutions,  $Rtn_a$  or  $Rtn_b$ , as a false one. This situation would arise, for instance, if we do not have any a priori knowledge about the true normal to the plane. In this case, we want to define an error function involving a combination of the true and false solutions:

$$\mathbf{e} = \begin{bmatrix} \mathbf{e}_t(\mathbf{t}_a, \mathbf{t}_b) \\ \mathbf{e}_r(\mathbf{r}_a, \mathbf{r}_b) \end{bmatrix}$$

where  $\mathbf{e}_t$  and  $\mathbf{e}_r$  are the functions defining the translation and orientation error, respectively. It is clear that this function should be symmetric, in the sense that, since we cannot distinguish which solution is the true one, we have no reason to weight one of them more than the other. On the other hand, we want that the closed-loop system resulting from this control law is stable and makes the system to converge to an equilibrium in which the current camera frame is coincident with the desired one. It will be shown that a control law based on the *average of the two possible solutions* can be used, such that the system will always converge, not to the mentioned desired equilibrium, but to another particular configuration in space.

Nevertheless, we will see that the system converges in such a way that we are always able to discard the false solution. Once the true solution has been identified, the camera can be controlled using only this solution, taking the system to the desired equilibrium. We describe next this averaged control law, and we will see that, taking advantage of the new analytic formulation for the homography decomposition problem, we are able to prove the stability of such a control law.

### 6.3.1 Mean-based control law

For simplicity in the upcoming development, the solution  $Rtn_a$  is supposed to be the unknown right one. That is, it gives the true position and orientation of the desired reference frame with respect to the current one. As a task function [10] to be minimized, we define a translation and orientation error:

$$\mathbf{e} = \begin{bmatrix} \mathbf{e}_t \\ \mathbf{e}_r \end{bmatrix} = \begin{bmatrix} \mathbf{t}_m \\ \mathbf{r}_m \end{bmatrix}$$

Being  $\mathbf{t}_m$  and  $\mathbf{r}_m$  the translation and orientation means, respectively, computed as follows:

$$\mathbf{t}_m = \frac{\mathbf{t}_a + \mathbf{t}_b}{2} \quad (133)$$

$$\mathbf{r}_m \Leftarrow \mathbf{R}_m = \mathbf{R}_a (\mathbf{R}_a^\top \mathbf{R}_b)^{1/2} \quad (134)$$

The rotation matrix,  $\mathbf{R}_m$ , average of  $\mathbf{R}_a$  and  $\mathbf{R}_b$ , computed in such way is defined as the *Riemmanian mean of two rotations* (for more details, see [8]). From  $\mathbf{R}_m$ , according to our rotation parametrization (122), we obtain  $\mathbf{r}_m$ . Using the given relations between the two solutions (102), (104) and (108), it is clear that we could write  $\mathbf{t}_m$  and  $\mathbf{R}_m$  only as a function of the presumed true solution:  $Rtn_a$ . Then, we can rewrite (130) as:

$$\begin{bmatrix} \dot{\mathbf{t}}_a \\ \dot{\mathbf{r}}_a \end{bmatrix} = \begin{bmatrix} \mathbf{I} & -[\mathbf{t}_a]_\times \\ \mathbf{0} & \mathbf{J}_\omega \end{bmatrix} \begin{bmatrix} \mathbf{v} \\ \boldsymbol{\omega} \end{bmatrix}$$

From the defined task error we can compute the input control action as:

$$\mathbf{v} = \begin{bmatrix} \mathbf{v} \\ \boldsymbol{\omega} \end{bmatrix} = -\lambda \mathbf{e} \quad (135)$$

where  $\lambda$  is a positive scalar, tuning the closed-loop convergence rate. The derivative of the task error is related to the velocity screw, according to some interaction matrix  $\mathbf{L}$  to be determined:

$$\dot{\mathbf{e}} = \mathbf{L} \mathbf{v}$$

Giving the following closed-loop system:

$$\dot{\mathbf{e}} = -\lambda \mathbf{L} \mathbf{e} \quad (136)$$

We are now interested in the computation and properties of the interaction matrix  $\mathbf{L}$ . We will identify the components of this matrix as:

$$\begin{aligned} \begin{bmatrix} \dot{\mathbf{e}}_t \\ \dot{\mathbf{e}}_r \end{bmatrix} &= \begin{bmatrix} \mathbf{L}_{11} & \mathbf{L}_{12} \\ \mathbf{L}_{21} & \mathbf{L}_{22} \end{bmatrix} \begin{bmatrix} \mathbf{v} \\ \boldsymbol{\omega} \end{bmatrix} \\ \begin{bmatrix} \dot{\mathbf{e}}_t \\ \dot{\mathbf{e}}_r \end{bmatrix} &= \begin{bmatrix} \frac{\partial \mathbf{e}_t}{\partial \mathbf{t}_a} & \frac{\partial \mathbf{e}_t}{\partial \mathbf{r}_a} \\ \frac{\partial \mathbf{e}_r}{\partial \mathbf{t}_a} & \frac{\partial \mathbf{e}_r}{\partial \mathbf{r}_a} \end{bmatrix} \begin{bmatrix} \mathbf{I} & -[\mathbf{t}_a]_{\times} \\ \mathbf{0} & \mathbf{J}_{\omega} \end{bmatrix} \begin{bmatrix} \mathbf{v} \\ \boldsymbol{\omega} \end{bmatrix} \\ \mathbf{L}_{11} &= \frac{\partial \mathbf{e}_t}{\partial \mathbf{t}_a} \\ \mathbf{L}_{12} &= -\frac{\partial \mathbf{e}_t}{\partial \mathbf{t}_a} [\mathbf{t}_a]_{\times} + \frac{\partial \mathbf{e}_t}{\partial \mathbf{r}_a} \mathbf{J}_{\omega} \\ \mathbf{L}_{21} &= \frac{\partial \mathbf{e}_r}{\partial \mathbf{t}_a} \\ \mathbf{L}_{22} &= -\frac{\partial \mathbf{e}_r}{\partial \mathbf{t}_a} [\mathbf{t}_a]_{\times} + \frac{\partial \mathbf{e}_r}{\partial \mathbf{r}_a} \mathbf{J}_{\omega} \end{aligned} \quad (137)$$

The following sections are devoted to the computation and analysis of the properties (when possible) of the sub-matrices  $\mathbf{L}_{11}$ ,  $\mathbf{L}_{12}$ ,  $\mathbf{L}_{21}$ ,  $\mathbf{L}_{22}$ . However, before continuing with the control issues of our scheme, we need to develop some more details regarding to the relation of  $\mathbf{r}_m$  and  $\{\mathbf{r}_a, \mathbf{r}_b\}$ . This is what the next subsection is devoted to.

### 6.3.2 Parametrization of the mean of two rotations

As said above, we use as a measure of the orientation error the average of the two rotations  $\mathbf{R}_a$  and  $\mathbf{R}_b$ .

$$\mathbf{R}_m = \mathbf{R}_a (\mathbf{R}_a^{\top} \mathbf{R}_b)^{1/2}$$

As we already know,  $\mathbf{R}_b$  can be written as a function of  $Rtn_a$ . Using this, we want to find an expression of our parametrization of the orientation mean,  $\mathbf{r}_m$ , as a function of  $\mathbf{r}_a$ . According to relation (115), that we rewrite here for convenience:

$$\mathbf{R}_b = \mathbf{R}_a \mathbf{R}_{ab}$$

$\mathbf{R}_b$  is the composition of these two rotations. Using this,  $\mathbf{R}_m$  can also be written as the composition of two rotations:

$$\mathbf{R}_m = \mathbf{R}_a \mathbf{R}_h = \mathbf{R}_a \mathbf{R}_{ab}^{1/2}$$

where we have called  $\mathbf{R}_h$  the "half" rotation corresponding to  $\mathbf{R}_{ab}$ , that is a rotation of half the angle,  $\theta_{ab}/2$ , about the same axis  $\mathbf{u}_{ab}$ . We have already got the expression for the

parametrization  $\mathbf{r}$  of a composition of two rotations, which was given in (121). Using this relation for the composition of  $\mathbf{r}_a$  and  $\mathbf{r}_h$ :

$$\mathbf{r}_m = \frac{\mathbf{r}_a + \mathbf{r}_h + \mathbf{r}_a \times \mathbf{r}_h}{1 - \mathbf{r}_a^\top \mathbf{r}_h} \quad (138)$$

where<sup>11</sup>

$$\mathbf{r}_h = \tan \frac{\theta_{ab}}{4} \mathbf{u}_{ab}$$

We had previously computed the expressions for  $\tan(\theta_{ab}/2)$  and  $\mathbf{u}_{ab}$ , which are given in (119) and (120), respectively. Making use of the trigonometric relation:

$$\tan \frac{\alpha}{2} = \frac{\pm \sqrt{1 + \tan^2 \alpha} - 1}{\tan \alpha}; \quad \text{for any angle } \alpha$$

and considering normalized angles,  $\theta_{ab} \in [-\pi, \pi]$ , then  $\theta_{ab}/4 \in [-\pi/4, \pi/4]$ , we can obtain the following relation without the plus/minus ambiguity:

$$\tan \frac{\theta_{ab}}{4} = \frac{\sqrt{1 + \tan^2(\theta_{ab}/2)} - 1}{\tan(\theta_{ab}/2)}$$

From this relation, using (119) and (120), we obtain the desired form for  $\mathbf{r}_h$ :

$$\mathbf{r}_h = \frac{\rho - (2 + \mathbf{n}_a^\top \mathbf{t}_a^*)}{\|\mathbf{n}_a \times \mathbf{t}_a^*\|^2} (\mathbf{n}_a \times \mathbf{t}_a^*) \quad (139)$$

being, as usual:

$$\mathbf{t}_a^* = \mathbf{R}_a^\top \mathbf{t}_a$$

As a conclusion, the expressions (138) and (139) give us the desired relation between  $\mathbf{r}_m$  and the elements in  $Rtn_a$ .

### Computation of $\mathbf{J}_\omega$

Previous to studying the interaction sub-matrices, we will find the expression for matrix  $\mathbf{J}_\omega$  in (130). This Jacobian relates our orientation parametrization to the angular velocity commanded to the system:

$$\dot{\mathbf{r}}_a = \mathbf{J}_\omega \boldsymbol{\omega}$$

The derivation of this Jacobian is easier if we consider the derivative of a quaternion and its relation with the angular velocity. As described in [10] (page 37), this relation is given by:

$$\frac{d \overset{\circ}{\mathbf{q}}}{dt} = \frac{1}{2} (\boldsymbol{\omega} \circ \overset{\circ}{\mathbf{q}})$$

<sup>11</sup>An experimental observation that may be helpful sometime is that it seems  $\mathbf{u}_m$  is always on the plane defined by  $\mathbf{u}_a$  and  $\mathbf{u}_b$ .



where  $\overset{\circ}{\mathbf{q}}$  is the unitary quaternion used as a representation of a rotation and  $\circ$  means for the quaternion product. As our orientation parametrization is close to the quaternion representation for a rotation, this relation is very useful. Developing the quaternion product:

$$\boldsymbol{\omega} \circ \overset{\circ}{\mathbf{q}} = \begin{bmatrix} 0 \\ \boldsymbol{\omega} \end{bmatrix} \circ \begin{bmatrix} \alpha \\ \boldsymbol{\beta} \end{bmatrix} = \begin{bmatrix} -\boldsymbol{\omega}^\top \boldsymbol{\beta} \\ \boldsymbol{\omega} \times \boldsymbol{\beta} + \alpha \boldsymbol{\omega} \end{bmatrix}$$

being  $\alpha$  and  $\boldsymbol{\beta}$  the real and pure parts, respectively, of  $\overset{\circ}{\mathbf{q}}$ . Then

$$\frac{d \overset{\circ}{\mathbf{q}}}{dt} = \begin{bmatrix} \dot{\alpha} \\ \dot{\boldsymbol{\beta}} \end{bmatrix} = \begin{bmatrix} -\frac{1}{2} \boldsymbol{\beta}^\top \boldsymbol{\omega} \\ \frac{1}{2} (\alpha \mathbf{I} - [\boldsymbol{\beta}]_\times) \boldsymbol{\omega} \end{bmatrix} \quad (140)$$

As our rotation parametrization,  $\mathbf{r}$ , can be obtained from the quaternion as:

$$\mathbf{r} = \frac{\boldsymbol{\beta}}{\alpha}$$

The time derivative of  $\mathbf{r}_a$  will be:

$$\dot{\mathbf{r}}_a = \frac{\alpha \dot{\boldsymbol{\beta}} - \dot{\alpha} \boldsymbol{\beta}}{\alpha^2}$$

replacing the expressions obtained in (140) for  $\dot{\alpha}$  and  $\dot{\boldsymbol{\beta}}$ , we can write:

$$\dot{\mathbf{r}}_a = \frac{1}{2\alpha^2} \left( \alpha^2 \mathbf{I} - \alpha [\boldsymbol{\omega}]_\times + \boldsymbol{\beta} \boldsymbol{\beta}^\top \right) \boldsymbol{\omega}$$

which can be put in terms of  $\mathbf{r}_a$ , providing the desired Jacobian:

$$\dot{\mathbf{r}}_a = \mathbf{J}_\omega \boldsymbol{\omega}; \quad \mathbf{J}_\omega = \frac{1}{2} (\mathbf{I} - [\mathbf{r}_a]_\times + \mathbf{r}_a \mathbf{r}_a^\top) \quad (141)$$

Using (125), another way of giving matrix  $\mathbf{J}_\omega$  is:

$$\mathbf{J}_\omega = \frac{1 + \|\mathbf{r}_a\|^2}{4} (\mathbf{I} + \mathbf{R}_a^\top) \quad (142)$$

From (126), we can easily write the expression for the inverse of this matrix:

$$\mathbf{J}_\omega^{-1} = \frac{2}{1 + \|\mathbf{r}_a\|^2} (\mathbf{I} + [\mathbf{r}_a]_\times)$$

### Computation of $\mathbf{L}_{11}$

The translation error was defined as the average of the two solutions for the translation vector:

$$\mathbf{e}_t = \mathbf{t}_m = \frac{\mathbf{t}_a + \mathbf{t}_b}{2} \quad (143)$$

$\mathbf{L}_{11}$  is then:

$$\mathbf{L}_{11} = \frac{\partial \mathbf{e}_t}{\partial \mathbf{t}_a} = \frac{1}{2} \left( \frac{\partial \mathbf{t}_b}{\partial \mathbf{t}_a} + \mathbf{I} \right)$$

From (102) and using:

$$\frac{\partial \|\mathbf{t}_a\|}{\partial \mathbf{t}_a} = \frac{\mathbf{t}_a}{\|\mathbf{t}_a\|}; \quad \frac{\partial \|\mathbf{t}_a\|^2}{\partial \mathbf{t}_a} = 2 \mathbf{t}_a; \quad \frac{\partial \rho}{\partial \mathbf{t}_a} = \frac{1}{\rho} (\mathbf{t}_a + 2 \mathbf{R}_a \mathbf{n}_a)$$

the expression of the Jacobian  $\mathbf{L}_{11}$  can be found:

$$\mathbf{L}_{11} = \frac{1}{2} \left[ 2\mu_1 \mathbf{n}'_a \mathbf{t}_a^\top + \mu_1 \mathbf{t}_a \mathbf{t}_a^\top - 4\mu_2 \mathbf{n}'_a \mathbf{n}'_a{}^\top - 2\mu_2 \mathbf{t}_a \mathbf{n}'_a{}^\top + \mu_3 \mathbf{I} \right] \quad (144)$$

where  $\mathbf{n}'_a$  means for

$$\mathbf{n}'_a = \mathbf{R}_a \mathbf{n}_a$$

and the scalars  $\mu_i$  are:

$$\mu_1 = \frac{1}{\rho \|\mathbf{t}_a\|} - \mu_2; \quad \mu_2 = \frac{\|\mathbf{t}_a\|}{\rho^3}; \quad \mu_3 = \frac{\|\mathbf{t}_a\|}{\rho} + 1 \quad (145)$$

### Computation of $\mathbf{L}_{12}$

For the computation of  $\mathbf{L}_{12}$ , the Jacobian  $\frac{\partial \mathbf{e}_t}{\partial \mathbf{r}_a}$  is needed (see (137)):

$$\frac{\partial \mathbf{e}_t}{\partial \mathbf{r}_a} = \frac{1}{2} \frac{\partial \mathbf{t}_b}{\partial \mathbf{r}_a}$$

as  $\mathbf{t}_a$  is independent from  $\mathbf{r}_a$ . We use  $\mathbf{n}'_a = \mathbf{R}_a \mathbf{n}_a$  as before, and write (102) and  $\rho$  as:

$$\mathbf{t}_b = \frac{\|\mathbf{t}_a\|}{\rho} (2 \mathbf{n}'_a + \mathbf{t}_a); \quad \rho = \sqrt{\|\mathbf{t}_a\|^2 + 4 \mathbf{t}_a^\top \mathbf{n}'_a + 4}$$

Then, using

$$\left[ \frac{\partial \rho}{\partial \mathbf{r}_a} \right]^\top = \left[ \frac{\partial \rho}{\partial \mathbf{n}'_a} \right]^\top \frac{\partial \mathbf{n}'_a}{\partial \mathbf{r}_a}; \quad \frac{\partial \rho}{\partial \mathbf{n}'_a} = \frac{2}{\rho} \mathbf{t}_a^\top$$

we compute  $\frac{\partial \mathbf{n}'_a}{\partial \mathbf{r}_a}$  in an indirect way. The time derivative of  $\mathbf{n}'_a$  is:

$$\frac{d\mathbf{n}'_a}{dt} = \dot{\mathbf{R}}_a \mathbf{n}_a = [\boldsymbol{\omega}]_\times \mathbf{R}_a \mathbf{n}_a = -[\mathbf{n}'_a]_\times \boldsymbol{\omega}$$

as  $\mathbf{n}_a$  is constant. As we have previously seen (141):

$$\boldsymbol{\omega} = \mathbf{J}_\omega^{-1} \dot{\mathbf{r}}_a$$

then, we have:

$$\frac{d\mathbf{n}'_a}{dt} = -[\mathbf{n}'_a]_{\times} \mathbf{J}_{\omega}^{-1} \dot{\mathbf{r}}_a$$

from what,  $\frac{\partial \mathbf{n}'_a}{\partial \mathbf{r}_a}$  can be written as:

$$\frac{\partial \mathbf{n}'_a}{\partial \mathbf{r}_a} = -[\mathbf{n}'_a]_{\times} \mathbf{J}_{\omega}^{-1} = -\mathbf{R}_a [\mathbf{n}_a]_{\times} \mathbf{R}_a^{\top} \mathbf{J}_{\omega}^{-1}$$

After some simple manipulations, we can write:

$$\frac{\partial \mathbf{e}_t}{\partial \mathbf{r}_a} = [2\mu_2 \mathbf{n}'_a \mathbf{t}_a^{\top} + \mu_2 \mathbf{t}_a \mathbf{t}_a^{\top} + (1 - \mu_3) \mathbf{I}] [\mathbf{n}'_a]_{\times} \mathbf{J}_{\omega}^{-1}$$

the coefficients  $\mu_2$  and  $\mu_3$  were defined in (145). From this, we can conclude that the intended Jacobian is (see again (137)):

$$\mathbf{L}_{12} = -\mathbf{L}_{11} [\mathbf{t}_a]_{\times} + [2\mu_2 \mathbf{n}'_a \mathbf{t}_a^{\top} + \mu_2 \mathbf{t}_a \mathbf{t}_a^{\top} + (1 - \mu_3) \mathbf{I}] [\mathbf{n}'_a]_{\times}$$

where, as already said,  $\mathbf{n}'_a$  is:

$$\mathbf{n}'_a = \mathbf{R}_a \mathbf{n}_a$$

After further reduction of this expression, an extremely closed form for  $\mathbf{L}_{12}$  is obtained:

$$\mathbf{L}_{12} = -[\mathbf{e}_t]_{\times} \quad (146)$$

This means that, in a similar way to  $\dot{\mathbf{t}}_a$ :

$$\dot{\mathbf{t}}_a = \mathbf{I} \mathbf{v} + (\boldsymbol{\omega} \times \mathbf{t}_a)$$

we can write:

$$\dot{\mathbf{e}}_t = \mathbf{L}_{11} \mathbf{v} + (\boldsymbol{\omega} \times \mathbf{e}_t)$$

or what is the same:

$$\dot{\mathbf{t}}_m = \mathbf{L}_{11} \mathbf{v} + (\boldsymbol{\omega} \times \mathbf{t}_m)$$

The interpretation of this is that, as long as the angular velocity is concerned, the same effect can be viewed on the average of the real and false solutions for the translation vector,  $\mathbf{t}_m$ , than on the real solution alone,  $\mathbf{t}_a$ .

### Computation of $\mathbf{L}_{21}$

Regarding to the interaction sub-matrix:

$$\mathbf{L}_{21} = \frac{\partial \mathbf{e}_r}{\partial \mathbf{t}_a}; \quad \mathbf{e}_r = \mathbf{r}_m$$

We first try to compute the total time derivative of  $\mathbf{e}_r$ , which can be written as:

$$\dot{\mathbf{r}}_m = \frac{\partial \mathbf{r}_m}{\partial \mathbf{r}_h} \dot{\mathbf{r}}_h + \frac{\partial \mathbf{r}_m}{\partial \mathbf{r}_a} \dot{\mathbf{r}}_a \quad (147)$$

It is easy to show that the first addend does not depend on  $\boldsymbol{\omega}$ . In fact, this addend can be written as:

$$\frac{\partial \mathbf{r}_m}{\partial \mathbf{r}_h} \dot{\mathbf{r}}_h = \frac{\partial \mathbf{r}_m}{\partial \mathbf{r}_h} \frac{\partial \mathbf{r}_h}{\partial \mathbf{t}_a^*} \mathbf{R}_a^\top \mathbf{v}$$

as

$$\dot{\mathbf{t}}_a^* = \frac{d [\mathbf{R}_a^\top \mathbf{t}_a]}{dt} = \mathbf{R}_a^\top \mathbf{v}$$

On the other hand, the second addend does not depend on  $\mathbf{v}$ . To check this, it is enough to remind that:

$$\dot{\mathbf{r}}_a = \mathbf{J}_\omega \boldsymbol{\omega}$$

From what, the second addend can be written as:

$$\frac{\partial \mathbf{r}_m}{\partial \mathbf{r}_a} \dot{\mathbf{r}}_a = \frac{\partial \mathbf{r}_m}{\partial \mathbf{r}_a} \mathbf{J}_\omega \boldsymbol{\omega}$$

This means that if we match the expression (147) with the following one:

$$\dot{\mathbf{e}}_r = \dot{\mathbf{r}}_m = \mathbf{L}_{21} \mathbf{v} + \mathbf{L}_{22} \boldsymbol{\omega} \quad (148)$$

the interaction sub-matrices  $\mathbf{L}_{21}$  and  $\mathbf{L}_{22}$  can be obtained as:

$$\mathbf{L}_{21} = \frac{\partial \mathbf{r}_m}{\partial \mathbf{r}_h} \frac{\partial \mathbf{r}_h}{\partial \mathbf{t}_a^*} \mathbf{R}_a^\top \quad (149)$$

$$\mathbf{L}_{22} = \frac{\partial \mathbf{r}_m}{\partial \mathbf{r}_a} \mathbf{J}_\omega \quad (150)$$

In this subsection, we are interested in  $\mathbf{L}_{21}$ . Then, going ahead with the first Jacobian in (149):

$$\frac{\partial \mathbf{r}_m}{\partial \mathbf{r}_h} = \frac{(1 + \|\mathbf{r}_a\|^2) \mathbf{I} + ([\mathbf{r}_a]_\times^2 + [\mathbf{r}_a]_\times) (\mathbf{I} + [\mathbf{r}_h]_\times)}{(1 - \mathbf{r}_a^\top \mathbf{r}_h)^2}$$

Using the relation (124),  $\mathbf{R}_a$  can be introduced here:

$$\frac{\partial \mathbf{r}_m}{\partial \mathbf{r}_h} = \frac{1 + \|\mathbf{r}_a\|^2}{2(1 - \mathbf{r}_a^\top \mathbf{r}_h)^2} [(\mathbf{R}_a + \mathbf{I}) + (\mathbf{R}_a - \mathbf{I}) [\mathbf{r}_h]_\times]$$

The second Jacobian to be determined in (149) is:

$$\frac{\partial \mathbf{r}_h}{\partial \mathbf{t}_a^*} = \frac{\frac{1}{\rho} \mathbf{z} \mathbf{t}_a^{*\top} + (\frac{2}{\rho} - 1) \mathbf{z} \mathbf{n}_a^\top + \sigma_1 \left( \mathbf{I} - \frac{2}{\|\mathbf{z}\|^2} \mathbf{z} \mathbf{z}^\top \right) [\mathbf{n}_a]_\times}{\|\mathbf{z}\|^2}$$

being the coefficient  $\sigma_1$  and the vector  $\mathbf{z}$ :

$$\mathbf{z} = \mathbf{n}_a \times \mathbf{t}_a^*; \quad \sigma_1 = \rho - (2 + \mathbf{n}_a^\top \mathbf{t}_a^*)$$

That is,  $\mathbf{r}_h$  can be put in terms of these elements as:

$$\mathbf{r}_h = \frac{\sigma_1}{\|\mathbf{z}\|^2} \mathbf{z}$$

When we multiply  $\frac{\partial \mathbf{r}_m}{\partial \mathbf{t}_h}$  and  $\frac{\partial \mathbf{r}_h}{\partial \mathbf{t}_a^*}$ , some simplification can be performed since all the terms involving the following product become null:

$$[\mathbf{r}_h]_\times \mathbf{z} = 0$$

as vectors  $\mathbf{r}_h$  and  $\mathbf{z}$  are parallel. Finally, it must be said that a closed form has not been obtained yet for this Jacobian. Nevertheless, we will see afterwards that we do not need to care about this matrix, whatever its form and complexity.

### Computation of $\mathbf{L}_{22}$

We consider here as a starting point the relation (150). Using also relation (138), the Jacobian  $\frac{\partial \mathbf{r}_m}{\partial \mathbf{r}_a}$  can be computed:

$$\frac{\partial \mathbf{r}_m}{\partial \mathbf{r}_a} = \frac{1 + \|\mathbf{r}_h\|^2}{2(1 - \mathbf{r}_a^\top \mathbf{r}_h)^2} [\mathbf{R}_h^\top (\mathbf{I} - [\mathbf{r}_a]_\times) + (\mathbf{I} + [\mathbf{r}_a]_\times)]$$

After post-multiplying this Jacobian by  $\mathbf{J}_\omega$ , we can obtain the following expression for  $\mathbf{L}_{22}$ :

$$\mathbf{L}_{22} = \frac{(1 + \|\mathbf{r}_a\|^2)(1 + \|\mathbf{r}_h\|^2)}{4(1 - \mathbf{r}_a^\top \mathbf{r}_h)^2} (\mathbf{I} + \mathbf{R}_m^\top)$$

That can be put into a very closed form:

$$\mathbf{L}_{22} = \frac{1 + \|\mathbf{r}_m\|^2}{4} (\mathbf{I} + \mathbf{R}_m^\top) \quad (151)$$

It can be seen that it has exactly the same structure as  $\mathbf{J}_\omega$  (142). This means that, in the same way we wrote:

$$\dot{\mathbf{r}}_a = \mathbf{0} \mathbf{v} + \mathbf{J}_\omega \boldsymbol{\omega}$$

we can write:

$$\dot{\mathbf{r}}_m = \mathbf{L}_{21} \mathbf{v} + \mathbf{J}_\omega(\mathbf{r}_m) \boldsymbol{\omega}$$

With the notation  $\mathbf{J}_\omega(\mathbf{r}_m)$  we mean *replace in the expression of  $\mathbf{J}_\omega$  the rotation  $\mathbf{r}_a$  by that corresponding to  $\mathbf{r}_m$ .*

## 6.4 Stability analysis

The stability of mean-based control presented at the beginning of this section is being analyzed. First, the stability of the translation error,  $\mathbf{e}_t$ , is considered.

### 6.4.1 Stability of the translation error $\mathbf{e}_t$

In order to prove the convergence of  $\mathbf{e}_t$  to zero, the following Lyapunov function candidate is proposed:

$$V_t = \frac{1}{2} \mathbf{e}_t^\top \mathbf{e}_t$$

Its time derivative is:

$$\dot{V}_t = \frac{d\|\mathbf{e}_t\|}{dt} = \mathbf{e}_t^\top \dot{\mathbf{e}}_t$$

The expression of  $\dot{\mathbf{e}}_t$  in terms of the components of the interaction matrix is:

$$\dot{\mathbf{e}}_t = \mathbf{L}_{11} \mathbf{v} + \mathbf{L}_{12} \boldsymbol{\omega}$$

Using the form (146) for  $\mathbf{L}_{12}$  and replacing the control inputs  $\mathbf{v}$  and  $\boldsymbol{\omega}$  using (135):

$$\dot{\mathbf{e}}_t = -\lambda \mathbf{L}_{11} \mathbf{e}_t - \lambda \mathbf{L}_{12} \mathbf{e}_r = -\lambda \mathbf{L}_{11} \mathbf{e}_t - \lambda [\mathbf{e}_t]_\times \mathbf{e}_r$$

giving

$$\dot{V}_t = -\lambda \mathbf{e}_t^\top \mathbf{L}_{11} \mathbf{e}_t$$

As  $\mathbf{L}_{11}$  is not, in general, a symmetric matrix, it is convenient to write the previous expression as:

$$\dot{V}_t = -\lambda \mathbf{e}_t^\top \mathbf{S}_{11} \mathbf{e}_t \quad (152)$$

being  $\mathbf{S}_{11}$  the symmetric part of matrix  $\mathbf{L}_{11}$ :

$$\mathbf{S}_{11} = \frac{\mathbf{L}_{11} + \mathbf{L}_{11}^\top}{2}$$

Then, the convergence of  $\mathbf{e}_t$  depends only on the positiveness of matrix  $\mathbf{S}_{11}$ . From (144), it can be seen that matrix  $\mathbf{S}_{11}$  has the form:

$$\mathbf{S}_{11} = \frac{1}{2} \left[ (\mu_1 - \mu_2) \left( \mathbf{n}'_a \mathbf{t}_a^\top + \mathbf{t}_a \mathbf{n}'_a{}^\top \right) + \mu_1 \mathbf{t}_a \mathbf{t}_a^\top - 4\mu_2 \mathbf{n}'_a \mathbf{n}'_a{}^\top + \mu_3 \mathbf{I} \right] \quad (153)$$

Given the structure of this matrix, its eigenvalues can be easily computed, being:

$$\begin{aligned} \lambda_1 &= \frac{\rho + \|\mathbf{t}_a\|}{2\rho} > 0 \\ \lambda_2 &= \frac{\|\mathbf{t}_a\| + 1}{2\rho} + \frac{1}{2} + \frac{\mathbf{t}_a^\top \mathbf{R}_a \mathbf{n}_a}{2\rho \|\mathbf{t}_a\|} > \lambda_3 \\ \lambda_3 &= \frac{\|\mathbf{t}_a\| - 1}{2\rho} + \frac{1}{2} + \frac{\mathbf{t}_a^\top \mathbf{R}_a \mathbf{n}_a}{2\rho \|\mathbf{t}_a\|} \geq 0 \end{aligned}$$

The condition for the first eigenvalue is clear as we know that  $\rho$  is positive. The second eigenvalue is greater than the third one, as their difference is:

$$\lambda_2 - \lambda_3 = \frac{1}{\rho} > 0$$

Finally, it can be proved that the third eigenvalue is always non-negative and it only becomes null in a particular configuration, namely

$$\frac{\mathbf{R}_a^\top \mathbf{t}_a}{\|\mathbf{t}_a\|} = -\mathbf{n}_a \quad (154)$$

The proof is given in Appendix D.1. The geometric interpretation of this condition is shown in the left drawing of Figure 5. In this figure, we can see that  $\mathbf{t}_a$ , if expressed in the same

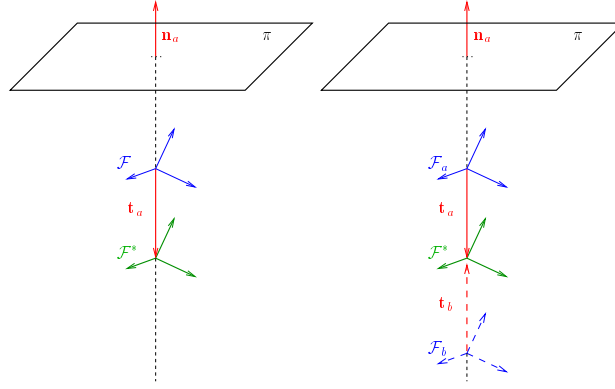


Figure 5: Geometric configuration in which  $\mathbf{L}_{11}$  becomes singular.

frame as  $\mathbf{n}_a$ , that is, frame  $\mathcal{F}^*$ , is parallel to the latter. According to relation (154), the only possible configuration should be the one depicted in the left figure, that is, the current frame between the desired frame and the object plane, so the translation vector points in the opposite direction to  $\mathbf{n}_a$ . However, it is easy to see that the other configuration, when the current frame is behind the desired frame is also possible. The reason is very simple, if we make notice of the peculiar relation existing between  $Rtn_a$  and  $Rtn_b$  in the configuration described by (154). In this particular case, (102)-(108) become:

$$\mathbf{t}_b = -\mathbf{t}_a; \quad \mathbf{n}_b = -\mathbf{n}_a; \quad \mathbf{r}_b = \mathbf{r}_a \quad (155)$$

This situation is depicted in the right-most drawing of Figure 5, where the "true" and "false" solutions are shown. During our developments, we have been assuming that  $Rtn_a$  corresponds to the true solution, and  $Rtn_b$  to the false one. However, in practice we assume there is no way of distinguishing between them. This means that,  $Rtn_b$  can be the true

solution, instead of  $Rtn_a$ . When this happens, we are in the situation when the real solution for the current frame is behind the desired one. Then we need to generalize the geometric configuration (154) by this new one:

$$\frac{\mathbf{R}_a^\top \mathbf{t}_a}{\|\mathbf{t}_a\|} = \pm \mathbf{n}_a \quad (156)$$

One further consideration, derived from the relations (155), is that one of the two solutions  $Rtn_a$ ,  $Rtn_b$  will not verify the visibility constraint in this configuration, as the normals are pointing in opposite directions. Resuming our study of  $\dot{V}_t$  (152) and according to the previous paragraphs, we can state that  $\dot{V}_t$  is always non-positive and it is null only at the equilibrium point,  $\mathbf{e}_t = \mathbf{0}$ . The reason is that the only eigenvalue of  $\mathbf{S}_{11}$  that can be zero,  $\lambda_3$ , only becomes effectively zero when the relation (156) holds. We know that in this configuration  $\mathbf{t}_b = -\mathbf{t}_a$ , what implies that the mean, and hence the translation error, are null.

$$\mathbf{e}_t = \mathbf{t}_m = \frac{\mathbf{t}_a + \mathbf{t}_b}{2} = 0$$

As a conclusion for  $\mathbf{e}_t$ , it always converges to the equilibrium point  $\mathbf{e}_t = \mathbf{0}$ , that coincides with the geometric configuration (156). Now we have proved  $\mathbf{e}_t$  always converges, there is another interesting question we need to answer. It can be posed as follows:

#### $\|\mathbf{t}_a\|$ never increases using the mean-based control law

We need to complete the previous analysis to make sure that, during the convergence of  $\mathbf{e}_t$ , the current camera frame does not go away, at the risk of losing visibility of the object. In fact, if the answer to the question is affirmative, we are proving that the current camera pose is always getting closer (or at least, never getting further) to the desired camera pose, as the system converges towards  $\mathbf{e}_t = 0$ . Recalling the expression:

$$\dot{\mathbf{t}}_a = \mathbf{v} - [\mathbf{t}_a]_\times \boldsymbol{\omega}$$

we analyze if the time derivative of the norm of  $\mathbf{t}_a$  can be positive:

$$\dot{V}_{t_a} = \frac{1}{2} \|\mathbf{t}_a\|^2 \implies \dot{V}_{t_a} = \mathbf{t}_a^\top \dot{\mathbf{t}}_a = \mathbf{t}_a^\top \mathbf{v}$$

Using our mean-based control law  $\mathbf{v} = -\lambda \mathbf{e}_t$ :

$$\dot{V}_{t_a} = -\lambda \mathbf{t}_a^\top \mathbf{t}_m = -\frac{\lambda}{2} \mathbf{t}_a^\top (\mathbf{t}_a + \mathbf{t}_b) \quad (157)$$

From relation (102) we can write  $\mathbf{t}_b$  as the product of a matrix and  $\mathbf{t}_a$ :

$$\mathbf{t}_b = \mathbf{M} \mathbf{t}_a; \quad \mathbf{M} = \frac{1}{\rho} \left( \frac{2}{\|\mathbf{t}_a\|} \mathbf{R}_a \mathbf{n}_a \mathbf{t}_a^\top + \|\mathbf{t}_a\| \mathbf{I} \right)$$



Using this expression in (157), we can write:

$$\dot{V}_{t_a} = -\frac{\lambda}{2} \mathbf{t}_a^\top \mathbf{A} \mathbf{t}_a; \quad \mathbf{A} = \mathbf{I} + \mathbf{M}$$

where the symmetric part of matrix  $\mathbf{A}$ , denoted by  $\mathbf{S}_A$ , can be introduced:

$$\dot{V}_{t_a} = -\frac{\lambda}{2} \mathbf{t}_a^\top \mathbf{S}_A \mathbf{t}_a$$

Computing the eigenvalues of matrix  $\mathbf{S}_A$ :

$$\begin{aligned} \lambda_1 &= 1 + \frac{\|\mathbf{t}_a\|}{\rho} \\ \lambda_2 &= 1 + \frac{\|\mathbf{t}_a\| + 1}{\rho} + \frac{\mathbf{t}_a^\top \mathbf{R}_a \mathbf{n}_a}{\rho \|\mathbf{t}_a\|} \\ \lambda_3 &= 1 + \frac{\|\mathbf{t}_a\| - 1}{\rho} + \frac{\mathbf{t}_a^\top \mathbf{R}_a \mathbf{n}_a}{\rho \|\mathbf{t}_a\|} \end{aligned}$$

which are exactly double of the eigenvalues of matrix  $\mathbf{S}_{11}$ , for which we concluded they were always positive, except at the equilibrium point,  $\mathbf{e}_t = \mathbf{0}$ , where  $\lambda_3 = 0$ . This confirms that  $\|\mathbf{t}_a\|$  is always non-increasing using the proposed mean-based control law.

#### 6.4.2 Stability in the orientation error $\mathbf{e}_r$

We define the following Lyapunov function candidate:

$$V_r = \frac{1}{2} \mathbf{e}_r^\top \mathbf{e}_r$$

being its time derivative:

$$\dot{V}_r = \frac{d\|\mathbf{e}_r\|}{dt} = \mathbf{e}_r^\top \dot{\mathbf{e}}_r$$

The expression for the derivative of  $\mathbf{e}_r$  is:

$$\dot{\mathbf{e}}_r = \mathbf{L}_{21} \mathbf{v} + \mathbf{L}_{22} \boldsymbol{\omega} = -\lambda \mathbf{L}_{21} \mathbf{e}_t - \lambda \mathbf{L}_{22} \mathbf{e}_r$$

Considering that  $\mathbf{e}_t$  always converges to zero, as we have just seen, the first addend goes to zero. This is why the particular form of  $\mathbf{L}_{21}$  does not matter, as said before. Regarding to the second addend, the positiveness of matrix  $\mathbf{L}_{22}$  has to be proved. As it is again a non-symmetric matrix, we analyze its symmetric part:

$$\mathbf{S}_{22} = \frac{\mathbf{L}_{22} + \mathbf{L}_{22}^\top}{2}$$

which has the form:

$$\mathbf{S}_{22} = \frac{1 + \|\mathbf{r}_m\|^2}{4} (2\mathbf{I} + \mathbf{R}_m + \mathbf{R}_m^\top)$$

The eigenvalues of  $(2\mathbf{I} + \mathbf{R}_m + \mathbf{R}_m^\top)$  are:

$$\lambda_1 = 4; \quad \lambda_2 = \lambda_3 = 2(1 + \cos\theta_m) \geq 0$$

$\lambda_2 = \lambda_3 = 0$  when  $\theta_m = \pm\pi$ . Even if we consider  $\pm\pi$  is a wide range for the mean angle, it is a limitation we can avoid if we realize the way  $\mathbf{L}_{22}$  takes part in the closed-loop equation (136). In this equation, we can see that  $\mathbf{L}_{22}$  appears as the product:

$$\mathbf{L}_{22} \mathbf{e}_r = \mathbf{L}_{22} \mathbf{r}_m$$

Replacing  $\mathbf{L}_{22}$  using (151), this product becomes:

$$\mathbf{L}_{22} \mathbf{r}_m = \frac{1 + \|\mathbf{r}_m\|^2}{4} (\mathbf{I} + \mathbf{R}_m^\top) \mathbf{r}_m$$

As  $\mathbf{r}_m$  is in the rotation axis of  $\mathbf{R}_m$ , it does not change with the rotation:

$$\mathbf{R}_m \mathbf{r}_m = \mathbf{r}_m$$

Hence, the product reduces to:

$$\mathbf{L}_{22} \mathbf{r}_m = \frac{1 + \|\mathbf{r}_m\|^2}{2} \mathbf{r}_m$$

This means that, as far as the closed-loop system is concerned,  $\mathbf{L}_{22}$  can be replaced in our interaction matrix by the following symmetric, positive-definite matrix:

$$\mathbf{L}'_{22} = \frac{1 + \|\mathbf{r}_m\|^2}{2} \mathbf{I}$$

Thus, we obtain:

$$\frac{d\|\mathbf{e}_r\|}{dt} \rightarrow -\lambda \mathbf{e}_r^\top \mathbf{L}_{22} \mathbf{e}_r = -\lambda \frac{1 + \|\mathbf{r}_m\|^2}{2} \mathbf{e}_r^\top \mathbf{e}_r$$

Since this is always non-positive, the conclusion for  $\mathbf{e}_r$  is that it always converges to  $\mathbf{e}_r = \mathbf{0}$ , that is,  $\mathbf{R}_a = \mathbf{R}_b = \mathbf{I}$ .

### 6.4.3 Conclusions on the stability of the mean-based control

At this point, the conclusion for the stability of the complete position-based control scheme is that global asymptotic stability can be achieved using the mean of the true and the false solutions. The only limitation is due to the use of  $\tan(\theta_m/2)$  in  $\mathbf{r}_m$ , that may produce saturation as the mean angle  $\theta_m$  goes to  $\pm\pi$ . Finally, it must be noticed that the achieved

equilibrium point,  $\mathbf{e} = \mathbf{0}$ , is not the desired configuration in which the current camera frame coincides with the desired one:

$$\mathbf{e} = \mathbf{0} \not\Rightarrow \begin{bmatrix} \mathbf{t}_a \\ \mathbf{r}_a \end{bmatrix} = \mathbf{0}$$

Instead, it corresponds to a line in the Cartesian space defined by:

$$\frac{\mathbf{R}_a^\top \mathbf{t}_a}{\|\mathbf{t}_a\|} = \pm \mathbf{n}_a; \quad \mathbf{R}_a = \mathbf{I} \quad (158)$$

$$\mathbf{e} = \mathbf{0} \Rightarrow \begin{bmatrix} \mathbf{t}_a \\ \|\mathbf{t}_a\| \\ \mathbf{r}_a \end{bmatrix} = \begin{bmatrix} \pm \mathbf{n}_a \\ \mathbf{0} \end{bmatrix}$$

That is, the current camera frame is properly oriented according to the reference frame, but the translation error always converges reaching a configuration parallel to the reference-plane normal. This will be overcome using a switching control law as we will see in the next section.

#### 6.4.4 Practical considerations bounding global stability

In our theoretical developments, we assumed that  $Rtn_a$  is the true solution among the four possible (131)-(132). If we compute  $Rtn_b$  from  $Rtn_a$  using the formulas, it may happen that  $Rtn_b$  does not verify the visibility constraint, in spite of the fact that  $Rtn_a$  does. This means that  $Rtn_{b-}$  should be chosen instead, and used together with  $Rtn_a$  to compute the mean-based control inputs. Moreover, in a practical situation, when controlling with the average of the true and false solutions, as we are assuming there is no mean of discerning which one is the true one, we must choose, from the four possible solutions, those two fulfilling the visibility constraint. Making this choice we are making sure that one of the two solutions is the true one, but the other is a false solution, may be the one obtained from the true one using the formulas or may be its opposite. This means that we need to prove also the convergence of the mean-based control law when using the couple  $\{Rtn_a, Rtn_{b-}\}$ , instead of  $\{Rtn_a, Rtn_b\}$  as done before. In consequence, consider the alternative mean control law:

$$\begin{aligned} \mathbf{t}_m &= \frac{\mathbf{t}_a - \mathbf{t}_b}{2} \\ \mathbf{r}_m &\Leftarrow \mathbf{R}_m = \mathbf{R}_a (\mathbf{R}_a^\top \mathbf{R}_b)^{1/2} \end{aligned}$$

instead of (133)-(134). The only difference with respect to the previous analysis is a new  $\mathbf{L}_{11-}$  matrix. Instead of (144), now we have:

$$\mathbf{L}_{11-} = \frac{1}{2} \left[ -2\mu_1 \mathbf{n}'_a \mathbf{t}_a^\top - \mu_1 \mathbf{t}_a \mathbf{t}_a^\top + 4\mu_2 \mathbf{n}'_a \mathbf{n}'_a{}^\top + 2\mu_2 \mathbf{t}_a \mathbf{n}'_a{}^\top + (2 - \mu_3) \mathbf{I} \right] \quad (159)$$

Instead of (153), the symmetric part of  $\mathbf{L}_{11-}$  is:

$$\mathbf{S}_{11-} = \frac{1}{2} \left[ (\mu_2 - \mu_1) \left( \mathbf{n}'_a \mathbf{t}_a^\top + \mathbf{t}_a \mathbf{n}'_a{}^\top \right) - \mu_1 \mathbf{t}_a \mathbf{t}_a^\top + 4\mu_2 \mathbf{n}'_a \mathbf{n}'_a{}^\top + (2 - \mu_3) \mathbf{I} \right] \quad (160)$$

The eigenvalues of which are:

$$\begin{aligned}\lambda_{1-} &= \frac{\rho - \|\mathbf{t}_a\|}{2\rho} \\ \lambda_{2-} &= \frac{1 - \|\mathbf{t}_a\|}{2\rho} + \frac{1}{2} - \frac{\mathbf{t}_a^\top \mathbf{R}_a \mathbf{n}_a}{2\rho \|\mathbf{t}_a\|} \\ \lambda_{3-} &= -\frac{1 + \|\mathbf{t}_a\|}{2\rho} + \frac{1}{2} - \frac{\mathbf{t}_a^\top \mathbf{R}_a \mathbf{n}_a}{2\rho \|\mathbf{t}_a\|}\end{aligned}$$

These eigenvalues verify:

$$\lambda_{1-} > 0; \quad \lambda_{2-} > \lambda_{3-}; \quad \lambda_{3-} \geq 0 \text{ if } \|\mathbf{t}_a\| \leq 1$$

The condition for the first eigenvalue is clear as  $\rho$  is:

$$\rho = \sqrt{\|\mathbf{t}_a\|^2 + 2\nu} > \|\mathbf{t}_a\|$$

and  $\nu > 0$ . The second eigenvalue is again greater than the third one, as their difference is:

$$\lambda_{2-} - \lambda_{3-} = \frac{1}{\rho} > 0$$

The condition for  $\lambda_{3-}$  is a sufficient condition and is proved in Appendix D.2. Actually, the necessary and sufficient condition proved in that appendix for  $\lambda_{3-}$  being non-negative is:

$$\|\mathbf{t}_a\| \leq \frac{4 - (1 + c_\alpha)^2}{2(1 - c_\alpha)} \quad (161)$$

being  $c_\alpha = \cos \alpha$ , and  $\alpha$  the angle between vectors  $\mathbf{n}_a$  and  $\mathbf{R}^\top \mathbf{t}_a$ . The conclusion from that proof is that  $\mathbf{L}_{11-}$  is always positive-semidefinite when (161) is verified (or using a more restrictive but simpler condition, when  $\|\mathbf{t}_a\| \leq 1$ ) and that it only becomes singular in the well-known configuration (156). A similar study to that in Section 6.4.1 allows us to state that:  $\|\mathbf{t}_a\|$  *never increases using the mean control law based on the couple*  $\{Rtn_a, Rtn_{b-}\}$ . This confirms that if we start from a configuration with a distance between the desired and current pose less than  $d^*$  (that is,  $\|\mathbf{t}_a\| \leq 1$ ),  $\mathbf{e}_t$  always converges, while keeping  $\|\mathbf{t}_a\| \leq 1$ , as this norm will never increase. According to this, the global asymptotic stability condition for the closed-loop system, has to be lowered to local asymptotic stability. Nevertheless, in all the simulation experiments made starting from a configuration not verifying condition (161), the system featured a perfectly stable behaviour. This suggests that, even if we have not been able to prove global stability in the second case ( $\mathbf{t}_m = \frac{\mathbf{t}_a - \mathbf{t}_b}{2}$ ) with the chosen Lyapunov function, it is likely that another candidate Lyapunov function could be found such that it guarantees global stability also in this case.

## 6.5 Switching control law

As it has been shown in the previous sections, the mean-based control law always takes the system to an equilibrium where (see (155)):

$$\mathbf{t}_b = -\mathbf{t}_a; \quad \mathbf{n}_b = -\mathbf{n}_a; \quad \mathbf{R}_b = \mathbf{R}_a = \mathbf{I}$$

This is not completely satisfactory, as  $\mathbf{t}_a$  can be different from zero, as would be required. Now we want to improve this control law so the desired equilibrium:

$$\begin{bmatrix} \mathbf{t}_a \\ \mathbf{r}_a \end{bmatrix} = \mathbf{0} \implies \begin{cases} \mathbf{t}_a = \mathbf{t}_b = \mathbf{0} \\ \mathbf{R}_a = \mathbf{R}_b = \mathbf{I} \end{cases} \quad (162)$$

is reached (as we know that the norm  $\mathbf{t}_b$  is always equal to the norm of  $\mathbf{t}_a$ , both solutions must have simultaneously null translation). As said before, in practice we choose two solutions that verify the visibility constraint at the beginning and use their average for controlling the system, until it converges to a particular configuration in the Cartesian space (158). During this convergence the true normal  $\mathbf{n}_a$  does not change, since the object does not move and the reference frame,  $\mathcal{F}^*$ , is also motionless. On the other hand, the false normal,  $\mathbf{n}_b$ , will change from its original direction until it becomes opposite to  $\mathbf{n}_a$ . This can be clearly understood with Figure 6, where the evolution of the false system,  $t_0$ , until the convergence of the system,  $t_\infty$ . During this continuous

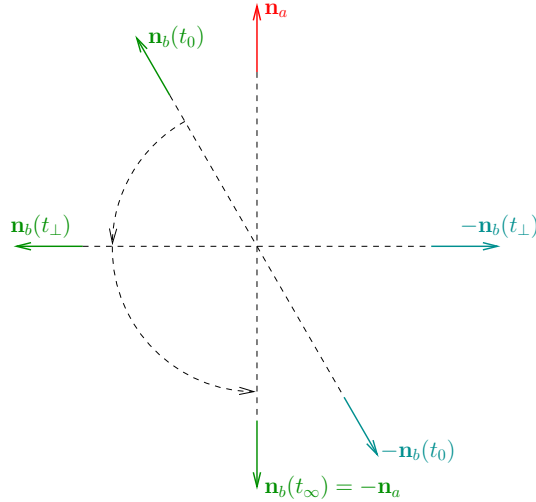


Figure 6: Evolution of the false plane normal  $\mathbf{n}_b$ .

evolution, it is clear that, at some point,  $\mathbf{n}_b$  no longer verifies the visibility constraint. This instant is indicated as  $t_\perp$  in the figure, but this can occur before or after the time when  $\mathbf{n}_b$  becomes perpendicular to  $\mathbf{n}_a$ , depending on the position of the reference points respect to

$\mathcal{F}^*$ . After that instant, is  $-\mathbf{n}_b$  the false normal that starts verifying the visibility constraint. Nevertheless, as it was a discarded solution from the beginning, it will not be considered. This means that the control based on the average of the two solutions drives the current frame in such a way that it is always possible to detect the false solution, among the two that verified the visibility constraint at the beginning. Then, it could be possible to control the system from this instant on, using just the true solution, that takes the system to the desired equilibrium (162). According to this, a switching control strategy can be proposed, in such a way that when one of the two solutions comes out to be a false one, we start making a smooth transition from the mean control to the control using only the true solution. A smooth transition is preferred to immediately discarding the false solution, in order to avoid any abrupt changes in the evolution of the control signals. Then, we can replace the average control law (133)-(134) by a weighted-average control law:

$$\begin{cases} \mathbf{t}_m = \frac{\alpha_a \mathbf{t}_a + \alpha_b \mathbf{t}_b}{2} \\ \mathbf{r}_m \Leftarrow \mathbf{R}_m = \mathbf{R}_a (\mathbf{R}_a^\top \mathbf{R}_b)^{\frac{\alpha_b}{2}} \end{cases}$$

The weighting coefficients  $\alpha_a$  and  $\alpha_b$  can be defined according to an exponentially decreasing time-function:

$$f(t) = e^{-\lambda_f (t-t_\perp)} \quad (163)$$

being:

$$\alpha_a = 2 - f(t); \quad \alpha_b = f(t)$$

In the previous analysis, when  $\mathbf{t}_b$  and  $\mathbf{n}_b$  appear, we should understand the translation and normal corresponding to either  $Rtn_b$  or  $Rtn_{b-}$ , the one verifying the visibility constraint. Another case can be mentioned for the sake of completeness, even not being of much practical use. We already know we can control with the average translation and rotation, computed from the true solution and either  $Rtn_b$  or  $Rtn_{b-}$ . What happens if we consider as the second solution the one not verifying the visibility constraint? According to Figure 6, this implies to compute the mean translation using:

$$\mathbf{t}_m = \frac{\mathbf{t}_a - \mathbf{t}_b}{2}$$

as  $-\mathbf{t}_b$  corresponds to the normal  $-\mathbf{n}_b$  in the figure. In this case, is the normal  $-\mathbf{n}_b$  the one that will converge to  $-\mathbf{n}_a$ . Now no change in the visibility condition of the false solution will be appreciated, as  $-\mathbf{n}_b$  did not verify the visibility constraint at the beginning and continues like that during the convergence. Graphically, we could say that the rotation of the normals corresponding to the false solutions,  $\mathbf{n}_b$  and  $-\mathbf{n}_b$ , is in the opposite sense to that shown in the figure.

### 6.5.1 Alternatives for the detection of the false solution

It has been just described how the false solution can be detected using the visibility constraint during the convergence of the system. Other alternatives that has been already used in other

works could also be applied to our case. One of them consists of taking advantage of the fact that, as we have seen, and in the absence of camera calibrations errors, the true normal keeps unchanged while the camera is moving towards the desired configuration. Hence, we can detect the false solution as that one that experiences a significant change respect to its initial value. This alternative is not incompatible with the mean-based control law, even if the false solution can be detected after two or three steps. The reason is that even in that case, a control law is needed for the first iterations that guarantees the stability of the system. The mean-based control law ensures convergence during the two, three, or whatever the number of steps needed to detect the false solution. On the other hand, it is not intended to perform arbitrary movements until the false solution can be detected, but being able of detect the false solution while keeping the system always under control.

## 6.6 Simulation results

As common parameters in all the experiments to be described, the initial orientation error is 36 degrees and the scalar  $\lambda$  used in the control law (135) is chosen  $\lambda = 1$ .

### 6.6.1 Control using the true solution

In this experiment, only the true solution, among the four possible (131)-(132), verifies the visibility constraint at the beginning. In this case, there is no need to use mean-based control, and the conventional position-based control takes the system to the desired equilibrium. In the upper part of Figure 7, the evolution of the translation and orientation errors are shown. In the lower plots, the required control vector is given. If we try to control using only the false solution instead, an unstable behavior is observed, even if that solution verifies the visibility constraint.

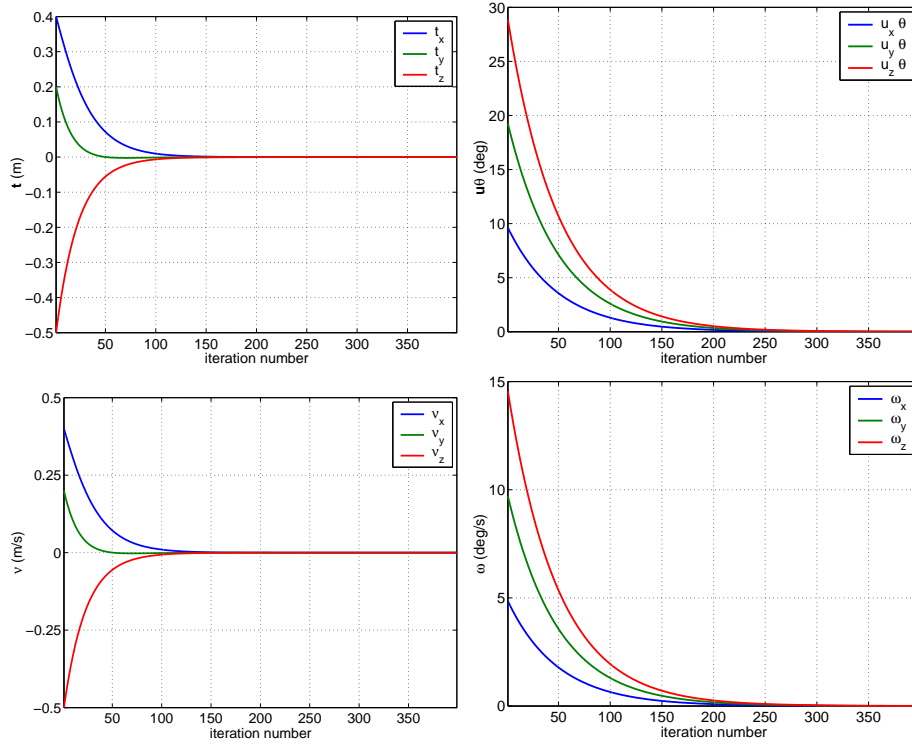


Figure 7: Simulation experiment using only the true solution.



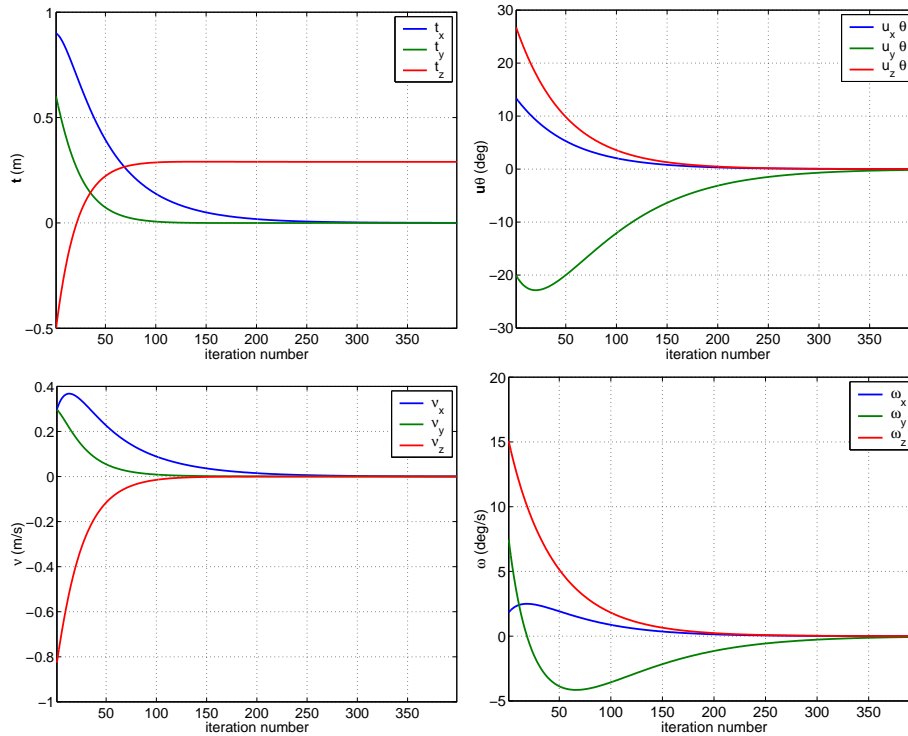


Figure 8: Simulation experiment using the mean of true and false solutions.

### 6.6.2 Mean-based control

In this experiment, shown in Figure 8, the mean-based control law is applied. The most adverse situation is simulated. That is, the two solutions verifying the visibility constraint at the beginning are  $Rtn_a$  and  $Rtn_b_-$ . In this case, convergence was only guaranteed when  $\|\mathbf{t}_a\|$  verifies condition (161). In this experiment, we initially have  $\|\mathbf{t}_a\| = 1.2$ , which not satisfies that condition. Hence, this also illustrates that  $\|\mathbf{t}_a\| \leq 1$  or even (161) is not a necessary condition for the system convergence. We can notice in the figure that, as expected,  $\mathbf{t}_a$  does not converge to zero. In particular, as in the experiment  $\mathbf{n}_a = [0, 0, 1]^T$ , we can see that only the third component of  $\mathbf{t}_a$  is different from zero at the equilibrium. At the convergence we obtain  $\mathbf{n}_b = -\mathbf{n}_a$  so we know then which is the true solution.

### 6.6.3 Switching control

In the last experiment, the performance of the switching control strategy is shown (see Figure 9). In particular, the control system starts switching at the 14th iteration, as one of the points becomes non-visible at that instant, according to the false solution.

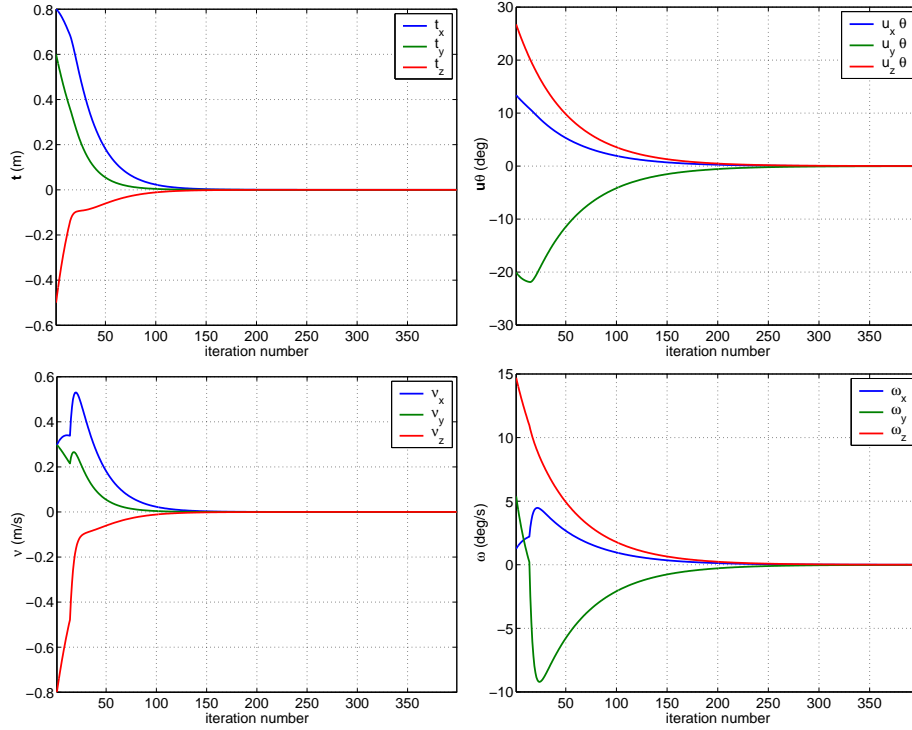


Figure 9: Simulation experiment using switching control.

The chosen value for the switching-rate parameter is  $\lambda_f = 0.25$ . It has been implemented as a discrete-time switching mechanism, as  $(t - t_\perp)$  in (163) has been replaced by  $(k - k_\perp)$ , being  $k$  the current iteration number and  $k_\perp$  the iteration number when the false solution was detected. As expected, it can be seen that the system converges to the equilibrium where the desired camera pose is reached.

## 7 Hybrid visual servoing based on analytical decomposition

The control scheme proposed in the previous section is based on the choice of the true normal vector. It implies introducing a switching control law, coming from the use of the mean between the two solutions for the translation vector. Instead, we can control only the mean rotation and the translation with image data. Thus, we obtain a hybrid visual servoing [12] but without needing to find the true solution of the homography decomposition. The task function can be defined as follows:

$$\mathbf{e} = \begin{bmatrix} (\mathbf{H} - \mathbf{I})\mathbf{m}^* \\ \mathbf{u}_m\theta_m \end{bmatrix}$$

where  $\mathbf{R}_m = \exp([\mathbf{u}_m\theta_m]_\times) = \mathbf{R}_v(\mathbf{R}_v^\top \mathbf{R}_f)^{(1/2)}$ . The derivative of the task function can be written as:

$$\dot{\mathbf{e}} = \mathbf{L}\mathbf{v}$$

and a simple control law is:

$$\mathbf{v} = -\lambda\widehat{\mathbf{L}}^{-1}\mathbf{e}$$

where  $\widehat{\mathbf{L}}$  is an approximation of the interaction matrix  $\mathbf{L}$ .

Figure 10 shows the simulation results with the proposed hybrid visual servoing scheme. As already mentioned, the main advantage of this scheme is that we avoid to choose between the two solutions (i.e. the switching of control laws proposed in the previous section). Another improvement proposed in this control law is the new rotation parametrization, that avoids the limitations of the previous method when  $\theta_m = \pm\pi$ . On the other hand, the stability analysis of the control law is more complicated. For the moment, we have obtained encouraging simulation results and we leave the theoretical proof of the stability as future work.

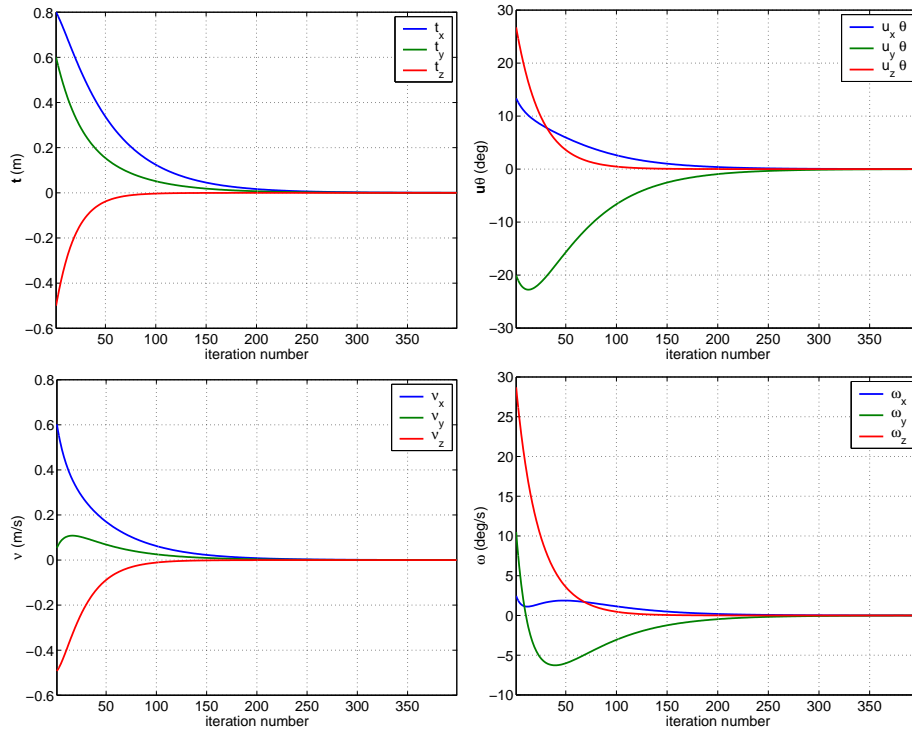


Figure 10: Simulation experiment using hybrid visual servoing.

## 8 Conclusions

In this report, we have presented a new analytical method to decompose the Euclidean homography matrix. As a result of this analytical procedure, we have been able to find the explicit relations among the different solutions for the Euclidean decomposition elements:  $\mathbf{R}$ ,  $\mathbf{t}$  and  $\mathbf{n}$ . Another result described in the report, also derived from the analytical formulation, is the statement of the stability conditions for a position-based control strategy that makes use of the two solutions of the homography decomposition (one of them being a false solution) assuming that there is no a priori knowledge that allows us to distinguish between them (such as an estimation of the normal to the object plane). It has been proved that, using this control law, the system evolves in such a way that, at some point, it is always possible to determine which one is the true solution. After the true solution has been identified, a switching strategy has been introduced in order to smoothly start using just the true solution. Another possible control law that we propose in this document uses only the mean of the solutions for the rotation, while the remaining d.o.f.s are controlled with image information resulting in a hybrid visual servoing scheme. This alternative solution allows us to avoid the choice of the true solution.

Future work will be focused on the study of the effects of camera calibration errors on the homography decomposition, taking advantage of the derived analytical expressions. Another future objective is to try to prove stability conditions of the hybrid visual servoing using the average of the two visible solutions, since, as we have seen, it is a very interesting alternative that avoids the need for a switching mechanism, required in the position-based visual servoing.

## Acknowledgments

The authors gratefully acknowledge INRIA, MEyC (grants HF2005-0200 and DPI2004-06419) and Egide for supporting this work which has been done in the PHC Picasso project "Robustness of vision-based control for positioning tasks".

## A Useful relations for the homography decomposition

Rodrigues' formula for a rotation matrix:

$$\mathbf{R} = \mathbf{I} + \sin(\theta)[\mathbf{u}]_{\times} + (1 - \cos(\theta))[\mathbf{u}]_{\times}^2 \quad (164)$$

$$\mathbf{R} - \mathbf{R}^{\top} = 2 \sin(\theta)[\mathbf{u}]_{\times}$$

$$\mathbf{H} - \mathbf{H}^{\top} = [2 \sin(\theta)[\mathbf{u}]_{\times} + [\mathbf{n}]_{\times} \mathbf{t}]_{\times}$$

Some trigonometric relations:

$$\sin(2x) = \frac{2 \tan(x)}{1 + \tan^2(x)}$$

$$\cos(2x) = \frac{1 - \tan^2(x)}{1 + \tan^2(x)}$$

$$1 - \cos(2x) = \frac{2 \tan^2(x)}{1 + \tan^2(x)}$$

$$1 + \cos(2x) = \frac{2}{1 + \tan^2(x)}$$

Relations useful when working with skew-symmetric matrices:

$$[\mathbf{u}]_{\times} [\mathbf{v}]_{\times} = \mathbf{v} \mathbf{u}^{\top} - (\mathbf{u}^{\top} \mathbf{v}) \mathbf{I}$$

$$[\mathbf{u}]_{\times}^2 = \mathbf{u} \mathbf{u}^{\top} - \|\mathbf{u}\|^2 \mathbf{I}$$

$$[\mathbf{u}]_{\times} [\mathbf{v}]_{\times} - [\mathbf{v}]_{\times} [\mathbf{u}]_{\times} = \mathbf{v} \mathbf{u}^{\top} - \mathbf{u} \mathbf{v}^{\top} = [[\mathbf{u}]_{\times} \mathbf{v}]_{\times}$$

$$[\mathbf{u}]_{\times} [\mathbf{v}]_{\times} [\mathbf{u}]_{\times} = -(\mathbf{u}^{\top} \mathbf{v}) [\mathbf{u}]_{\times}$$

$$[\mathbf{u}]_{\times}^3 = -\|\mathbf{u}\|^2 [\mathbf{u}]_{\times}$$

$$[\mathbf{u}]_{\times}^4 = -\|\mathbf{u}\|^2 [\mathbf{u}]_{\times}^2$$

If  $\mathbf{u}$  is a unitary vector, we have some interesting properties involving derivatives:

$$\mathbf{u}^{\top} \mathbf{u} = 1 \implies \mathbf{u}^{\top} \dot{\mathbf{u}} = 0$$

then

$$[\mathbf{u}]_{\times} [\dot{\mathbf{u}}]_{\times} = \dot{\mathbf{u}} \mathbf{u}^{\top}$$

$$[\mathbf{u}]_{\times} [\dot{\mathbf{u}}]_{\times} [\mathbf{u}]_{\times} = 0$$

$$\dot{\mathbf{u}} = -[\mathbf{u}]_{\times}^2 \dot{\mathbf{u}}$$

Inversion of a particular matrix appearing in the developments:

$$(\mathbf{I} + \mathbf{x} \mathbf{y}^{\top})^{-1} = \mathbf{I} - \frac{1}{1 + \mathbf{x}^{\top} \mathbf{y}} \mathbf{x} \mathbf{y}^{\top}$$

If we consider matrix:

$$\mathbf{H}^\top \mathbf{H} = \mathbf{S} + \mathbf{I}$$

it has a special eigenvector associated with the unitary eigenvalue:

$$(\mathbf{S} + \mathbf{I}) \mathbf{v} = \mathbf{v}; \quad \mathbf{v} = [\mathbf{n}]_\times \mathbf{R}^\top \mathbf{t}$$

## B On the normalization of the homography matrix

In general, after retrieving an estimation of the homography matrix,  $\hat{\mathbf{H}}$ , we need to obtain the normalized homography matrix:

$$\mathbf{H} = \frac{\hat{\mathbf{H}}}{\gamma}$$

being the scale factor  $\gamma$ :

$$\gamma = \text{med}(\text{svd}(\hat{\mathbf{H}}))$$

In order to illustrate that this normalizing factor can also be computed from the components of matrix  $\hat{\mathbf{H}}$  using an analytical expression, we just need to solve the third order equation:

$$\det(\hat{\mathbf{H}}^\top \hat{\mathbf{H}} - \lambda \mathbf{I}) = 0 \implies \text{svd}(\hat{\mathbf{H}}) = \sqrt{\lambda}$$

The equation can be written as:

$$\lambda^3 + a_2 \lambda^2 + a_1 \lambda + a_0 = 0$$

where:

$$\begin{aligned} a_2 &= -(m_{11} + m_{22} + m_{33}) \\ a_1 &= m_{11} m_{22} + m_{11} m_{33} + m_{22} m_{33} - (m_{12}^2 + m_{13}^2 + m_{23}^2) \\ a_0 &= m_{12}^2 m_{33} + m_{13}^2 m_{22} + m_{23}^2 m_{11} - m_{11} m_{22} m_{33} - 2 m_{12} m_{13} m_{23} \end{aligned}$$

Being  $m_{ij}$  the components of the symmetric matrix  $\mathbf{M} = \hat{\mathbf{H}}^\top \hat{\mathbf{H}}$ .

The solutions of such a third order equation can be obtained using Cardano's formula:

$$\begin{aligned} \lambda_1 &= -\frac{a_2}{3} + (S + T) \\ \lambda_2 &= -\frac{a_2}{3} - \frac{1}{2}(S + T) - \frac{\sqrt{3}}{2}(S - T)i \\ \lambda_3 &= -\frac{a_2}{3} - \frac{1}{2}(S + T) + \frac{\sqrt{3}}{2}(S - T)i \end{aligned} \tag{165}$$

where

$$\begin{aligned} i &= \sqrt{-1} \\ S &= \left( R + \sqrt{Q^3 + R^2} \right)^{1/3} \\ T &= \left( R - \sqrt{Q^3 + R^2} \right)^{1/3} \end{aligned}$$

and finally:

$$\begin{aligned} Q &= \frac{3 a_1 - a_2^2}{9} \\ R &= \frac{9 a_2 a_1 - 27 a_0 - 2 a_2^3}{54} \end{aligned}$$

It can be verified that, when all the solutions of the cubic polynomial are real (as in our case, where  $\mathbf{M}$  is a symmetric matrix),  $(S + T)$  is always positive and  $(S - T)$  is always an imaginary positive value. From this, it is clear that the solutions can be ordered as:

$$\lambda_1 \geq \lambda_2 \geq \lambda_3$$

Then, we conclude that the normalizing factor,  $\gamma$ , is given by the square root of formula (165).

## C Proofs of several properties

### C.1 Proof of properties on minors of matrix $\mathbf{S}$

In this section we want to prove the non-positivity of the principal minors of matrix  $\mathbf{S}$  in (29). The proof is straightforward if we consider the form of matrix  $\mathbf{S}$  in terms of the components of vectors  $\mathbf{x}$  and  $\mathbf{y}$ :

$$\mathbf{S} = \mathbf{xy}^\top + \mathbf{yx}^\top + \mathbf{yy}^\top = \begin{bmatrix} 2x_1y_1 + y_1^2 & x_1y_2 + x_2y_1 + y_1y_2 & x_1y_3 + x_3y_1 + y_1y_3 \\ x_1y_2 + x_2y_1 + y_1y_2 & 2x_2y_2 + y_2^2 & x_2y_3 + x_3y_2 + y_2y_3 \\ x_1y_3 + x_3y_1 + y_1y_3 & x_2y_3 + x_3y_2 + y_2y_3 & 2x_3y_3 + y_3^2 \end{bmatrix} \quad (166)$$

The opposite of each principal minor (minor corresponding to the diagonal element  $s_{kk}$ , eliminating column  $k$  and row  $k$ ) has the form:

$$M_{\mathbf{S}_{kk}} = - \begin{vmatrix} 2x_iy_i + y_i^2 & x_iy_j + x_jy_i + y_iy_j \\ x_iy_j + x_jy_i + y_iy_j & 2x_jy_j + y_j^2 \end{vmatrix}; \quad i, j, k = 1, 2, 3, \quad i, j \neq k$$

Developing this determinant, the proposed condition is clear:

$$\begin{aligned} M_{\mathbf{S}_{11}} &= (x_2y_3 - x_3y_2)^2 \geq 0 \\ M_{\mathbf{S}_{22}} &= (x_1y_3 - x_3y_1)^2 \geq 0 \\ M_{\mathbf{S}_{33}} &= (x_1y_2 - x_2y_1)^2 \geq 0 \end{aligned}$$



We can also prove the relations:

$$M_{\mathbf{S}_{12}} = \epsilon_{12} \sqrt{M_{\mathbf{S}_{11}}} \sqrt{M_{\mathbf{S}_{22}}} \quad (167)$$

$$M_{\mathbf{S}_{13}} = \epsilon_{13} \sqrt{M_{\mathbf{S}_{11}}} \sqrt{M_{\mathbf{S}_{33}}} \quad (168)$$

$$M_{\mathbf{S}_{23}} = \epsilon_{23} \sqrt{M_{\mathbf{S}_{22}}} \sqrt{M_{\mathbf{S}_{33}}} \quad (169)$$

In order to do so, we define the following variables:

$$m_1 = x_3 y_2 - x_2 y_3 \Rightarrow \sqrt{M_{\mathbf{S}_{11}}} = |m_1| \quad (170)$$

$$m_2 = x_3 y_1 - x_1 y_3 \Rightarrow \sqrt{M_{\mathbf{S}_{22}}} = |m_2| \quad (171)$$

$$m_3 = x_2 y_1 - x_1 y_2 \Rightarrow \sqrt{M_{\mathbf{S}_{33}}} = |m_3| \quad (172)$$

As an example, we will prove it for  $M_{\mathbf{S}_{13}}$ :

$$M_{\mathbf{S}_{13}} = x_1 x_3 y_2^2 + x_2^2 y_1 y_3 - x_1 x_2 y_2 y_3 - x_2 x_3 y_1 y_2 = m_1 m_3 \quad (173)$$

From what it is obvious that:

$$M_{\mathbf{S}_{13}} = \epsilon_{13} \sqrt{M_{\mathbf{S}_{11}}} \sqrt{M_{\mathbf{S}_{33}}}$$

## C.2 Geometrical aspects related to minors of matrix $\mathbf{S}$

In this section, we will show what the geometrical meaning of the minors of matrix  $\mathbf{S}$  becoming null ( $M_{\mathbf{S}_{ii}} = 0$ ) is.

Using the definitions of  $\mathbf{x}$  and  $\mathbf{y}$  in (46)-(47) and using also (170)-(172), we can write:

$$m_1 = t_3^* n_2 - t_2^* n_3$$

$$m_2 = t_3^* n_1 - t_1^* n_3$$

$$m_3 = t_2^* n_1 - t_1^* n_2$$

where  $n_i$  and  $t_i^*$  are the components of vectors  $\mathbf{n}$  and  $\mathbf{t}^*$ , respectively. Consider the following vector:

$$[\mathbf{n}]_{\times} \mathbf{t}^* = \begin{bmatrix} m_1 \\ -m_2 \\ m_3 \end{bmatrix} = \begin{bmatrix} \text{sign}(m_1) |m_1| \\ -\text{sign}(m_2) |m_2| \\ \text{sign}(m_3) |m_3| \end{bmatrix}$$

or what is the same:

$$[\mathbf{n}]_{\times} \mathbf{t}^* = \begin{bmatrix} \text{sign}(m_1) \sqrt{M_{\mathbf{S}_{11}}} \\ -\text{sign}(m_2) \sqrt{M_{\mathbf{S}_{22}}} \\ \text{sign}(m_3) \sqrt{M_{\mathbf{S}_{33}}} \end{bmatrix}$$

According to (173), we knew that:

$$M_{\mathbf{S}_{12}} = m_1 m_2$$

$$M_{\mathbf{S}_{13}} = m_1 m_3$$

$$M_{\mathbf{S}_{23}} = m_2 m_3$$

From this, it can be easily proved that:

$$\begin{bmatrix} \text{sign}(m_1) \\ \text{sign}(m_2) \\ \text{sign}(m_3) \end{bmatrix} = \pm \begin{bmatrix} \epsilon_{23} \\ \epsilon_{13} \\ \epsilon_{12} \end{bmatrix}$$

being  $\epsilon_{ij} = \text{sign}(M_{\mathbf{S}_{ij}})$ . Then, we can find the following relation:

$$[\mathbf{n}]_{\times} \mathbf{t}^* = \pm \mathbf{m}; \quad \mathbf{m} = \begin{bmatrix} \epsilon_{23} \sqrt{M_{\mathbf{S}_{11}}} \\ -\epsilon_{13} \sqrt{M_{\mathbf{S}_{22}}} \\ \epsilon_{12} \sqrt{M_{\mathbf{S}_{33}}} \end{bmatrix}$$

Hence, when any of the components of this vector product is null, the corresponding minor  $M_{\mathbf{S}_{ii}}$  is also null. We can look for a geometrical meaning of this situation. We can say that, whenever the vector product of  $\mathbf{n}$  and  $\mathbf{t}^*$  lies on any of the canonical planes ( $XY$ ,  $XZ$  or  $YZ$ ), the corresponding minor is null ( $M_{\mathbf{S}_{11}}$ ,  $M_{\mathbf{S}_{22}}$  or  $M_{\mathbf{S}_{33}}$ , respectively). There is another way to depict this. We can consider that each one of the components  $m_i$  is the scalar product of vectors obtained projecting  $\mathbf{n}$  and  $\mathbf{t}^*$  onto a particular canonical plane. For instance, in order to get  $m_3$ , we project the normal and the translation vectors onto the plane  $XY$ , these are vectors  $\mathbf{n}_{XY} = [n_1, n_2, 0]^T$  and  $\mathbf{t}_{XY}^* = [t_1^*, t_2^*, 0]^T$  in Fig. 11. Then we obtain the vector perpendicular to the second one on the same plane:  $\mathbf{t}_{XY}^{*\perp} = [t_2^*, -t_1^*, 0]^T$ , and compute the scalar product of this vector and  $\mathbf{n}_{XY}$ :

$$m_3 = \mathbf{n}_{XY}^T \mathbf{t}_{XY}^{*\perp}$$

This means that, when we are moving from the current frame to the reference frame in a direction such that its projection on plane  $XY$  is parallel to the object-plane normal, projected on this same plane,  $M_{\mathbf{S}_{33}}$  is null. In general:

$$\begin{aligned} \mathbf{n}_{YZ} \parallel \mathbf{t}_{YZ}^* &\implies M_{\mathbf{S}_{11}} = 0 \\ \mathbf{n}_{XZ} \parallel \mathbf{t}_{XZ}^* &\implies M_{\mathbf{S}_{22}} = 0 \\ \mathbf{n}_{XY} \parallel \mathbf{t}_{XY}^* &\implies M_{\mathbf{S}_{33}} = 0 \end{aligned}$$

That means that the plane defined by  $\mathbf{n}$  and  $[0 \ 0 \ 1]^T$  (in blue in Fig. 11) divides the space in two regions, being  $\mathbf{t}^*$  in either of these parts, the sign of the corresponding  $M_{\mathbf{S}_{ij}}$  (in this case,  $M_{\mathbf{S}_{12}}$ ) changes. Being  $\mathbf{t}^*$  on that plane,  $M_{\mathbf{S}_{33}}$  is null.

### C.3 Components of vectors $\mathbf{x}$ and $\mathbf{y}$ are always real

In order to prove that the components of vectors  $\mathbf{x}$  and  $\mathbf{y}$  are always real, we need to prove that the solutions for  $\omega$  in (74) are real and positive. On the one hand, the discriminant appearing in the computation of  $w_{num}$  should be always positive. It can be shown that, after some simple manipulations, this discriminant can be written as:

$$\begin{aligned} b^2 - ac &= 4 (\text{trace}(\mathbf{S}) + 1 + s_{11}s_{22} + s_{22}s_{33} + s_{11}s_{33} - s_{12}^2 - s_{23}^2 - s_{13}^2) \\ &= 4 (\text{trace}(\mathbf{S}) + 1 - M_{\mathbf{S}_{11}} - M_{\mathbf{S}_{22}} - M_{\mathbf{S}_{33}}) \end{aligned}$$

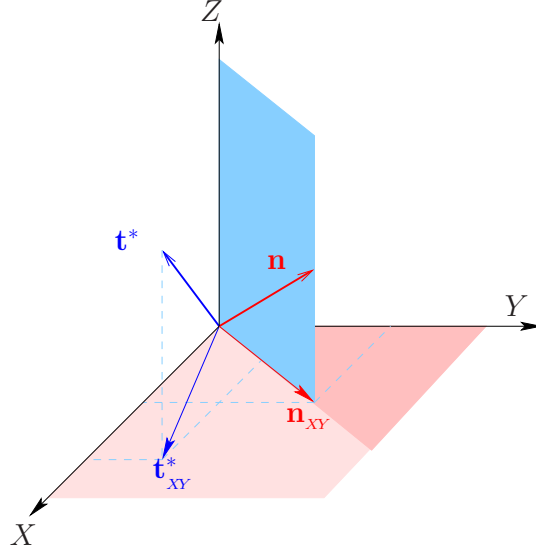


Figure 11: In blue, plane where  $\mathbf{t}^*$  must lie for  $M_{\mathbf{S}_{33}}$  becoming null.

The condition for the discriminant being non-negative can be written as:

$$\text{trace}(\mathbf{S}) + 1 \stackrel{?}{\geq} M_{\mathbf{S}_{11}} + M_{\mathbf{S}_{22}} + M_{\mathbf{S}_{33}}$$

According to the form of matrix  $\mathbf{S}$  (166) and its principal minors, the left member of this inequality can be written as:

$$\text{trace}(\mathbf{S}) + 1 = \|\mathbf{y}\|^2 + 2\mathbf{x}^\top \mathbf{y} + 1$$

while the right member can be developed in the following way:

$$y_1^2(x_2^2 + x_3^2) + y_2^2(x_1^2 + x_3^2) + y_3^2(x_1^2 + x_2^2) - 2(x_1x_2y_1y_2 + x_1x_3y_1y_3 + x_2x_3y_2y_3)$$

Recalling that  $\mathbf{x}$  is a unitary vector, we can write instead:

$$y_1^2(1 - x_1^2) + y_2^2(1 - x_2^2) + y_3^2(1 - x_3^2) - 2(x_1x_2y_1y_2 + x_1x_3y_1y_3 + x_2x_3y_2y_3)$$

From this, we can put the right member in a more convenient form:

$$\|\mathbf{y}\| - x_1y_1(x_1y_1 + x_2y_2 + x_3y_3) - x_2y_2(x_1y_1 + x_2y_2 + x_3y_3) - x_3y_3(x_1y_1 + x_2y_2 + x_3y_3) = \|\mathbf{y}\| - (\mathbf{x}^\top \mathbf{y})^2$$

Then, the condition to be proved becomes:

$$\|\mathbf{y}\| + 2\mathbf{x}^\top \mathbf{y} + 1 \stackrel{?}{\geq} \|\mathbf{y}\| - (\mathbf{x}^\top \mathbf{y})^2$$

or what is the same:

$$(\mathbf{x}^\top \mathbf{y})^2 + 2 \mathbf{x}^\top \mathbf{y} + 1 = (\mathbf{x}^\top \mathbf{y} + 1)^2 \geq 0$$

which is always true. On the other hand, after it has been stated that the discriminant is non-negative, the condition that  $w \geq 0$  is verified as  $a$  and  $c$  ((71) and (73), respectively) are always positive.

#### C.4 Proof of the equivalence of different expressions for $\nu$

In this brief section, we want to prove that the coefficients  $\nu$  defined in (88) and that introduced in (84) are the same. We will call  $\nu_1$  and  $\nu_2$  to the first and second ones, respectively. For the second one, we can write (see (89)):

$$\nu_2 = 2 + \text{trace}(\mathbf{S}) - \|\mathbf{t}_e\|^2$$

For the first one, we had:

$$\nu_1 = 2 (1 + \mathbf{n}^\top \mathbf{R}^\top \mathbf{t})$$

From the definitions of vectors  $\mathbf{x}$  and  $\mathbf{y}$  given in (46) and (47), we can write:

$$\nu_1 = 2 (1 + \mathbf{y}^\top \mathbf{x})$$

The scalar product appearing here can be computed using (56)-(58):

$$\mathbf{y}^\top \mathbf{x} = \frac{1}{2} (s_{11} + s_{22} + s_{33} - (y_1^2 + y_2^2 + y_3^2)) = \frac{1}{2} (\text{trace}(\mathbf{S}) - \|\mathbf{y}\|^2)$$

Then, we get the same expression as for  $\nu_2$

$$\nu_1 = 2 + \text{trace}(\mathbf{S}) - \|\mathbf{t}_e\|^2$$

what proves the equivalence of both definitions.

#### C.5 Proof of condition $\rho > 1$

Given coefficient  $\rho$ , that was defined as:

$$\rho = \|2 \mathbf{n}_e + \mathbf{R}_e^\top \mathbf{t}_e\|; \quad e = \{a, b\}$$

we want to prove in this section that this coefficient verifies:

$$\rho > 1$$

For that purpose, we can compute the scalar product:

$$\mathbf{n}_e^\top (2 \mathbf{n}_e + \mathbf{R}_e^\top \mathbf{t}_e) = \|2 \mathbf{n}_e + \mathbf{R}_e^\top \mathbf{t}_e\| \cos \phi$$

where  $\phi$  is the angle between both vectors involved in the scalar product. This product can also be written as:

$$\mathbf{n}_e^\top (2\mathbf{n}_e + \mathbf{R}_e^\top \mathbf{t}_e) = 2 + \mathbf{n}_e^\top \mathbf{R}_e^\top \mathbf{t}_e > 1$$

where (76) has been used. Then we have:

$$\|2\mathbf{n}_e + \mathbf{R}_e^\top \mathbf{t}_e\| \cos \phi > 1$$

This condition means, on the one hand, that the angle  $\phi$  must be:

$$\frac{-\pi}{2} < \phi < \frac{\pi}{2} \quad (174)$$

Also, as  $\cos \phi \leq 1$ , the condition for  $\rho$  is proved:

$$\rho = \|2\mathbf{n}_e + \mathbf{R}_e^\top \mathbf{t}_e\| > 1$$

## D Stability proofs

### D.1 Positivity of matrix $\mathbf{S}_{11}$

In this Appendix, it is proved that the third eigenvalue of matrix  $\mathbf{S}_{11}$ , in Section 6.3.2, is always positive, or can be null only along a particular configuration in Cartesian space. The expression for this eigenvalue was:

$$\lambda_3 = \frac{\|\mathbf{t}_a\| - 1}{2\rho} + \frac{1}{2} + \frac{\mathbf{t}_a^\top \mathbf{R}_a \mathbf{n}_a}{2\rho \|\mathbf{t}_a\|}$$

that, we can rewrite:

$$\lambda_3 = \frac{\|\mathbf{t}_a\| - 1}{2\rho} + \frac{1}{2} + \frac{\mathbf{n}_a^\top \mathbf{t}_a^*}{2\rho \|\mathbf{t}_a\|}; \quad \text{being: } \mathbf{t}_a^* = \mathbf{R}_a^\top \mathbf{t}_a$$

We want to verify the condition:

$$\lambda_3 = \frac{\|\mathbf{t}_a\|^2 - \|\mathbf{t}_a\| + \rho \|\mathbf{t}_a\| + \mathbf{n}_a^\top \mathbf{t}_a^*}{2\rho \|\mathbf{t}_a\|} \stackrel{?}{\geq} 0$$

This is the same as:

$$\frac{\|\mathbf{t}_a\| - 1 + \rho + c_\alpha}{2\rho} \stackrel{?}{\geq} 0 \quad (175)$$

being  $c_\alpha = \cos \alpha$ , and  $\alpha$  the angle between vectors  $\mathbf{n}_a$  and  $\mathbf{t}_a^*$ :

$$\mathbf{n}_a^\top \mathbf{t}_a^* = \|\mathbf{t}_a\| c_\alpha$$

In order to prove this, we need to put  $\rho$  in terms of  $\mathbf{n}_a^\top \mathbf{t}_a^*$ . This is done by means of cosines. Consider the following scalar product:

$$\mathbf{n}_a^\top (2\mathbf{n}_a + \mathbf{t}_a^*) = 2 + \mathbf{n}_a^\top \mathbf{t}_a^*$$

that is also equal to:

$$\mathbf{n}_a^\top (2\mathbf{n}_a + \mathbf{t}_a^*) = \|2\mathbf{n}_a + \mathbf{t}_a^*\| c_\phi = \rho c_\phi; \quad \text{being: } c_\phi = \cos \phi$$

and  $\phi$  is the angle between vectors  $\mathbf{n}_a$  and  $(2\mathbf{n}_a + \mathbf{t}_a^*)$ . According to this, we can write:

$$\rho c_\phi = 2 + \mathbf{n}_a^\top \mathbf{t}_a^* = 2 + \|\mathbf{t}_a\| c_\alpha$$

On the other hand, from the proof that  $\rho > 1$ , we know that  $c_\phi$  must be positive (see (174)):

$$\phi \in (-\pi/2, \pi/2) \implies c_\phi > 0$$

Multiplying both sides of (175) by  $c_\phi$ , then, does not change the inequality:

$$\frac{\|\mathbf{t}_a\| c_\phi - c_\phi + 2 + \|\mathbf{t}_a\| c_\alpha + c_\alpha c_\phi}{2\rho} \stackrel{?}{\geq} 0$$

As the denominator of this expression is always positive, we can simply analyze:

$$\|\mathbf{t}_a\| (c_\phi + c_\alpha) + [2 + c_\phi(c_\alpha - 1)] \stackrel{?}{\geq} 0 \quad (176)$$

From this, as  $2 + c_\phi(c_\alpha - 1) \geq 0$ , a sufficient condition for this being satisfied is:

$$\|\mathbf{t}_a\| (c_\phi + c_\alpha) \stackrel{?}{\geq} 0$$

Finally, the condition to be proved is:

$$c_\phi \stackrel{?}{\geq} -c_\alpha$$

This will be done in two steps:

- First, we suppose that  $\alpha \in [-\pi/2, \pi/2]$ . A geometric interpretation of angles  $\alpha$  and  $\phi$  can help us seeing that in this case, the condition is always verified. In the following figure, we picture vectors  $\mathbf{n}_a$  and  $\mathbf{t}_a^*$  on the plane they define: As  $\phi$  must always verify  $\text{abs}(\phi) \leq \text{abs}(\alpha)$ , and we are in the first or fourth quadrants, it is clear that  $c_\phi \geq -c_\alpha$ , as both cosines are positive.
- Now, lets see what happens when  $\alpha \in [-\pi, \pi/2) \cup (\pi/2, \pi]$ . This case is not so simple. In this case,  $\mathbf{t}_a^*$  is in the second or third quadrant. In this case, we must limit the norm of  $\mathbf{t}_a^*$  so the condition can be verified. This is illustrated in Figure 13 In this

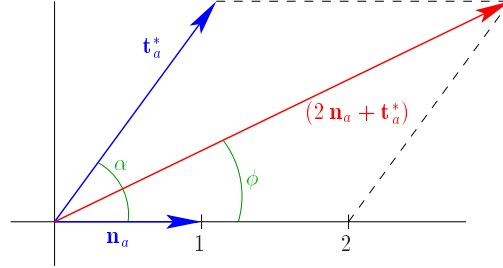
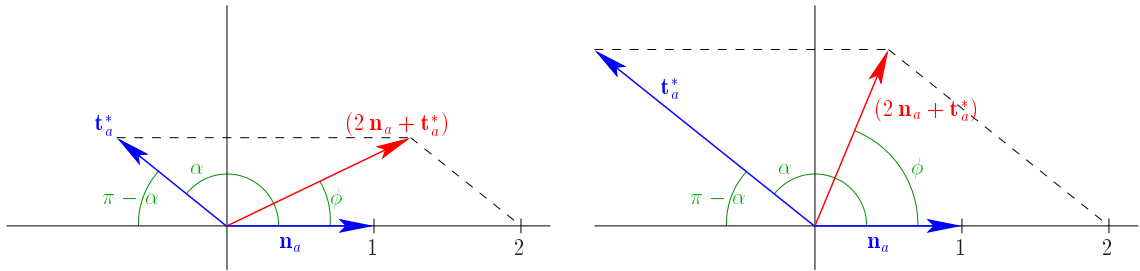
Figure 12: Angles  $\alpha$  and  $\phi$ . Case  $\alpha \in [-\pi/2, \pi/2]$ Figure 13: Angles  $\alpha$  and  $\phi$ . Case when  $\mathbf{t}_a^*$  is in the second or third quadrant. Left: condition is verified. Right: condition is not verified.

figure we see, that if do not limit  $\|\mathbf{t}_a^*\|$   $\phi$  may be:

$$\phi > \pi - \alpha \implies c_\phi < c_{\pi - \alpha} = -c_\alpha$$

From condition (76), we know that the limitation in the norm of  $\mathbf{t}_a^*$  is such that:

$$\mathbf{n}_a^\top \mathbf{t}_a^* > -1$$

that can be written as:

$$\mathbf{n}_a^\top \mathbf{t}'_a < 1; \quad \mathbf{t}'_a = -\mathbf{t}_a^*$$

If we consider the worst case (already not possible), when this projection reaches its limit value,  $\mathbf{n}_a^\top \mathbf{t}'_a = 1$ , that corresponds to the camera hitting the object plane. The vector

$$2\mathbf{n}_a + \mathbf{t}_a^* = 2\mathbf{n}_a - \mathbf{t}'_a$$

can be drawn as shown in Figure 14. Several possibilities are drawn in red for this vector and in blue for the corresponding  $\mathbf{t}'_a$ . These are included just to make clear that no one can pass to the right side of vertical line in 1. Considering the instances

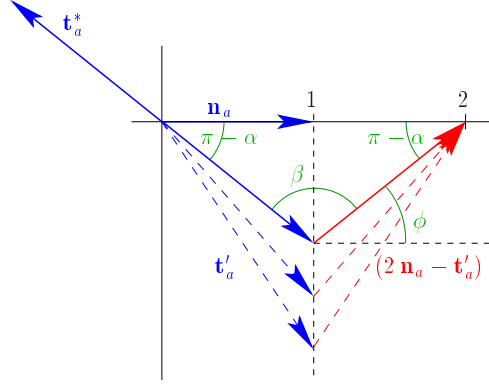


Figure 14: Geometric interpretation of condition  $\mathbf{n}_a^\top \mathbf{t}'_a = 1$ .

of  $\mathbf{t}'_a$  and  $2\mathbf{n}_a - \mathbf{t}'_a$  in solid lines, the angles shown in the figure verify:

$$2(\pi - \alpha) + \beta = \pi \implies \beta = 2\alpha - \pi$$

On the other hand,

$$\frac{\beta}{2} + \phi = \frac{\pi}{2}$$

Combining these two relations, the conclusion is:

$$\phi = \pi - \alpha \implies c_\phi = -c_\alpha$$

This is the limit case, as said before. If we take the norm of  $\mathbf{t}_a$  such that:

$$\|\mathbf{t}'_a\| / \mathbf{n}_a^\top \mathbf{t}'_a < 1$$

instead, we have the situation depicted in Figure 15. Then, we see that always:

$$\phi < \phi_{lim} \implies c_\phi > c_{\phi_{lim}} = -c_\alpha$$

With all this, we finally have the required proof, that always:

$$c_\phi \geq -c_\alpha$$

and then:

$$\lambda_3 \geq 0$$



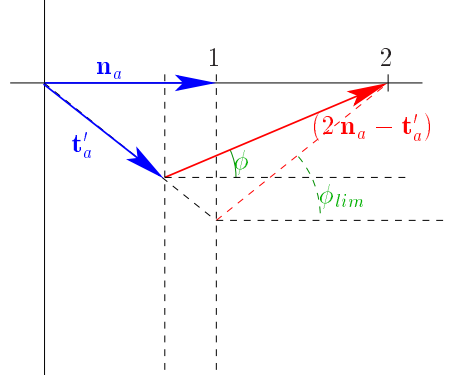


Figure 15: Geometric interpretation of condition  $\mathbf{n}_a^\top \mathbf{t}'_a < 1$ .

### D.1.1 When is $\mathbf{S}_{11}$ singular ?

We want now to determine when is  $\lambda_3 = 0$ . We can start the analysis from the expression (176), and try to find when it becomes zero:

$$\|\mathbf{t}_a\| (c_\phi + c_\alpha) + [2 + c_\phi(c_\alpha - 1)] = 0$$

Since both addends are non-negative, for the whole expression to become zero, both must be zero:

$$\begin{aligned} 2 + c_\phi(c_\alpha - 1) = 0 &\implies c_\alpha = -1 \quad \text{and} \quad c_\phi = 1 \\ \|\mathbf{t}_a\| (c_\phi + c_\alpha) = 0 &\implies c_\alpha = -c_\phi \end{aligned}$$

Obviously, both conditions are simultaneously verified if:

$$c_\alpha = -1 \quad \text{and} \quad c_\phi = 1$$

That is,

$$\alpha = \pm\pi \quad \text{and} \quad \phi = 0$$

On the one hand, as  $\alpha$  is the angle between vectors  $\mathbf{n}_a$  and  $\mathbf{t}_a^*$ , this means that  $\mathbf{t}_a^*$  is in the opposite direction of the plane normal:

$$\mathbf{t}_a^* = -\|\mathbf{t}_a^*\| \mathbf{n}_a$$

Or in terms of  $\mathbf{t}_a$ :

$$\frac{\mathbf{R}_a^\top \mathbf{t}_a}{\|\mathbf{t}_a\|} = -\mathbf{n}_a \tag{177}$$

On the other hand,  $c_\phi = 1$ ,

$$c_\phi = \frac{\mathbf{n}_a^\top (2\mathbf{n}_a + \mathbf{R}_a^\top \mathbf{t}_a)}{\|2\mathbf{n}_a + \mathbf{R}_a^\top \mathbf{t}_a\|}$$

If we particularize this expression using (177), we get:

$$\begin{aligned}\mathbf{n}_a^\top (2 \mathbf{n}_a + \mathbf{R}_a^\top \mathbf{t}_a) &= (2 - \|\mathbf{t}_a\|) \mathbf{n}_a \\ \|2 \mathbf{n}_a + \mathbf{R}_a^\top \mathbf{t}_a\| &= \text{abs}(2 - \|\mathbf{t}_a\|) = 2 - \|\mathbf{t}_a\|\end{aligned}$$

From the second equality, we have removed the *abs()*. This is possible because of the reference-plane non-crossing constraint. This constraint, applied to our situation, in which we are moving exactly in the direction of the normal, becomes:

$$\|\mathbf{t}'_a\| = \|\mathbf{t}_a\| < 1$$

Then,  $c_\phi$  is:

$$c_\phi = \frac{2 - \|\mathbf{t}_a\|}{2 - \|\mathbf{t}_a\|} = 1$$

Hence, the condition  $c_\alpha = -1$  already implies  $c_\phi = 1$ , and no additional conditions are needed. In Section 6.3.2, the interpretation of the geometric locus corresponding to relation (177) is given. Finally, we will also compute the eigenvector corresponding to the null eigenvalue, in case they are needed. If we particularize the matrix  $L_{S_{11}}$  in (177), we obtain:

$$L_{S_{11}}^\bullet = \frac{1}{2 - \|\mathbf{t}_a\|} (\mathbf{I} - \mathbf{R}_a \mathbf{n}_a \mathbf{n}_a^\top \mathbf{R}_a^\top)$$

With  $L_{S_{11}}^\bullet$  we mean *the value of  $S_{11}$  in the points of the geometric locus (177)*. The corresponding eigenvalues, particularized for this case are:

$$\lambda_1^\bullet = \lambda_2^\bullet = \frac{1}{2 - \|\mathbf{t}_a\|}; \quad \lambda_3^\bullet = 0$$

The corresponding eigenvectors are:

$$\begin{aligned}\mathbf{v}_1^\bullet &= \kappa_1 [n_{a_2}, -n_{a_1}, 0]^\top \\ \mathbf{v}_2^\bullet &= \kappa_2 [0, -n_{a_3}, n_{a_2}]^\top \\ \mathbf{v}_3^\bullet &= \kappa_3 \mathbf{R}_a \mathbf{n}_a\end{aligned}\tag{178}$$

where  $\kappa_i$  are scalars and  $n_{a_i}$  are the components of  $\mathbf{R}_a \mathbf{n}_a$ :

$$\mathbf{R}_a \mathbf{n}_a = [n_{a_1}, n_{a_2}, n_{a_3}]^\top$$

## D.2 Positivity of matrix $S_{11-}$

In this Appendix, we want to prove that the third eigenvalue of matrix  $S_{11-}$  (see (160)) is always positive, or that it can be null only along a particular configuration in Cartesian space, assuming some conditions.

The expression for this eigenvalue was:

$$\lambda_{3-} = -\frac{1 + \|\mathbf{t}_a\|}{2\rho} + \frac{1}{2} - \frac{\mathbf{n}_a^\top \mathbf{t}_a^*}{2\rho \|\mathbf{t}_a\|}; \quad \text{being: } \mathbf{t}_a^* = \mathbf{R}_a^\top \mathbf{t}_a$$

We want to verify the condition:

$$\lambda_{3-} = \frac{-\|\mathbf{t}_a\|^2 - \|\mathbf{t}_a\| + \rho \|\mathbf{t}_a\| - \mathbf{n}_a^\top \mathbf{t}_a^*}{2\rho \|\mathbf{t}_a\|} \stackrel{?}{\geq} 0$$

This is equivalent to:

$$\rho \stackrel{?}{\geq} \|\mathbf{t}_a\| + 1 + c_\alpha$$

being the cosine  $c_\alpha$ , as before:

$$\mathbf{n}_a^\top \mathbf{t}_a^* = \|\mathbf{t}_a\| c_\alpha$$

As both members in the inequality are positive, the condition holds if the squared inequality does:

$$\rho^2 \stackrel{?}{\geq} (\|\mathbf{t}_a\| + 1 + c_\alpha)^2$$

After some elemental manipulations, we obtain:

$$4 \stackrel{?}{\geq} (1 + c_\alpha)^2 + 2\|\mathbf{t}_a\|(1 - c_\alpha) \quad (179)$$

Then, the condition for  $\lambda_{3-}$  being also positive is:

$$\|\mathbf{t}_a\| \leq \frac{4 - (1 + c_\alpha)^2}{2(1 - c_\alpha)} \quad (180)$$

In particular, if we assume  $\|\mathbf{t}_a\| \leq 1$ , we can write:

$$(1 + c_\alpha)^2 + 2(1 - c_\alpha) \geq (1 + c_\alpha)^2 + 2\|\mathbf{t}_a\|(1 - c_\alpha) \quad (181)$$

Then, it is sufficient to prove:

$$4 \stackrel{?}{\geq} (1 + c_\alpha)^2 + 2(1 - c_\alpha)$$

This is equivalent to:

$$4 \geq 3 + c_\alpha^2 \quad (182)$$

which is always true. This proves that:

$$\lambda_{3-} \geq 0 \quad \text{if } \|\mathbf{t}_a\| \leq 1$$

as desired.

### D.2.1 When is $\mathbf{S}_{11_-}$ singular ?

We want now to determine when is  $\lambda_{3_-} = 0$ . In order to see when the inequality (179) becomes an identity, we go back to the inequalities (181) and (182):

$$4 \geq 3 + c_\alpha^2 \geq (1 + c_\alpha)^2 + 2 \|\mathbf{t}_a\| (1 - c_\alpha)$$

both inequalities change into equalities when  $c_\alpha = 1$ . As  $\alpha$  is the angle between vectors  $\mathbf{n}_a$  and  $\mathbf{t}_a^*$ , both vectors must be parallel, corresponding to the already known Cartesian configuration:

$$\frac{\mathbf{R}_a^\top \mathbf{t}_a}{\|\mathbf{t}_a\|} = \pm \mathbf{n}_a$$

## References

- [1] O. Faugeras and F. Lustman, "Motion and structure from motion in a piecewise planar environment", in *International Journal of Pattern Recognition and Artificial Intelligence*, 2(3):485–508, 1988.
- [2] S. Hutchinson, G. D. Hager and P. I. Corke, "A tutorial on Visual Servo Control", in *IEEE Transaction on Robotics and Automation*, 12(5):651–670, October 1996.
- [3] E. Malis, F. Chaumette and S. Boudet, "2 1/2 D Visual Servoing", in *IEEE Transaction on Robotics and Automation*, 15(2):234–246, April 1999.
- [4] E. Malis, "Hybrid vision-based robot control robust to large calibration errors on both intrinsic and extrinsic camera parameters", in *European Control Conference*, pp. 2898–2903, Porto, Portugal, September 2001.
- [5] Y. Fang, D.M. Dawson, W.E. Dixon, and M.S. de Queiroz, "Homography-Based Visual Servoing of Wheeled Mobile Robots", in *Proc. IEEE Conf. Decision and Control*, pp. 2866–282871, Las Vegas, NV, Dec. 2002.
- [6] E. Malis and F. Chaumette, "Theoretical improvements in the stability analysis of a new class of model-free visual servoing methods", in *IEEE Transaction on Robotics and Automation*, 18(2):176–186, April 2002.
- [7] S. Benhimane and E. Malis, "Real-time image-based tracking of planes using efficient second-order minimization", in *IEEE/RSJ International Conference on Intelligent Robots Systems*, Sendai, Japan, October 2004.
- [8] M. Moakher., "Means and averaging in the group of rotations", in *SIAM Journal on Matrix Analysis and Applications*, Vol. 24, Number 1, pp. 1-16, 2002.

- 
- [9] M. Vargas and E. Malis, “Visual servoing based on an analytical homography decomposition”, in *44th IEEE Conference on Decision and Control and European Control Conference ECC 2005 (CDC-ECC'05)*, Seville, Spain, December 2005.
  - [10] C. Samson, M. Le Borgne, and B. Espiau. *Robot control: the task function approach*, Vol. 22 of *Oxford Engineering Science Series*. Clarendon Press, Oxford, UK, 1991.
  - [11] Z. Zhang, and A.R. Hanson. “3D Reconstruction based on homography mapping”, in *Proc. ARPA96*, pp. 1007-1012, 1996.
  - [12] E. Malis, F. Chaumette “Theoretical improvements in the stability analysis of a new class of model-free visual servoing methods”, in *IEEE Transaction on Robotics and Automation*, 18(2):176-186, April 2002.



---

Unité de recherche INRIA Sophia Antipolis  
2004, route des Lucioles - BP 93 - 06902 Sophia Antipolis Cedex (France)

Unité de recherche INRIA Futurs : Parc Club Orsay Université - ZAC des Vignes  
4, rue Jacques Monod - 91893 ORSAY Cedex (France)

Unité de recherche INRIA Lorraine : LORIA, Technopôle de Nancy-Brabois - Campus scientifique  
615, rue du Jardin Botanique - BP 101 - 54602 Villers-lès-Nancy Cedex (France)

Unité de recherche INRIA Rennes : IRISA, Campus universitaire de Beaulieu - 35042 Rennes Cedex (France)

Unité de recherche INRIA Rhône-Alpes : 655, avenue de l'Europe - 38334 Montbonnot Saint-Ismier (France)

Unité de recherche INRIA Rocquencourt : Domaine de Voluceau - Rocquencourt - BP 105 - 78153 Le Chesnay Cedex (France)

---

Éditeur

INRIA - Domaine de Voluceau - Rocquencourt, BP 105 - 78153 Le Chesnay Cedex (France)

<http://www.inria.fr>

ISSN 0249-6399